THE STATUS OF ($N = 1$) SUPERSYMMETRY

J. F Gunion, Barcelona (September, 1997)

- WHY is it attractive?
- WHAT do we expect to see?
- HOW do we see what is predicted?

WHY?

- SUSY = only non-trivial extension of Lorentz group at heart of QFT: $\Rightarrow$ introduce spinorial extension of space to θ ($\theta^2 = 0$). Taylor expansions in θ then yield [spin-0 $\leftrightarrow$ spin-1/2].
- If SUSY formulated as a *local* symmetry $\Rightarrow$ spin-2 (graviton) field $\Rightarrow$ SUGRA (which reduces to general relativity in appropriate limit).
- SUSY appears in Superstrings.
- Adding Lorentz group to QM required antiparticle for every particle; why should history not repeat — SUSY + QFT requires sparticle for every particle.

WHY below a TeV?

- String theory solutions with non-supersymmetric *ground* state are quite problematic.
- SUSY solves hierarchy problem, *e.g.* $m_{\rm Higgs}^2 < (1~{\rm TeV})^2$ (as required to avoid non-perturbative WW sector) via spin-1/2 loop cancellation

of spin-0 loop quadratic divergence

$$m_H^2 \sim [m_H^0]^2 + \lambda^2(m_{\rm boson}^2 - m_{\rm fermion}^2)\ln\frac{\Lambda^2}{\langle m_b^2, m_f^2\rangle}, \quad (m_f \sim m_{\rm SUSY}) \tag{0.1}$$

provided $m_f^2 \lesssim (1\ \mathrm{TeV})^2$.

- SUSY $\Rightarrow$ gauge coupling unification (at $M_U \sim$ few $\times\, 10^{16}$ GeV) if $m_{\rm SUSY} \lesssim 1 - 10$ TeV + desert — smaller α_s prefers larger $m_{\rm SUSY}$. Subsidiary points:
  - a) perturbative unification requires $N_{\rm families}^{\lesssim 1\ \rm TeV} \leq 4$.
  - b) is $M_U < M_S = M_{\rm Planck}/\sqrt{8\pi} \sim 2 \times 10^{18}$ GeV a problem? 'Non-perturbatively, M_S can be anything' even as low as a TeV (Lykken).
  - c) unification "ok" only if exactly 2 Higgs doublets (+ singlets) below M_U. Anomaly cancellation requires 2 doublets.
- Electroweak Symmetry Breaking (EWSB) is 'derived' from RGE equations if $m_t \sim 175$ GeV — $m_{H_2}^2$ driven < 0 at energy scale in vicinity of 100 GeV by large λ_t if $m_{H_2}^2 < (1\ \mathrm{TeV})^2$ at M_U.
- In many cases, the LSP = cold dark matter candidate (GMSB?,$\not R$?).

WHAT do we expect to see?

A) Sparticles

$$\begin{array}{llcc} [u,d,c,s,t,b] & g & \underbrace{W^\pm, H^\pm} & \underbrace{\gamma, Z, H_1^0, H_2^0} \\ \left[\tilde{u},\tilde{d},\tilde{c},\tilde{s},\tilde{t},\tilde{b}\right]_{L,R} & \tilde{g} & \widetilde{\chi}^\pm_{1,2} & \widetilde{\chi}^0_{1,2,3,4} \end{array}$$

B) A **very** special Higgs sector.

$$h^0, H^0, A^0, H^\pm$$

with $m_{h^0} \lesssim 130$ GeV (150 GeV if add singlets)

$m_{H^0} \sim m_{A^0} \sim m_{H^\pm} \gtrsim 200$ GeV probable in models with auto EWSB

Many possible versions of A) $\Rightarrow$ many different HOW?'s. Except for h^0, need $\sqrt{s} \gtrsim 2m_{\rm SUSY}$ at $q\overline{q}$ or $e^+e^-, \mu^+\mu^-$ level (unless $\not{R}$).

Possibilities for Sparticles

W =superpotential is well-determined, but SU$\not{S}$Y $\Rightarrow$ many scenarios. In model with minimal particle content, we have the SM sparticle partners with masses determined by **soft**-supersymmetry-breaking. (**soft**$\equiv$preserves hierarchy solution.)

- gaugino masses: $M_i\lambda_i\lambda_i$ where $i = 3,2,1$ for SU(3),SU(2),U(1) and λ_i =spin-1/2 partner of corresponding gauge field.

- scalar masses:

$$m_{H_1}^2|H_1|^2 + m_{H_2}^2|H_2|^2 + m^2_{(\tilde{t},\tilde{b})_L}(\tilde{t}_L^\star\tilde{t}_L + \tilde{b}_L^\star\tilde{b}_L) + m^2_{\tilde{t}_R}\tilde{t}_R^\star\tilde{t}_R + m^2_{\tilde{b}_R}\tilde{b}_R^\star\tilde{b}_R \quad (0.2)$$

- 'A' terms: *e.g.* $A_t\lambda_t(\tilde{t}_LH_2^0 - \tilde{b}_LH_2^+)\tilde{t}_R^\star$.

- 'B': $B\mu(H_1^0 H_2^0 - H_1^+ H_2^-)$, where μ is the parameter appearing the superpotential term $W \ni \mu \widehat{H}_1 \widehat{H}_2$.

Altogether $\Rightarrow$ 105 (106?) independent and unknown (perhaps limited by hierarchy/naturalness) parameters beyond the SM. Is this Good or Bad?

- Bad: if you want to know ahead of time exactly what to look for.
- Good: if you want to be confident you will learn something from what you observe.

Hope to discover an underlying organization for the 105 parameters (by evolving the low-E parameters up to M_U) that will define the GUT/String model visible sector properties.

Different models $\Rightarrow$ vastly different low-E parameters and expectations.

$\Rightarrow$ machine builders + experimentalists must be prepared for a wide range of possibilities as to HOW? we see and fully explore SUSY. The rest of the talk reviews some of the many possibilities discussed to date.

SPARTICLE SECTOR

Phenomenology determined by boundary conditions, nature and source of supersymmetry breaking, and whether or not R-parity is broken. A selection of possibilities is discussed below, beginning with

Minimal Supergravity (mSUGRA)

(assuming SU$\not{S}$Y at M_U and no $\not{R}$)

- At M_U the parameters are universal:
  - $m_{H_1} = m_{H_2} = m_{\tilde{q}_i} = m_{\tilde{\ell}_i} \ldots = m_0$
  - $M_3 = M_2 = M_1 = m_{1/2}$
  - $A_{ijk} = A_0$
  - $|\mu|$, B
  - sign(μ)
- At m_W, some rules of thumb:
  - $M_3 : M_2 : M_1 = \alpha_3 : \alpha_2 : \alpha_3$ (1-loop) $\sim 6 :\sim 2 :\sim 1$;
  - $m_{\tilde{q}_i} = m_0$ (universal) at $M_U \Rightarrow$ small FCNC for first two generations (but starting at M_S?) — stop = lightest squark;
  - automatic EWSB — trade $|\mu|$ and B for $\tan\beta$ and (known) m_Z;
  - $|\mu|$, $m_{A^0} \sim m_{H^0} \sim m_{H^\pm} \sim$ "big" ($\gtrsim$ 200 GeV) unless $\tan\beta \gg 1$;
  - $\widetilde{\chi}_1^0 \simeq \widetilde{B}$ = good (cold) dark matter candidate if no $\not{R}$;
  - if $m_0^2 \gg m_{1/2}^2 \Rightarrow$ squarks, sleptons, ... heavier than $\widetilde{\chi}$'s and $\approx$ degenerate.
  - if $m_0^2 \ll m_{1/2}^2 \Rightarrow m_{\tilde{\ell}} < m_{\tilde{q}}$ and $m_{\tilde{t}_1}$ distinctly smaller than other $m_{\tilde{q}_i}$;

- Signatures: $m_{\widetilde{\chi}^0_{3,4}} \sim m_{\widetilde{\chi}^\pm_2} > m_{\widetilde{\chi}^0_2,\widetilde{\chi}^\pm_1} > m_{\widetilde{\chi}^0_1} \Rightarrow$ chain decays — *e.g.*

$$\tilde{g} \to q\overline{q}\widetilde{\chi}^\pm_1 \to q\overline{q} + \begin{cases} \ell^\pm\nu\widetilde{\chi}^0_1 \\ q\overline{q}\widetilde{\chi}^0_1 \end{cases} \quad \text{with}$$

– large $\not{E}_T$

– energetic jets and leptons

♢ <u>LHC</u>

$\Rightarrow pp \to \tilde{g}\tilde{g} \to$ jets + $\not{E}_T$ and like-sign dileptons+jets+$\not{E}_T$,

$\to m_{\tilde{g}} - m_{\widetilde{\chi}^\pm_1}$ from jet spectra end points, $m_{\widetilde{\chi}^\pm_1} - m_{\widetilde{\chi}^0_1}$ from ℓ spectra end points, absolute scale from hemispheric $m_{\tilde{g}}$ ($\pm 15\%$).

$\Rightarrow pp \to \widetilde{\chi}^\pm_1\widetilde{\chi}^0_1 \to$ trileptons.

♢ <u>NLC</u> or <u>MC</u>

$\Rightarrow e^+e^- \to \widetilde{\chi}^+_1\widetilde{\chi}^-_1 \to (q\overline{q}\widetilde{\chi}^0_1$ or $\ell\nu\widetilde{\chi}^0_1) + (q\overline{q}\widetilde{\chi}^0_1$ or $\ell\nu\widetilde{\chi}^0_1)$

$\to m_{\widetilde{\chi}^\pm_1}, m_{\widetilde{\chi}^0_1}$ to very good accuracy from spectra end points

$\Rightarrow$ $\tilde{q}$ and (if m_0 big) $\tilde{\ell}$ often too heavy for $\sqrt{s} = 500$ GeV pair production — if $m_0 \sim 1$ TeV, is required energy more easily achieved at NMC or expanded NLC?

'Standard' Snowmass Point

$m_0 = 200$ GeV, $m_{1/2} = 100$ GeV, $A_0 = 0$, $\tan\beta = 2$, $\mu < 0$

$\Rightarrow$ lots of light SUSY, in particular $m_{\tilde{g}} = 285$, $m_{\tilde{b}_L} = 266$ GeV

$\Rightarrow$, at LHC, millions of spectacular events with $\tilde{g} \to b\tilde{b}_L \to \ldots$

$\Rightarrow$, at NLC or MC, $\tilde{q}\tilde{q}$ threshold $> \sqrt{s} = 500$ GeV, but $\tilde{\ell}\tilde{\ell}$ and $\widetilde{\chi}^+_1\widetilde{\chi}^-_1, \widetilde{\chi}^0_{1,2}\widetilde{\chi}^0_{1,2}$ accessible.

String/SUGRA Motivated mSUGRA Models

♣ No-Scale: $m_{1/2} \neq 0$, $m_0 = A_0 = 0$ (*e.g.* SU(5)×U(1) flipped still attractive);

♣ Dilaton or Dilaton-Like: $m_{1/2} = -A_0 = \sqrt{3}m_0$

— To deviate significantly from dilaton b.c. in Calabi-Yau and Orbifold models requires having $\sin\theta_{\rm goldstino} \ll 1^*$

— Vacuum stability against color breaking ... currently looking ok; metastability and/or non-perturbative effects can cure apparent difficulty

Both models

⇒ light sleptons,

⇒ excellent LEPII, TeV33, LHC, NLC/MC prospects, depending on overall mass scale, $m_{1/2}$.

Unification at M_S?

If coupling constant unification at M_U is taken to be only apparent, and we introduce intermediate scale matter in such a way that the couplings actually unify at M_S, then detailed phenomenology changes somewhat in the mSUGRA models.

⇒ this is good, since we want to be able to determine if there is intermediate scale stuff using low-E experimental observations.

---

*This is because in the absence of loop corrections the dilaton boundary conditions apply with $m_{1/2} = m_{3/2}\sin\theta_{\rm goldstino}$ and it is only when $m_{3/2}\sin\theta_{\rm goldstino}$ gets small compared to loop corrections that we can move away from dilaton b.c.

Beyond mSUGRA Models

- many possible sources of non-universality
  - gaugino mass non-universality
  - scalar mass non-universality
- R-parity breaking
  - hard (*i.e.* tri-linear superpotential terms — restricted by proton decay)
  - soft (*i.e.* $\tilde{\ell}$-Higgs mixing at quadratic level)
- SU$\not{S}$Y at lower scales

Models that have some form of reasonable motivation continue to multiply. Exotic ones include:

- strange-event-motivated models.
- the light gluino scenario.
- heavy gluino=LSP scenarios.

Non-Universal Gaugino Masses

- O-II Orbifold String model: all matter fields in $n = -1$ untwisted sector, SU$\not{S}$Y dominated by overall size modulus (not dilaton).

  Only model where limit of pure modulus (no dilaton) SU$\not{S}$Y is possible without charge and/or color breaking.

  – Gaugino masses from 1-loop terms of form present in any theory $\Rightarrow M_U$ b.c.:

  $$M_a^0 \sim \sqrt{3} m_{3/2}[-(b_a + \delta_{GS})K\eta], \;\; m_0^2 = m_{3/2}^2[-\delta_{GS}K'], \;\; A_0 = 0 \tag{0.3}$$

  where b_a = gauge RGE coefficients ($b_3 = 3$, $b_2 = -1$, $b_1 = -33/5$), δ_{GS} = Green-Schwarz mixing parameter (a negative integer in the O-II model, with $\delta_{GS} = -4, -5$ preferred), and $\eta = \pm 1$. Estimates are $K = 4.6 \times 10^{-4}$ and $K' = 10^{-3}$

  $\Rightarrow m_{\widetilde{\ell}}, m_{\widetilde{q}} \gg M_a$.

  – General relation of M_a to b_a, δ_{GS} more general than O-II model; likely to survive non-perturbative corrections. Relation between K and K' is model-dependent.

- F-term breaking with $F \neq$ SU(5) singlet:

  – M_a arise from a chiral superfield Φ that appears linearly in the gauge kinetic function with $\langle F \rangle \neq 0$ for auxiliary component.

  $$\mathcal{L} = \int d^2\theta W_a W_b \frac{\Phi_{ab}}{M_{\rm Planck}} + h.c. \sim \frac{\langle F_\Phi \rangle_{ab}}{M_{\rm Planck}} \lambda_a \lambda_b \,, \tag{0.4}$$

  $\lambda_{a,b}$ $(a, b = 1, 2, 3)$ = gaugino fields.

– If F = SU(5) singlet $\Rightarrow \langle F_\Phi \rangle_{ab} \propto c\delta_{ab} \Rightarrow M_1 = M_2 = M_3$ (at M_U).

– More generally,

$$\Phi, F_\Phi \in (\mathbf{24}\times\mathbf{24})_{\text{symmetric}} = \mathbf{1} \oplus \mathbf{24} \oplus \mathbf{75} \oplus \mathbf{200}\,. \qquad (0.5)$$

For higher reps, only F_Φ component that is 'neutral' wrp to SU(3), SU(2), U(1) has vev if groups unbroken after SU$\not{S}$Y

$\Rightarrow \langle F_\Phi \rangle_{ab} = c_a \delta_{ab}$, with c_a depending on rep. (arbitrary superposition of reps also possible).

	M_U			m_Z		
F_Φ	M_3	M_2	M_1	M_3	M_2	M_1
1	1	1	1	~ 6	~ 2	~ 1
24	2	-3	-1	~ 12	~ -6	~ -1
75	1	3	-5	~ 6	~ 6	~ -5
200	1	2	10	~ 6	~ 4	~ 10
$O-II$ $\delta_{GS}=-4$	1	5	$\frac{53}{5}$	~ 6	~ 10	$\sim \frac{53}{5}$

Table 1: M_a at M_U and m_Z for the four F_Φ irr. reps. and in the O-II model with $\delta_{GS} \sim -4$.

Phenomenology

- In **200** and O-II, $m_{\widetilde{\chi}_1^0} \sim \min(M_1, M_2)$, $m_{\widetilde{\chi}_1^\pm} \sim M_2 \Rightarrow m_{\widetilde{\chi}_1^\pm} \simeq m_{\widetilde{\chi}_1^0}$ (winos) since $M_2 \lesssim M_1$, *e.g.* Snowmass point $m_{\widetilde{g}} \sim 285$ GeV masses:
- At the NLC or MC: not necessarily straightforward.
  – In **1** and **24**: masses for $\widetilde{\ell}_L$, $\widetilde{\ell}_R$, $\widetilde{\chi}_1^\pm$, $\widetilde{\chi}_1^0$ and $\widetilde{\chi}_2^0 \Rightarrow$ standard array of SUSY discovery signals — mass splittings substantial.
  – In **75**: $\widetilde{\chi}_1^+\widetilde{\chi}_1^-$ and $\widetilde{\chi}_2^0\widetilde{\chi}_2^0$ barely allowed at $\sqrt{s} = 500$ GeV; $\widetilde{\chi}_1^0\widetilde{\chi}_2^0$ only somewhat better. $\Rightarrow$ signals weak; fruitful to look for $e^+e^- \rightarrow \gamma\widetilde{\chi}_1^0\widetilde{\chi}_1^0$?

	1	**24**	**75**	**200**	$O-II$ $\delta_{GS}=-4.7$
$m_{\widetilde{g}}$	285	285	287	288	313
$m_{\widetilde{u}_R}$	302	301	326	394	big
$m_{\widetilde{t}_1}$	255	257	235	292	big
$m_{\widetilde{t}_2}$	315	321	351	325	big
$m_{\widetilde{b}_L}$	266	276	307	264	big
$m_{\widetilde{b}_R}$	303	303	309	328	big
$m_{\widetilde{\ell}_R}$	207	204	280	437	big
$m_{\widetilde{\ell}_L}$	216	229	305	313	big
$m_{\widetilde{\chi}_1^0}$	44.5	12.2	189	174.17	303.09
$m_{\widetilde{\chi}_2^0}$	97.0	93.6	235	298	337
$m_{\widetilde{\chi}_1^\pm}$	96.4	90.0	240	174.57	303.33
$m_{\widetilde{\chi}_2^\pm}$	275	283	291	311	big
m_{h^0}	67	67	68	70	82

Table 2: Sparticle masses for the Snowmass comparison point.

- In **200**: $e^+e^- \to \widetilde{\chi}_1^+\widetilde{\chi}_1^-$ allowed at $\sqrt{s}=500$ GeV NLC, but hard to see since (invisible) $\widetilde{\chi}_1^0$ would take all of $\widetilde{\chi}_1^\pm$ energy. $\Rightarrow$ use $e^+e^- \to \gamma\widetilde{\chi}_1^+\widetilde{\chi}_1^-$ which is ok at $\sqrt{s}=500$ GeV.
- The O-II model with δ_{GS} near $-4 \Rightarrow m_{\widetilde{\chi}_1^\pm}, m_{\widetilde{\chi}_1^0} \sim m_{\widetilde{g}}$ and $e^+e^- \to \widetilde{\chi}_1^+\widetilde{\chi}_1^-, \widetilde{\chi}_1^0\widetilde{\chi}_1^0$ *not* kinematically allowed. SM-like h^0 = only SUSY 'signal'.

- At the LHC, $\tilde{g}\tilde{g}$ at Snowmass point $\Rightarrow$

$$\mathbf{1}: \ \tilde{g} \stackrel{90\%}{\to} \tilde{b}_L\overline{b} \stackrel{99\%}{\to} \widetilde{\chi}_2^0 b\overline{b} \stackrel{33\%}{\to} \widetilde{\chi}_1^0(e^+e^- \text{ or } \mu^+\mu^-)b\overline{b}$$
$$\stackrel{8\%}{\to} \widetilde{\chi}_1^0\nu\overline{\nu}b\overline{b}$$
$$\stackrel{38\%}{\to} \widetilde{\chi}_1^0 q\overline{q}b\overline{b}$$
$$\stackrel{8\%}{\to} \widetilde{\chi}_1^0 b\overline{b}b\overline{b}$$
$$\mathbf{24}: \ \tilde{g} \stackrel{85\%}{\to} \tilde{b}_L\overline{b} \stackrel{70\%}{\to} \widetilde{\chi}_2^0 b\overline{b} \stackrel{99\%}{\to} h^0\widetilde{\chi}_1^0 b\overline{b} \stackrel{28\%}{\to} \widetilde{\chi}_1^0 b\overline{b}b\overline{b}$$
$$\stackrel{69\%}{\to} \widetilde{\chi}_1^0\widetilde{\chi}_1^0\widetilde{\chi}_1^0 b\overline{b}$$

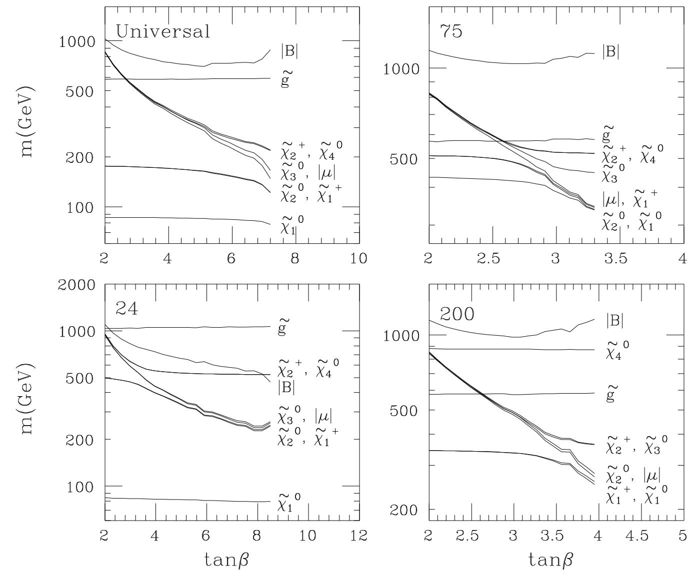

Figure 1: Physical (pole) gaugino masses as a function of $\tan\beta$ for the **1** (universal), **24**, **75**, and **200** F representation choices. Also shown are $|B|$ and $|\mu|$. We take $m_0 = 1$ TeV and $M_a(M_U) = m_{1/2} = 200$ GeV times number appearing in Table 1.

$$
\begin{aligned}
\mathbf{75}: \ \tilde{g} &\stackrel{43\%}{\rightarrow} \widetilde{\chi}^0_1 g \text{ or } \widetilde{\chi}^0_1 q\overline{q} \\
&\stackrel{10\%}{\rightarrow} \widetilde{\chi}^0_1 b\overline{b} \\
&\stackrel{20\%}{\rightarrow} \widetilde{\chi}^0_2 g \text{ or } \widetilde{\chi}^0_2 q\overline{q} \\
&\stackrel{10\%}{\rightarrow} \widetilde{\chi}^0_2 b\overline{b} \\
&\stackrel{17\%}{\rightarrow} \widetilde{\chi}^\pm_1 q\overline{q} \\
\mathbf{200}: \ \tilde{g} &\stackrel{99\%}{\rightarrow} \tilde{b}_L\overline{b} \stackrel{100\%}{\rightarrow} \widetilde{\chi}^0_1 b\overline{b} \\
\mathrm{O-II}: \ \tilde{g} &\stackrel{51\%}{\rightarrow} \widetilde{\chi}^\pm_1 q\overline{q} \\
&\stackrel{17\%}{\rightarrow} \widetilde{\chi}^0_1 g \\
&\stackrel{26\%}{\rightarrow} \widetilde{\chi}^0_1 q\overline{q} \\
&\stackrel{6\%}{\rightarrow} \widetilde{\chi}^0_1 b\overline{b}
\end{aligned}
$$

– **1**: $\not{E}_T$, $\ell^+\ell^-$, $4b$'s;

– **24**: $\not{E}_T$, no $\ell^+\ell^-$, $8b$'s, with 2 pairs having mass m_{h^0}.

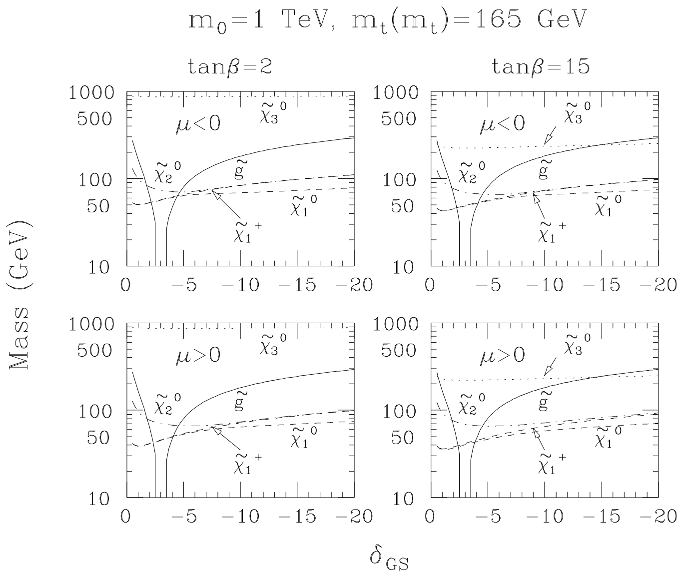

Figure 2: $m_{\widetilde{\chi}_1^0}$, $m_{\widetilde{\chi}_2^0}$, $m_{\widetilde{\chi}_3^0}$, $m_{\widetilde{\chi}_1^+}$, and $m_{\widetilde{g}}$ as functions of δ_{GS} at $\tan\beta = 2, 15$ for $\mu > 0$ and $\mu < 0$.

- **75**: traditional signals;
- **200**: $\not\!\!E_T$, $4b$'s, no leptons;
- O-II: $\tilde{g} \to \widetilde{\chi}_1^\pm, \widetilde{\chi}_1^0$ + soft and $\widetilde{\chi}_1^\pm \to \widetilde{\chi}_1^0$ + very soft; need soft jet cuts $\to$ sensitivity reduced, but not zero.

Low $m_{\widetilde{g}}$ $\Rightarrow$ spectrum end-points give mass differences (O-II hard).

- Very generally, distinguishing scenarios should be very easy.
- $M_2 < M_1$ scenarios $\Rightarrow$ new dark matter phenomenology:
  - For preferred $|\delta_{GS}|$ in O-II model, $\widetilde{\chi}_1^0\widetilde{\chi}_1^0$ annihilation is small — $\widetilde{\chi}_1^0 \sim$ pure SU(2) gaugino $\to$ weak couplings to h^0 and Z (higgsino component required) and sfermions very heavy.
  - $m_{\widetilde{\chi}_1^\pm} \simeq m_{\widetilde{\chi}_1^0} \Rightarrow$ similar $\widetilde{\chi}_1^\pm, \widetilde{\chi}_1^0$ densities (due to very similar Boltzmann factors) at freeze-out $\to$ $\widetilde{\chi}_1^0\widetilde{\chi}_1^\pm$ co-annihilation $\to$ greatly reduced relic density.

Non-Universal Scalar Masses

- D-terms from new chiral $\Phi, \overline{\Phi}$ (SM singlets):

$$V = V_0 + m^2|\Phi|^2 + \overline{m}^2|\overline{\Phi}|^2 + \frac{g_X^2}{2}\left[|\Phi|^2 - |\overline{\Phi}|^2 + X_i|\phi_i|^2\right]^2$$

  $\Rightarrow \Delta m_i^2 \sim X_i D_X$ $(D_X \sim m_Z^2)$

  Example is gauged $B-L$ with $X = -\frac{5}{3}(B-L) + \frac{4}{3}Y$.

- Yukawa influences:

  SUSY-breaking scalar masses at M_U are influenced by the Yukawa couplings of the corresponding quarks/leptons. Example: Hall/Randall, perturbing about $[U(3)]^5$ symmetry present in absence of Yukawa couplings $\Rightarrow$

$$m^2_{\widetilde{Q}} = m_0^2(I + c_Q\lambda_u^\dagger\lambda_u + c'_Q\lambda_d^\dagger\lambda_d + \ldots) \tag{0.6}$$

$$m^2_{\widetilde{U}^c} = m_0^2(I + c_U\lambda_u\lambda_u^\dagger + \ldots) \tag{0.7}$$

$$m^2_{\widetilde{D}^c} = m_0^2(I + c_D\lambda_d\lambda_d^\dagger + \ldots) \tag{0.8}$$

  Q = squark partners of left-handed quark doublets, U^c (D^c) = partners of left-handed up (down) antiquarks. The m^2's, I and λ_u, λ_d are 3×3 matrices in generation space, the latter containing the Yukawa couplings. The $\ldots = \mathcal{O}(\lambda^4)$ and higher. A, c_Q, c'_Q, c_U and $c_D \sim$ same $\Rightarrow \lambda_t$ dominates $\rightarrow$ primary deviations in $m^2_{\tilde{t}_L}$, $m^2_{\tilde{b}_L}$ (equally and in the same direction) and $m^2_{\tilde{b}_R}$.

  $\Rightarrow m^2_{\tilde{t}_L}$ and $m^2_{\tilde{b}_L}$ are equally shifted

  Differs from A terms that mix the Q and U^c, D^c squark fields, with

$$A_U = A_0(\lambda_u + \ldots)\,, \quad A_D = A_0(\lambda_d + \ldots)\,, \tag{0.9}$$

where A_U (A_D) describes $Q - U^c$ ($Q - D^c$) mixing.

$\Rightarrow \tilde{t}_L - \tilde{t}_R$ mixing $\rightarrow m_{\tilde{t}_1} < m_{\tilde{b}_1}$.

- F-vev dominance:

$$\mathcal{L} \propto \frac{\langle F_\Phi F_\Phi \rangle_{ij}}{M^2_{\rm Planck}} \phi_i^\dagger \phi_j \, . \tag{0.10}$$

  $\phi_{i,j}$ = scalar fields.

  Since the (left-handed) SM fermion and antifermion scalar fields $\in$ $\overline{\mathbf{5}}, \mathbf{10}$ but $H_1, H_2 \in \mathbf{5}$, $\Rightarrow$

  $\mathbf{R_\Phi} \times \mathbf{R_\Phi}$ must overlap $\mathbf{10} \times \overline{\mathbf{10}} = \mathbf{1} \oplus \mathbf{24} \oplus \mathbf{75}$ and $\mathbf{5} \times \overline{\mathbf{5}} = \mathbf{1} \oplus \mathbf{24}$.

  For example, $\mathbf{R_\Phi} = \mathbf{1}$ and $\mathbf{R_\Phi} = \mathbf{24}$ are ok; a single F_Φ could simultaneously $\rightarrow$ both gaugino and squark soft mass terms.

  - $\mathbf{1} \Rightarrow$ universal scalar masses.
  - $\mathbf{24} \Rightarrow$ non-universality.

- No time to discuss phenomenology of all these different cases, but signals can change dramatically and we should have good chance to sort things out if event rates are high enough.

$\not{R}$

- Hard: $W_{\not{R}} = \lambda_{ijk}(\widehat{L}_i\widehat{L}_j)\overline{\widehat{E}}_k + \lambda'_{ijk}(\widehat{L}_i\widehat{Q}_j)\overline{\widehat{D}}_k + \lambda''_{ijk}\overline{\widehat{U}}_i\overline{\widehat{D}}_j\overline{\widehat{D}}_k \Rightarrow$
  - $\lambda, \lambda' \Rightarrow \not{L}$; $\lambda'' \Rightarrow \not{B}$.
  - $\not{B} = 0 \Rightarrow \lambda, \lambda' \neq 0$ and $\lambda'' = 0$ or vice versa.
  - Otherwise, current constraints not strong: λ's $\lesssim 0.1 - 0.01$.
  - Unless λ's are *very* small, $\widetilde{\chi}^0_1$ decays inside the detector (no $\not{E}_T$)

LHC:

- If $\lambda'' \neq 0$, $\widetilde{\chi}^0_1 \to 3j \Rightarrow$ need like-sign dilepton signal from $\widetilde{\chi}^\pm_1$ decays = ok unless $m_{\widetilde{\chi}^\pm_1} \sim m_{\widetilde{\chi}^0_1}$ (= **very** bad LHC case).
- If $\lambda \neq 0$, $\widetilde{\chi}^0_1 \to \mu^\pm e^\mp \nu, e^\pm e^\mp \nu \Rightarrow$ very distinctive leptonic signals.
- If $\lambda' \neq 0$, $\widetilde{\chi}^0_1 \to \ell 2j$ again $\Rightarrow$ leptonic signals.

NLC:

- $\widetilde{\chi}^0_1\widetilde{\chi}^0_1 \to \underbrace{(3j)(3j)}_{\lambda''\neq 0}, \quad \underbrace{(2\ell\nu)(2\ell\nu)}_{\lambda\neq 0}, \quad \underbrace{(\ell 2j)(\ell 2j)}_{\lambda'\neq 0}$ all ok.

HERA:

- λ'_{121} or λ'_{131} near upper limits could yield lepto-quark type signal. Implications for Drell-Yan Tevatron data, ...

  More precisely: to explain HERA excess, need $\lambda'_{1j1} \sim 0.04/\sqrt{BF_{ed}}$ where $BF_{ed} = BF(\tilde{q}_j \to e^+ d)$ and $j = 2(\tilde{c}_L)$ or $3(\tilde{t}_L)$ (note L's required because of superpotential form). Meanwhile, atomic parity violation limits one to $|\lambda'_{1j1}| \lesssim 0.055(\tilde{q}_L/200 \text{ GeV})$. Combining, we require $BF_{ed} \gtrsim 0.3 - 0.5$.

However, the Tevatron requires $BF_{ed} \lesssim 0.5$ (no problem if there are some R-parity conserving decays of the squark), which is just on boundary of what is allowed above.

NLC, MC:

– $\lambda \neq 0 \Rightarrow$ possibility of $e^+e^- \to \tilde{\nu}_\tau$ (λ_{131}) and/or $\tilde{\nu}_\mu$ (λ_{121}) and $\mu^+\mu^- \to \tilde{\nu}_\tau$ (λ_{232}) and/or $\tilde{\nu}_e$ (λ_{122}). Some details include:

  * Lightest $\tilde{\nu}$ probably $\tilde{\nu}_\tau$, for which limits on λ_{131} and λ_{232} are relatively weak, $\lambda \lesssim 0.1$.
  * $\lambda_{121} \lesssim 0.04$ and $\lambda_{212} \lesssim 0.04$ limits are not much stronger.
  * Scenarios for decay are:
    · $\tilde{\nu}_\ell \to \nu_\ell \widetilde{\chi}^0_1$ if $m_{\widetilde{\chi}^0_1} < m_{\tilde{\nu}}$ (with $\widetilde{\chi}^0_1$ in turn decaying via virtual $\tilde{\nu}$'s);
    · $\tilde{\nu}_\ell \to \ell^{+\prime}\ell^{-\prime}$ (if $\lambda' \ll \lambda$);
    · $\tilde{\nu}_\ell \to q\overline{q}$ (if $\lambda \ll \lambda'$).
  * Cross section depends on $\Gamma^{\rm tot}_{\tilde{\nu}}$ vs. $\sigma_{\sqrt{s}}$ (the Gaussian width in $\sqrt{s}$): $\Rightarrow$ substantial sensitivity, especially if $\Gamma^{\rm tot}_{\tilde{\nu}}$ is small and $\sigma_{\sqrt{s}}$ is comparable or smaller.
  * In most likely case, LHC and/or normal NLC data show $\not{R}$ and $\Rightarrow$ some knowledge of $m_{\tilde{\nu}}$.

    But, *actual magnitude of λ and λ' will not be easily extracted.*

  MC technique depends upon R and $\Gamma^{\rm tot}_{\tilde{\nu}}$.

– One example:

  $\lambda' = 0$, $\lambda = 0.1$, $m_{\tilde{\nu}} = 100$ GeV, $m_{\widetilde{\chi}^0_1} = 90$ GeV ($\tilde{\nu} \to \nu\widetilde{\chi}^0_1$ decay allowed), $\Gamma^{\rm tot}_{\tilde\nu}=0.051$ GeV.

* For this case, $R=0.003\%\Rightarrow$ best results — correspondingly assume $L=0.1~{\rm fb}^{-1}$/yr, reduced by $\epsilon=0.5$ efficiency factor.
* $\Rightarrow\tilde\nu$ is observable at $S/\sqrt{B}=3$ level if accumulate $L=0.0008~{\rm fb}^{-1}$ at $\sqrt{s}=m_{\tilde\nu}$. To scan 1 GeV interval (expected NLC uncertainty) requires ~ 20 settings, or $L=0.0168~{\rm fb}^{-1}$ (a fraction of a year).
* Then, center and scan $\tilde\nu$ peak with $L=0.1~{\rm fb}^{-1}$,

  $\Rightarrow$ about $L=0.05~{\rm fb}^{-1}$ equivalent on-peak measurement of $\mu^+\mu^-\to\tilde\nu\to\mu^+\mu^-$ rate $\propto[BF(\tilde\nu\to\mu^+\mu^-)]^2$ — $S=1.23\times10^6$, $B=1.28\times10^3\to$ accuracy systematics dominated, lets say $\pm5\%$.

  $\Rightarrow$ very accurate determination of $\Gamma^{\rm tot}_{\tilde\nu}$ since $\sigma_{\sqrt{s}}\sim0.002$ GeV $\ll\Gamma^{\rm tot}_{\tilde\nu}$ — lets say $\pm5\%$ (must run program still).
* $\lambda^4\propto[\Gamma^{\rm tot}_{\tilde\nu}]^2[BF(\tilde\nu\to\mu^+\mu^-)]^2$ determination to $\lesssim\pm10\%$, corresponding to λ determination to $\lesssim\pm2.5\%$!!

– Much worse $\sigma_{\sqrt{s}}$ ($R\sim3\%$ effectively) at e^+e^- collider implies really need the much higher luminosity possible for interaction region especially designed for high $\mathcal{L}$ at low $\sqrt{s}$.

- Soft: $W_{\not R}=\mu_i\widehat{L}_i\widehat{H}_1\Rightarrow$
  - B conserved automatically;
  - $\widetilde\chi^0_1\to\ell+\ldots\Rightarrow$ good LHC,NLC,MC signals;
  - ν masses generated.
- Dark Matter??: = neutrinos? (but then only hot).

Event-Motivated Models (non-GMSB)

- CDF $ee\gamma\gamma$ event $= \tilde{e}\tilde{e}$, $\widetilde{\chi}_1^+\widetilde{\chi}_1^-$, ... production? (Kane *et al.*):

$\tilde{e}\tilde{e}$

If $\widetilde{\chi}_2^0 \to \gamma\widetilde{\chi}_1^0$ (1-loop) *and* $BF(\tilde{e} \to e\widetilde{\chi}_2^0) \gg BF(\tilde{e} \to e\widetilde{\chi}_1^0)$, $\Rightarrow$

$$\tilde{e}\tilde{e} \to (e\widetilde{\chi}_2^0)(e\widetilde{\chi}_2^0) \to (e\gamma\widetilde{\chi}_1^0)(e\gamma\widetilde{\chi}_1^0)$$

Only way to get $m_{\widetilde{\chi}_2^0} - m_{\widetilde{\chi}_1^0} \gtrsim 20$ GeV (required by observed E_γ) and suppress tree-level $\widetilde{\chi}_2^0$ decay graphs is

$$\widetilde{\chi}_2^0 = \tilde{\gamma} \quad \text{and} \quad \widetilde{\chi}_1^0 = \text{higgsino}$$

This requires: $M_1 \sim M_2 \quad 1 \lesssim \tan\beta \lesssim 3 \quad |\mu| < M_{1,2} \quad \mu < 0.$

This + kinematics and cross section requirements $\Rightarrow$

Table 3: Masses in the $\tilde{e}_L\tilde{e}_L$ and $\tilde{e}_R\tilde{e}_R$ scenarios for the $e^+e^-\gamma\gamma + \not{E}_T$ CDF event obtained by requiring $BF(\tilde{e}\tilde{e} \to e^+e^-\gamma\gamma\widetilde{\chi}_1^0\widetilde{\chi}_1^0) \geq 0.5$ and $\sigma(\tilde{e}\tilde{e}) \times BF \geq 4$ fb.

$\tilde{e}_L$	$\tilde{e}_R$
$100 \lesssim m_{\tilde{e}_L} \lesssim 130$ GeV	$100 \lesssim m_{\tilde{e}_R} \lesssim 122$ GeV
$50 \lesssim M_1 \lesssim 92$ GeV	$60 \lesssim M_1 \lesssim 85$ GeV
$50 \lesssim M_2 \lesssim 105$ GeV	$40 \lesssim M_2 \lesssim 85$ GeV
$0.75 \lesssim M_2/M_1 \lesssim 1.6$	$0.6 \lesssim M_2/M_1 \lesssim 1.15$
$-65 \lesssim \mu \lesssim -35$ GeV	$-60 \lesssim \mu \lesssim -35$ GeV
$0.5 \lesssim |\mu|/M_1 \lesssim 0.95$	$0.5 \lesssim |\mu|/M_1 \lesssim 0.8$
$1 \lesssim \tan\beta \lesssim 3$	$1 \lesssim \tan\beta \lesssim 2.2$
$33 \lesssim m_{\widetilde{\chi}_1^0} \lesssim 55$ GeV	$32 \lesssim m_{\widetilde{\chi}_1^0} \lesssim 50$ GeV
$58 \lesssim m_{\widetilde{\chi}_2^0} \lesssim 95$ GeV	$60 \lesssim m_{\widetilde{\chi}_2^0} \lesssim 85$ GeV
$88 \lesssim m_{\widetilde{\chi}_3^0} \lesssim 105$ GeV	$88 \lesssim m_{\widetilde{\chi}_3^0} \lesssim 108$ GeV
$100 \lesssim m_{\widetilde{\chi}_4^0} \lesssim 145$ GeV	$110 \lesssim m_{\widetilde{\chi}_4^0} \lesssim 132$ GeV
$62 \lesssim m_{\widetilde{\chi}_1^\pm} \lesssim 95$ GeV	$65 \lesssim m_{\widetilde{\chi}_1^\pm} \lesssim 90$ GeV
$100 \lesssim m_{\widetilde{\chi}_2^\pm} \lesssim 150$ GeV	$100 \lesssim m_{\widetilde{\chi}_2^\pm} \lesssim 125$ GeV

♡ At the Tevatron with current $L = 100$ pb^{-1} of data:

$u\overline{d} \to W^{+\star} \to \tilde{e}_L \tilde{\nu}_L \to (e\gamma\widetilde{\chi}_1^0)(e\widetilde{\chi}_1^{\pm}) \to e\gamma e W^{\star} + \not{E}_T$ ... events. For either $\tilde{e}_L\tilde{e}_L$ or $\tilde{e}_R\tilde{e}_R$ interpretation of $e^+e^-\gamma\gamma + \not{E}_T$ event one finds:

$$N(2\ell + X + \not{E}_T) \geq 30 \quad N(\gamma\gamma + X + \not{E}_T) \geq 2$$

$$N(\ell\gamma + X + \not{E}_T) \geq 15 \quad N(2\ell\gamma + X + \not{E}_T) \geq 4$$

$$N(\ell 2\gamma + X + \not{E}_T) \geq 2 \quad N(3\ell + X + \not{E}_T) \geq 2$$

♡ At LEP190 with $L = 500$ pb^{-1}:

$$N(2\ell + X + \not{E}_T) \geq 50 \quad N(2\gamma + X + \not{E}_T) \geq 3$$

plus, for $\tilde{e}_R\tilde{e}_R$ explanation of CDF event only,

$$N(\ell\gamma + X + \not{E}_T) \geq 5 \quad N((2\ell\gamma + X + \not{E}_T) \geq 5$$

♡ At LEP161 with $L = 25$ pb^{-1}:

$\tilde{e}_R\tilde{e}_R$ interpretation of CDF event $\Rightarrow$

$$N(\ell\gamma + X + \not{E}_T) \geq 2$$

In above, X =additional leptons,photons,jets.

To distinguish $\tilde{e}_L\tilde{e}_L$ from $\tilde{e}_R\tilde{e}_R$ look for $\tilde{e}_L\tilde{\nu}_L$, which must also be present if $\tilde{e}_L$ is light. With $\tilde{\nu}_L \to e\widetilde{\chi}_1^{\pm}$ and $\widetilde{\chi}_1^{\pm} \to W^{\star}\widetilde{\chi}_1^0 \Rightarrow ee\gamma W^{\star} + \not{E}_T$ events excess.

♡ Are there hints in 161 and 172 GeV ($L = 10$ pb^{-1} each) data?

- The 4 experiments report 6 events for $e^+e^- \to \gamma\gamma + \not{E}_T$ with $\not{M} > m_Z + 10$ GeV.

  These would be from $e^+e^- \to \widetilde{\chi}_2^0(\to \gamma\widetilde{\chi}_1^0)\widetilde{\chi}_2^0(\to \gamma\widetilde{\chi}_1^0)$. For $m_{\widetilde{\chi}_2^0} - m_{\widetilde{\chi}_1^0} > 20$ GeV (for CDF event kinematics), the signal has $E_\gamma > 8$ GeV, whereas background peaks at 0. With cut at $E_\gamma > 8$ GeV, only 1.3 bkgnd evts. expected for $\not{M} > m_Z + 20$ GeV, which is where entire signal would be since $\not{M} \geq 2m_{\widetilde{\chi}_1^0} \sim 100$ GeV.

- A problem is that dozens of $e^+e^- \to \widetilde{\chi}_1^0\widetilde{\chi}_3^0$ events should have been present, but they were not observed. To avoid observation, one can take

$$m_{\widetilde{\chi}_3^0} \gtrsim m_{\widetilde{\chi}_1^\pm} > m_{\tilde{\nu}} > m_{\widetilde{\chi}_1^0}.$$

  * $\tilde{\nu}\tilde{\nu}$ production is unobservable since $\tilde{\nu} \to \nu\widetilde{\chi}_1^0$ is invisible and $BF(\tilde{\nu} \to \nu\widetilde{\chi}_2^0(\to \gamma\widetilde{\chi}_1^0))$ is small.
  * $\widetilde{\chi}_3^0 \to \tilde{\nu}\nu$ (which is dominant) is then also invisible.
  * This scenario leads to $e^+e^- \to \gamma + \not{E}_T$ events via $\widetilde{\chi}_2^0(\to \gamma\widetilde{\chi}_1^0)\widetilde{\chi}_3^0$ production. 2 of the 4 experiments show an interesting excess over bckgnd. in the high $\not{M} > m_{\widetilde{\chi}_1^0} + m_{\tilde{\nu}}, 2m_{\tilde{\nu}}$ region required.
  * For charginos, we have $\widetilde{\chi}_1^+\widetilde{\chi}_1^-$ production with $\widetilde{\chi}_1^\pm \to \ell^\pm\tilde{\nu}$ with very soft ℓ's, requiring tricky search.

This scenario is also good for $b \to s\gamma$ and R_b.

- <u>CDF (event A and B) and D0 'di-lepton top events' that don't look like top events (Barnett and Hall):</u>

  Distributions for top $\rightarrow$ very low probability (Fig.).

  Explanation?: $\tilde{q} \rightarrow q\widetilde{\chi} \rightarrow q(\nu\tilde{\ell})$ with $\tilde{\ell} \rightarrow \ell\widetilde{\chi}_1^0$, where $\widetilde{\chi} = \widetilde{W}_3, \widetilde{W}^{\pm}$.

  Requires (kinematics + cross section):

$$\begin{array}{ll} m_{\tilde{g}} \simeq 330 & m_{\tilde{q}} \simeq 310 \\ m_{\tilde{\ell}_L} \simeq 220 & m_{\tilde{\nu}_L} \sim 220 \\ m_{\tilde{\ell}_R} \simeq 130 & \mu \sim -400 \\ M_1 \simeq 50 & M_2 \simeq 260 \end{array}$$

  Note inconsistency with $ee\gamma\gamma$ explanation.

- Both the above require non-universal gauginos masses and the small μ value in Kane requires $m_{H_1}^2 \neq m_{\tilde{q},\tilde{\ell}}^2$ soft mass non-universality.

- <u>Four-Jet 'Signal' at ALEPH (Carena *et al.* sample interpretation):</u>

  Observation of 4-jet signal with $M + M' \sim 106$ GeV and $M - M' \sim 10$ GeV, *i.e.* $M \sim 58, M' \sim 48$ GeV, significant 'rapidity-weighted' jet charge and no b jets is interpreted as $\tilde{e}_L\tilde{e}_R$ production with $\tilde{e}_L, \tilde{e}_R \rightarrow 2j$ via $R\!\!\!/$ coupling $W_{R\!\!\!/} \ni \lambda'_{ijk}(\widehat{L}^i\widehat{Q}^j)_L\widehat{\overline{D}}_R^k$.

  Points:

  - $\tilde{e}_L\tilde{e}_L$ and $\tilde{e}_R\tilde{e}_R$ production are β^3 suppressed whereas $\tilde{e}_L\tilde{e}_R$ is $\propto \beta$ $\Rightarrow \tilde{e}_L\tilde{e}_R$ dominance ok.
  - Production is via neutralino exchange: keeping only $\widetilde{\chi}_1^0 \sim \widetilde{B}$,

$$\frac{d\sigma}{dt}(e^+e^- \rightarrow \tilde{e}_R^{\pm}\tilde{e}_L^{\mp}) = \frac{g^4 \tan\theta_W^4}{64\pi s}\frac{M_1^2}{(t - M_1^2)^2}$$

and $M_1 \lesssim 100$ GeV is required for $\sigma \sim 1-2$ pb needed.

– For $M_1 \sim 80-100$ GeV, $\tilde{e}_L\tilde{e}_L, \tilde{e}_R\tilde{e}_R$ are suppressed also by destructive interference between γ, Z exchange and t-channel $\widetilde{\chi}^0_1$ exchange. To suppress $\tilde{e}\tilde{\nu}_{e\,L}$ production need largest $m_{\tilde{\nu}_L}$ possible: $m^2_{\tilde{\nu}_L} = m^2_{\tilde{e}_L} + (1-\sin\theta^2_W)\cos 2\beta m^2_Z \Rightarrow$ choose $\tan\beta \sim 1$. This $\Rightarrow \lambda_t$ blowing up and other problems if evolve to M_U.

– For $\Gamma(\tilde{e}_L \to \overline{u}_j d_k) = \frac{3\lambda^2_{1jk}}{16\pi} m_{\tilde{e}_L}$ to dominate over more standard decays via W and $\widetilde{\chi}^0_1$ exchange to $ee\tilde{e}_R$, requires $\lambda_{1jk} \gtrsim \mathrm{few}\times 10^{-4}$ — no problem with bounds.

– $\tilde{e}_R$ decays by mixing to $\tilde{e}_L$: $\Rightarrow$ above width $\times \sin^2\phi$, ϕ= mixing angle.

$$\sin\phi \sim \frac{m_e(A-\mu\tan\beta)}{m^2_{\tilde{e}_L} - m^2_{\tilde{e}_R}} \sim \frac{A-\mu\tan\beta}{200\ \mathrm{GeV}} \times 10^{-4}$$

$\tilde{e}_R \to \overline{u}_j d_k$ wins over $\tilde{e}_R \to ee\overline{u}d$ from virtual $\widetilde{\chi}^0_1, \tilde{e}_L$ exchange if $\sin\phi \gtrsim 10^{-4}$.

– Displaced vertex might be observable:

$$(\beta c\tau)_{\tilde{e}_R} \sim \left(\frac{10^{-4}}{\sin\phi}\right)^2 \left(\frac{10^{-2}}{\lambda_{1jk}}\right)^2 50 \text{ to } 80\ \mu m.$$

– Absence of $\widetilde{\mu}$ and $\tilde{\tau}$ pair signals + no destructive t-channel diagrams in $e^+e^- \to \widetilde{\mu}\widetilde{\mu}, \tilde{\tau}\tilde{\tau} \Rightarrow$ heavier masses required for these. $\Rightarrow$ non-universality for slepton masses, since for universality $\tilde{\tau}_1$ would be the lightest slepton.

– Lots of stuff expected at $\sqrt{s} = 186$ GeV and $\sqrt{s} = 195$ GeV: for $M_1 = 100$ GeV, $m_{\tilde{\nu}_L} = 58$ and $\sqrt{s} = 186$ GeV,

$\sigma(\tilde{e}_L\tilde{e}_R, \tilde{e}_L\tilde{e}_L, \tilde{e}_R\tilde{e}_R, \tilde{\nu}_{e\,L}\tilde{\nu}_{e\,L}, \widetilde{\chi}^0_1\widetilde{\chi}^0_1) = 1.33, 0.23, 0.2, 0.29, 0.62$ pb

- Light gluino (Farrar . . .)

  =Direct opposite of the no-scale scenario:

$$M_i = A = 0, \quad m_0 \neq 0$$

  $M_i = 0$ can arise if the gauge kinetic function, f, in $\int f_{ab}(\Phi) W_a W_b d^2\theta$ is particularly trivial: e.g. it can be chosen to be independent of Φ, in which case the normal linear term in the expansion $f(\Phi) =\sim 1 + \Phi/M_{\rm Planck} + \ldots$ that we used earlier is absent. A is generated in a similar fashion and can also be 0. Thus, it is not unnatural for all dimension-3 SU$\not{S}$Y terms to be 0.

  Motivation: CP violation arising from phases in the SU$\not{S}$Y parameters will generically lead to large CP violation (*e.g.* NDM, EDM) from SUSY loops. The easy way to avoid this problem is to set enough of the SU$\not{S}$Y parameters to 0 so that all remaining phases (namely in μ and B) can be rotated away (by R and U(1) transformations) $M_i = A = 0$ is sufficient. (But, so are dilaton b.c. and no-scale b.c.)

  Basic features:

  - Gaugino masses arise at one loop.
  - Proper EWSB requires substantial sfermion and Higgs soft m_0's $(100 - 300$ GeV).
  - $\widetilde{\chi}^0_1 \sim \tilde{\gamma}$ is the LSP with $m_{\widetilde{\chi}^0_1} \sim 0.1 - 1.5$ GeV (from 1-loop quark-squark and wino/higgsino-Higgs/vector boson diagrams).
  - $m_{\tilde{g}} \sim 10 - 600$ MeV (1-loop quark-squark diagrams), but it forms bound states of mass $> m_{\widetilde{\chi}^0_1}$: $R_0 = (\tilde{g}g)$, $S_0 = (\tilde{g}uds)$ with masses ~ 1.5 GeV (lattice estimates). There is also a $(\tilde{g}\tilde{g})$ state: enough

ambiguous states exist in $\eta', \ldots$ (*e.g.* $\eta(1410)$) spectroscopy that such a state would be helpful.

– proper EWSB requires $\mu \lesssim 100$ GeV and $\tan\beta \lesssim 2$.

–
$$m^2_{\widetilde{\chi}^\pm_{1,2}} = \frac{1}{2}\left[\mu^2 + 2m_W^2 \pm \sqrt{\mu^4 + 4m_W^4\cos^2 2\beta + 4m_W^2\mu^2}\right]$$
$\Rightarrow m_{\widetilde{\chi}^\pm_1} \leq m_W$; $m_{\widetilde{\chi}^\pm_1} \to m_W$ for small μ, decreasing as μ increases.

– If $\mu \ll m_W$ then $\widetilde{\chi}^0_2 =$ higgsino and $m_{\widetilde{\chi}^0_2} \sim \mu$; $m_{\widetilde{\chi}^0_3} \sim m_{\widetilde{\chi}^0_4} \sim m_Z$. At larger μ, $m_{\widetilde{\chi}^0_3}$ declines below m_Z.

Phenomenology:

– R_0 is long-lived: $\tau \gtrsim 10^{-10}$s. So R_0 energy is degraded (it has a strong-interaction σ and thus degradation occurs over $10-15$cm) before decay, implying that beam dump and missing energy limits (which assume prompt decay transmits most of the original R_0 energy to the $\widetilde{\chi}^0_1$) are not applicable.

  In short, a produced $\tilde{g}$ acts much like a jet.

– $\widetilde{\chi}^0_1 = \tilde{\gamma}$ implies $Z \to \widetilde{\chi}^0_1\widetilde{\chi}^0_1$ and $Z \to \widetilde{\chi}^0_1\widetilde{\chi}^0_2$ are small.

– Largest e^+e^- couplings are to $\widetilde{\chi}^+_1\widetilde{\chi}^-_1$, $\widetilde{\chi}^0_2\widetilde{\chi}^0_2$, $\widetilde{\chi}^0_2\widetilde{\chi}^0_3$ and $\widetilde{\chi}^0_2\widetilde{\chi}^0_4$ pair production.

– Non-observation of $Z \to \widetilde{\chi}^+_1\widetilde{\chi}^-_1$ and $Z \to \widetilde{\chi}^0_2\widetilde{\chi}^0_2$ places lower bounds of $m_{\widetilde{\chi}^\pm_1} \gtrsim 47$ GeV and $m_{\widetilde{\chi}^0_2} \gtrsim$ a $\tan\beta$-dependent lower bound. As a result, $\mu \lesssim 87$ GeV and $0.46 \lesssim \tan\beta \lesssim 1.8$ is required.

– Since $\tan\beta$ is near 1, must have big $m_{\tilde{t}}$ to get m_{h^0} above current limits, $\Rightarrow$ large non-universality in m_0's and other non-standard b.c.'s.

– At $\sqrt{s} = 183$ GeV, the minimum $\sigma(e^+e^- \to \widetilde{\chi}^0\widetilde{\chi}^0 + \widetilde{\chi}^+\widetilde{\chi}^-)$ is $\sim$ 2 pb. Signals depend somewhat on whether R-parity is violated or not. Still, existing and soon available data should find an anomaly in final state.

– Interpretation of ALEPH events as $\widetilde{\chi}_1^+\widetilde{\chi}_1^-$ with $\widetilde{\chi}_1^\pm \to q'\tilde{q}^* \to q'q\tilde{g}$ and $m_{\widetilde{\chi}_1^\pm} \sim 53$ GeV (two soft jets missed in jet reconstruction) questionable in light of other experiments.

– Hadronic $2j$ and $4j$ event shapes in Z decay constrain running of α_s via $b_0 = (11/6)C_A/C_F - (2/3)n_f T_F/C_F$. A light $\tilde{g}$ acts like 3 new flavors, *i.e.* would increase n_f from ~ 5 to ~ 8. Analysis is in controversial state with Farrar claiming that theoretical uncertainties (associated with ALEPH analysis) are large enough that n_f is poorly determined and a light $\tilde{g}$ is only slightly disfavored.

– $\widetilde{\chi}_1^0$ relic abundance can be ok for dark matter if $m_{\widetilde{\chi}_1^0} \geq m_{R_0}/1.8$.

– Beams designed for K's (FNAL *e.g.*) contain R_0's. For some range of parameters, $R_0 \to \pi^+\pi^-\widetilde{\chi}_1^0$ occurs rapidly enough to appear in detectors, but is hard to see given above dark matter mass relation — $\pi\pi$ mass is close to m_K implying large backgrounds. Of course the R_0 lifetime could also be sufficiently long as the escape the experiment.

– The S_0 can also be stable (if $m_{S_0} < m_p + m_e + m_{\widetilde{\chi}_1^0}$ and R-parity is ok). It could then provide an explanation for very high E cosmic rays.

- Experiments to detect stable or pseudo-stable R_0 and S_0 could be mounted. Technique would be to measure time of flight and kinetic energy (using a timed calorimeter). Then

$$m = KE[1/\sqrt{1-\beta^2} - 1]^{-1}.$$

  A low energy beam like that at BNL allows access to $m < 2$ GeV.

LSP=heavy gluino

In O-II model, for $\delta_{GS} \sim -3$ (the preferred value in the model), the gluino is the LSP. There is also a GMSB model by Raby in which this is the case. What is the phenomenology? What are the current limits? This subject is quite messy, and what I give below is in a state of flux.

Heavy stable particles with charge have been extensively discussed and there are many limits, but heavy stable neutral particles (with a strong-interaction-like cross section) have received limited attention. For a heavy gluino, the actual physical LSP would be either the $R_0 = (\tilde{g}g)$ or the $\tilde{\rho}^0 = (\tilde{g}[u\overline{u} - d\overline{d}])$, or really most likely a mixture of the usual type with multi g and $q\overline{q}$ components in the usual Fock space mixture picture.

We generically denote this particle by X. We assume that the charged versions of the X such $\tilde{\rho}^+$ (and baryonic equivalents) have short lifetimes.

Obvious limits derive from:

– mass spectrometer searches for heavy isotopes of H or O;

– accelerator fixed target searches for heavy new particles.

The latter have all focused on charged heavy particles, and we will thus ignore them.

If the neutral X binds to some charged nucleon or nucleus then limits will be strong if it is sufficiently abundant. Since our X has strong van der Waals forces, we expect such binding to occur. (Raby thinks

R_0 would bind more weakly than $\tilde{\rho}^0$, due to $m_{\rm glueball} \gg m_\pi \Rightarrow$ short range interaction for former; Fock space picture argues against such a clear distinction.)

I will review discussions by Starkman *et al.* and, more recently, by Mohapatra and Nussinov. Important ingredients in the limits are:

– the expected relic density.

Estimates by Mohapatra and Nussinov, using standard freeze-out arguments and $\sigma_{\rm an} \sim \alpha_s^2/M_X^2$, give a relic density of roughly $\frac{n_X}{n_B} \sim 10^{-3} M_X(\text{ TeV})$, whereas Raby says $\frac{n_X}{n_B} \sim 10^{-7} M_X(\text{ TeV})$. I have not had time to trace these calculations carefully to see where the difference lies. For relic densities a la Mohapatra,

$$\frac{n_X}{n_\gamma} \sim 5 \times 10^{-13} M_X(\text{ TeV}),$$

which converts to

$$\frac{\rho_X}{\rho_B} = \frac{n_X M_X}{n_B m_B} \sim \left(\frac{M_X}{1\text{ TeV}}\right)^2 .$$

Thus, something else would be needed for dark matter if $M_X \lesssim$ 1 TeV, the region we are considering.

– the extent to which the galactic halo is comprised of relic X's that have clustered into the halo.

Given that $M_X \lesssim 1$ TeV almost certainly implies that X's are not the dark matter, it seems unlikely that the halo is entirely made of X's. Even for M_X large enough to explain dark matter, very substantial gravitational clustering after freeze out is required for X's to be the halo. Starkman *et al.* limits assume the halo (which has $\rho = 0.4$ GeV/cm^3) is comprised of X's entirely.

– the elastic low-energy cross section, $\sigma_X(A)$. If the $X-A$ interaction is coherent on nuclei (2 gluon exchange?), then $\sigma_X(A) = A^2 m_r^2(A)/m_r^2(1)\sigma_X(p)$. This is the Starkman *et al.* choice. Mohapatra and Nussinov take $\sigma \sim \pi A^{2/3}\mathrm{fm}^2$, *i.e.* generally speaking much smaller.

Several experimental limits are crucial when $\sigma_X(p)$ is hadronic-like.

– Dark-matter balloon/mine detection experiments:

  Starkman *et al.* analysis finds that these require $\sigma_X(p) \geq 1 - 10$ mb for $M_X \leq 1$ TeV — larger $\sigma_X(p)$ results in large enough energy degradation before hitting detector that no signal is produced. Relic-like densities would give weaker limit.

  Mohapatra and Nussinov do not appear to take into account energy degradation (perhaps because of the smaller $\sigma_X(A)$ employed), and conclude that X's should have been seen for any M_X, even if X particles only have relic, rather than halo, density (see fluxes computed later).

– Capture and co-annihilation in the Earth (Starkman) (to produce ν's detected in proton decay detectors, at least as secondary products of primary annihilation) or capture and co-annihilation in the halo (MN) to produce energetic γ's that are detected:

  The rates depend upon the annihilation cross section and the fraction of the annihilation product energy appearing in the relevant channel, as well as whether or not the relevant density is halo or relic. For both types of observation, the conclusion seems to be that events would be likely to have been seen if the density is halo-like, but probably not if relic-like.

– Limits on heavy isotopes:

If the halo density is dominated by X's, and using velocity of movement of earth through the halo ($v_X \sim 2-3\times 10^7$ cm/s), the flux of X's from the galactic halo would be

$$\phi_X \sim 10^4 \frac{1\ \text{TeV}}{M_X} \text{cm}^{-2}\text{s}^{-1}.$$

For a strong cross section, these would accumulate in the ocean, probably binding to water molecules. Limits on such heavy water are (Mohapatra, Nussinov; Starkman *et al.* quote still stronger limits)

$$n_X/n_{\text{H}_20} \lesssim 3\times 10^{-15} M_X(\ \text{TeV})$$

to be compared to predicted ratio of

$$n_X/n_{\text{H}_20} \sim 3\times 10^{-14} \phi_X \frac{t_{\text{acc}}}{100\text{Myr}}$$

(assuming 10 km ocean depth and good mixing). Together these require

$$\phi_X \lesssim 0.1 M_X(\ \text{TeV}) \left(\frac{100\text{Myr}}{t_{\text{acc}}}\right).$$

Consistency of this limit with the predicted halo flux requires $M_X > 100$ TeV. If the X were to bind to H vs. O, then limits would be much stronger.

For relic density a la MN and using $n_\gamma \sim 300\text{cm}^{-3}$, we get $n_X \sim 2\times 10^{-10} M_X \text{cm}^{-3}$ and

$$\phi_X \sim n_X v_X \sim 6\times 10^{-3} M_X(\ \text{TeV})\text{cm}^{-2}\text{s}^{-1}.$$

This is no longer in conflict with heavy isotope limit on ϕ_X.

However, Raby argues that even for $n_X/n_B \sim 10^{-7} M_X(\text{ TeV})$ if the X's bind to hydrogen (which we are assuming is possible), then they are excluded. He claims that not all X's will have been reprocessed into stars and that the terrestrial abundance of XH bound states should be similar to the above relic abundance. Ocean analysis limits this ratio to $\lesssim 10^{-20}$ or better.

In summary, it appears that we can escape these types of limits for $M_X \lesssim 1$ TeV so long as the heavy gluino state is not responsible for the halo dark matter (as is consistent with its clearly not being responsible for all dark matter) and the X's were not captured into the earth at the same level as the relic abundance ratio.

What would be the signature of a X if produced at an accelerator? Well, as in light gluino case, we would want to look for a delayed calorimeter signal. As M_X increases, the KE as a fraction of M_X that appears in the calorimeter becomes smaller and smaller and to a large extent the X is simply stopped in the detector, its mass disappearing as missing energy. Stopping rate will depend upon the cross section size. A high luminosity, high energy $\sqrt{s} \gtrsim$ several TeV beam dump experiment, with mass spectrometer or chemical analysis of the dump could be used to rule out X's.

Hints from Higgs Limits, Precision Data and FCNC

General point: SUSY decouples for large SUSY masses ($\gtrsim 300$ GeV). $\Rightarrow$ SUSY can be as good as the SM.

Interesting question: can some sparticles be light?

- Higgs non-observation:

  For large m_{A^0}, m_{h^0} depends largely on $m_{\tilde{t}_2}$ (the mass of the heavier stop). For $\tan\beta \sim 1.5$, $m_{h^0} \gtrsim 60(80)$ GeV requires $m_{\tilde{t}_2} \gtrsim 300(400)$ GeV. For $\tan\beta \sim 10$, $m_{h^0} \gtrsim 60(80)$ GeV requires $m_{\tilde{t}_2} \gtrsim 150(200)$ GeV.

  Thus, $m_{\tilde{t}_2}$ cannot be too light.

- Oblique corrections to S, T, U:

  Large custodial SU(2) breaking via 3rd family sfermions is possible because $m_t \gg m_b$; e.g. for small mixing

$$m^2_{\tilde{t}_L} = m^2_{\tilde{q}_L} + m^2_t + (\tan^2\beta - 1)/(\tan^2\beta + 1)(m^2_Z - 4m^2_W)$$

$$m^2_{\tilde{b}_L} = m^2_{\tilde{q}_L} + m^2_b + (\tan^2\beta - 1)/(\tan^2\beta + 1)(m^2_Z + 2m^2_W)$$

  $\Rightarrow$ too large ΔT unless $m_{\tilde{q}_L} \gtrsim 300 - 400$ GeV. R sbottom and stop masses not constrained, nor are squarks of first two generations, nor are slepton soft masses.

  Since $\tilde{t}_2$ is normally mainly $\tilde{t}_L$, this is consistent with m_{h^0} limit needs.

  Non-zero mixing can reduce the lower bounds on soft masses from ΔT.

  There are no problems with $\sin^2\theta_{\text{eff}}$ in the $m_{h^0} \geq 60$ GeV domain. Constraints from m_W vs. m_t are even less constraining.

- Could one have $\tilde{t}$ of mass 200 GeV with large L component for HERA? This conflicts with ΔT unless there is large mixing to lower $m^2_{\tilde{t}_1}$ closer to $m^2_{\tilde{b}_L}$. This requires inverse hierarchy for m_U vs. m_Q soft masses. Using $m^2_{\tilde{t}_1} \sim m^2_Q + m^2_t(1 - \widetilde{A}^2_t/m^2_U)$ ($\widetilde{A}_t = A_t - \mu/\tan\beta$), we get smaller $m_{\tilde{t}_1}$ if $\widetilde{A}_t \sim m_U$, and $\tilde{t}_1$ is mainly L and light if $m_U \gg m_Q$ ($m_U \sim 2$ TeV is typically required). This looks pretty unnatural.

- $b \to s\gamma$ FCNC:

  SM predicts $BF(b \to s\gamma)$ a little too big compared to CLEO limits.

  If all sparticles heavy, then $m_{H^\pm} \sim m_{A^0} \gtrsim 500$ GeV required, since the $t - H^\pm$ loop increases BF.

  To get a negative correction, need a $\tilde{t}_R - \widetilde{\chi}^\pm_1$ loop with a light $\tilde{t}_R$ and a light $\widetilde{\chi}^\pm_1$ that is higgsino-like (so that coupling to $\tilde{t}_R$ is $\propto m_t$). This conflicts with HERA game where it is the $\tilde{t}_L$ that should be light — if both are light, then we are entering a region where m_{h^0} can fall below lower bound.

- $K - \overline{K}$ and $B - \overline{B}$ mixing etc.:

  $H^\pm - t$ and $\tilde{t} - \widetilde{\chi}^\pm_1$ boxes contribute. Is there room for a light $\tilde{t}_R$ and $\widetilde{\chi}^\pm_1$? In general, the answer is that there is some room: the η (phase) and ρ parameters of the CKM matrix would have to flex from SM values.

Gauge-Mediated SU$\not{S}$Y (GMSB) (Dine,Nelson, ..)

SUSY almost certainly = exact, local symmetry, as in strings. $\Rightarrow$ if not accidental, then spontaneously broken $\Rightarrow$ $\mathcal{L}_{\rm eff}$, with inverse mass scale characterized by 'hidden sector'.

♣ For gravity-mediated (super string) source of soft SU$\not{S}$Y masses, this scale is most naturally $\sim M_{\rm Planck}$.

$$\mathcal{L} = \int d^2\theta W_a W_a \frac{\Phi}{M_{\rm Planck}} + h.c. \sim \frac{\langle F_\Phi \rangle}{M_{\rm Planck}} \lambda_a \lambda_a \sim m_W \lambda_a \lambda_a \,,$$

requires

$$\langle F_\Phi \rangle \equiv m^2_{\rm S\not{U}SY} \sim m_W M_{\rm Planck} \sim (10^{10}~{\rm GeV})^2$$

FCNC Problem:

- Although gravity = 'flavor blind' argument suggests universal masses in this scenario, bad terms are possible in Kahler potential and (since not forbidden by symmetry) are generated at some level by radiative corrections, even if not present at tree-level.

- FCNC, $\not{L}$, *etc.* can arise from $M_S \to M_U$ evolution (if τ and t are in same multiplet above M_U), although $M_S \sim M_U$ is also not impossible non-perturbatively.

- Although EWSB semi-automatic from RGE's, it is not totally so.

♣ In GMSB, $M_{\rm Planck} \to M$ (M = mass scale of messenger sector) and $m^2_{\rm S\not{U}SY} \sim m_W M$ can be much lower — $m_{\rm S\not{U}SY} \sim 10 - 100$ TeV is often discussed. Popular realization is gauge-mediated picture:

- $\Rightarrow$ rather few parameters, at least in simplest incarnations.

Figure 3: Schematic of Gauge-mediated S$\not{U}$SY scenario.

General Features:

- SU$\not{S}$Y occurs in a 'hidden' sector and is communicated to a messenger sector.

- The messenger sector contains particles which transform under SU(3), SU(2) and U(1) that in turn communicate the SU$\not{S}$Y to the usual low-energy superpartners of the SM particles (*i.e.* the squarks, sleptons *etc.*) via normal gauge interactions.

- FCNC *etc.* problems solved since gauge interactions are flavor-blind and thus so are soft terms. Also soft masses are decoupled from any higher energy sector where GUT might place τ and t in same rep.

- In order to preserve gauge unification at M_U, which is much higher than the messenger sector mass scale, M, the messengers should form complete GUT representations.

Simple Model based on SU(5) GUT group:

- Choose messenger sector to contain a SU(3),SU(2),U(1) singlet superfield $\widehat{S}$ and messengers belonging to $\mathbf{5}+\overline{\mathbf{5}}$ of SU(5). Denote the superfield messengers $= \hat{h} = \hat{q}, \hat{\ell}$ (for the triplet and doublet components of the $\mathbf{5}$, respectively). As in gravity mediated case, the simplest choice will be for $\widehat{S}$ to be an SU(5) singlet, but this is not required.

- Couple the messengers to $\widehat{S}$ via $W = \lambda_1 \widehat{S}\hat{q}\hat{\overline{q}} + \lambda_2 \widehat{S}\hat{\ell}\hat{\overline{\ell}} \sim \lambda \widehat{S}\hat{h}\hat{\overline{h}}$. Different $\widehat{S}$ components would appear in W if $\widehat{S}$ not SU(5) singlet.

- SU$\not{S}$Y from the hidden sector is communicated to the messenger sector in the form $\langle S\rangle \neq 0$ and $\langle F_S\rangle \neq 0$. An important ratio is
$$\Lambda \equiv \frac{\langle F_S\rangle}{\langle S\rangle}.$$

- To get the masses of the messenger sector particles, we use the usual SUSY rules, according to which a $\widehat{W}$ expressed as a cubic gauge-invariant function of matter superfields A_i yields: $M^{ij}_{\rm fermion} \propto \partial^2 W/\partial A_i \partial A_j$ and $M^2_{\rm boson}$ derives from the scalar potential $V = \frac{1}{2}D^a D^a + F_i^\star F_i$ with $F_i = \langle F_i\rangle + \partial W/\partial A_i$ and $D^a = g A_i^\star T^a_{ij} A_j$ (which we drop). Roughly, this results in
$$M \equiv M_{f_{\rm mess.}} \sim \lambda\langle S\rangle; \quad M^2_{b_{\rm mess.}} \sim \begin{pmatrix} \lambda^2\langle S\rangle^2 & \lambda\langle F_S\rangle \\ \lambda\langle F_S\rangle & \lambda^2\langle S\rangle^2 \end{pmatrix},$$
where the boson mass-squared matrix is written in $(\overline{h}^\star \ h) M^2_{b_{\rm mess.}} \begin{pmatrix} \overline{h} \\ h^\star \end{pmatrix}$ space, the diagonal terms coming from $|F_h|^2$ and $|F_{\overline{h}}|^2$ and off-diagonal terms from $|F_S|^2$. From $M^2_{b_{\rm mess.}}$ we see that $\lambda\langle S\rangle^2 > \langle F_S\rangle$ is required to avoid negative eigenvalue. Ratios of $M^2_{b_{\rm mess}}$ eigenvalues < 30 (no fine tuning) suggests $\frac{M}{\Lambda} = \frac{\lambda\langle S\rangle^2}{\langle F_S\rangle} \gtrsim 1.05$.

- Integrate out messengers at scale $M \Rightarrow$ b.c. at scale M. Gaugino masses arise at one loop:

$$M_i(M) = k_i N_m g\left(\frac{\Lambda}{M}\right)\frac{\alpha_i(M)}{4\pi}\Lambda$$

where $k_2 = k_3 = 1, k_1 = 5/3$, and $N_m =$ no. of $\mathbf{5} + \overline{\mathbf{5}} + 3$ times no. of $\mathbf{10} + \overline{\mathbf{10}}$ reps. $N_m \leq 4$ to avoid Landau poles.

- To get $M_1(m_W) \sim 100$ GeV, $\Rightarrow \Lambda = \frac{\langle F_S\rangle}{\langle S\rangle} \sim 80$ TeV$/N_m$.

- Note: $\widehat{S} =$ SU(5) singlet assumed: $\Rightarrow$ usual $M_3 : M_2 : M_1 = 6-7 : 2 : 1$.

- Scalar masses arise at 2-loops $\Rightarrow m_i^2(M) =$

$$2\Lambda^2 N_m f\left(\frac{\Lambda}{M}\right)\left[c_3\left(\frac{\alpha_3(M)}{4\pi}\right)^2 + c_2\left(\frac{\alpha_2(M)}{4\pi}\right)^2 + \frac{5}{3}\left(\frac{Y}{2}\right)^2\left(\frac{\alpha_1(M)}{4\pi}\right)^2\right]$$

with $c_3 = 4/3$ (triplets) $c_2 = 3/4$ (weak doublets), $Y/2 = Q - T_3$. Note: degeneracy among families broken only by effects of order quark or lepton Yukawa couplings.

- In above, $g(\Lambda/M), f(\Lambda/M) \to 1$ for M/Λ not too near 1. For $\Lambda = M$, $g(1) = 1.4, f(1) = 0.7$.

- Above $\Rightarrow$ (for $g = f = 1$)

$$m_{\tilde{q}} : m_{\tilde{\ell}_L} : m_{\tilde{\ell}_R} : M_1 = 11.6 : 2.5 : 1.1 : \sqrt{N_m}$$

$\Rightarrow$ NLSP (next to lightest supersymmetric particle – goldstino=lightest) $= \widetilde{B}$ for $N_m = 1$, $\tilde{\ell}_R$ for $N_m \geq 2$. Other subtleties $\Rightarrow$ more freedom.

- μ and B do not arise from ansatz and are 'model-dependent', but EWSB driven by negative $m^2_{H_2^0}$ completely automatic.

- Meanwhile, in the hidden sector, spontaneous SU$\not{S}$Y $\Rightarrow$ goldstone fermion, the Goldstino G. (In local SUSY, G = longitudinal component of gravitino.) G acquires mass determined by F, the goldstino decay constant where $F \sim$ largest F-term vev;

$$m_G = \frac{F}{\sqrt{3} M_{\text{Planck}}} \sim 2.5 \left(\frac{\sqrt{F}}{100 \text{ TeV}} \right)^2 \text{ eV}$$

- Constraints:
  - $m_G \lesssim 1$ keV (or very big) required to avoid overclosing universe. $\Rightarrow \sqrt{F} \lesssim 2000$ TeV
  - $\sqrt{F} \sim 100$ TeV required for G=hot dark matter candidate.
  - $m_G \lesssim 10\% m_i$ to avoid return of flavor degeneracy worry. $\Rightarrow$

$$\langle S \rangle \lesssim 0.1 \sqrt{N_m} \frac{\alpha}{4\pi} M_{\text{Planck}} \sim \sqrt{N_m} 10^{12} \text{ TeV}$$

- G couplings are fixed by supersymmetric Goldberger-Treiman:

$$\mathcal{L} = -\frac{1}{F} j^{\mu\alpha} \partial_\mu G_\alpha + h.c.$$

where j = supercurrent taking superpartner to partner.

- $\Rightarrow$ For $\sqrt{F} \lesssim 2000$ TeV, superparticle decays to G are suppressed so that all except the NLSP decay as usual, but decay to G often not in the detector unless $\sqrt{F} \lesssim 200$ TeV (see below).

- What is relation of F to $\langle F_S \rangle$: Write $F \equiv f\langle F_S \rangle \Rightarrow$
  - In canonical models $f \sim \left(\frac{g_m^2}{16\pi^2}\right)^{-2} \sim 2.5 \times 10^4/g_m^4$ where g_m refers to gauge group responsible for SU$\not{S}$Y . $g_m \lesssim 1$ is preferred.
  - Meanwhile, $\langle F_S \rangle / \langle S \rangle \sim (80\text{ TeV}/N_m)(M_1/100\text{ GeV})$ is required. The result for $f = F/\langle F_S \rangle$ is:

$$f = \left(\frac{\sqrt{F}}{2000\text{ TeV}}\right)^2 \frac{625\lambda N_m^2}{(M/\Lambda)} \left(\frac{100\text{ GeV}}{M_1}\right)^2 .$$

  - This may be rewritten as:

$$(\sqrt{F}/2000\text{ TeV}) \geq \sqrt{F/F_S}(m_{\widetilde{\ell}_R}/100\text{ GeV})/(27.5\sqrt{N_m}).$$

  - For $m_{\widetilde{\ell}_R} \geq 45$ GeV (the rough LEP limit) and the two-loop communication value of $F/F_S = 2.5 \times 10^4$, $\sqrt{F} \geq 5200$ TeV ($\sqrt{F} \geq 2600$ TeV) for $N_m = 1$ ($N_m = 4$); *i.e.* even allowing for a factor of 2 or 3 uncertainty in the approximate lower bound, $\sqrt{F}$ must lie near its upper limit and the NLSP decay length will be long.
  - For a model with $F/F_S \sim 1$ (requiring that the hidden sector and messenger sector be one and the same),

$$\sqrt{F} \geq (73\text{ TeV}/\sqrt{N_m})(m_{\widetilde{\ell}_R}/100\text{ GeV})$$

    can be small, although nothing prohibits $\sqrt{F}$ values much larger than this lower limit.
  - Thus, in phenomenological studies $\sqrt{F}$ should be regarded as a model-dependent parameter.

Signals for GMSB

- Depend upon M, F and Λ; it is popular to assume M/Λ in $1.05-2$ range (as consistent as possible with $F/\langle F_S\rangle$ constraint) and $\sqrt{F}\leq 2000$ TeV. Most typically, $\sqrt{F}\sim 100$ TeV to 1000 TeV is assumed (which is difficult for models with separate hidden and messenger sectors).

- Consequent signals of GMSB depend on NLSP identity and $\sqrt{F}$. Let us first review the small $\sqrt{F}$ (prompt decay) signals.

  1. NLSP $=\widetilde\chi^0_1\sim\widetilde B$ ($N_m=1$):
     $\widetilde B\to G+\gamma$ with

     $$(c\tau)_{\widetilde\chi^0_1}\sim 130\left(\frac{100\text{ GeV}}{M_{\widetilde B}}\right)^5\left(\frac{\sqrt{F}}{100\text{ TeV}}\right)^4\mu m$$

     Notes:

     – If $\sqrt{F}\sim 2000$ TeV, then $c\tau\sim 21m$ for $M_{\widetilde B}=100$ GeV! (Such a large $M_{\widetilde B}$ is not really consistent with $f\sim 2.5\times 10^4/g_m^4$ for $\sqrt{F}$ this small when $N_m=1$ unless $g_m>1$.)

     – $F\sim 100$ TeV $\Rightarrow$ short decay length but need model with $F/\langle F_S\rangle\sim 1$, which would seem to require that the hidden sector and messenger sector be one and the same rather than connected by some type of gauge interactions.

     – For $m_{\widetilde B}>m_Z$, $\widetilde B\to G+Z$ as well.

     – $\widetilde\ell^\pm_R\to\widetilde B\ell^\pm(\text{soft})\to\ell^\pm\gamma G$ and $\widetilde\ell_L$ similar but with $\ell^\pm(\text{harder})$.

     Signals if $c\tau$ small

     Tevatron/LHC:

– $\widetilde{\chi}^0_1\widetilde{\chi}^0_1$ small, but $\widetilde{\chi}^+_1\widetilde{\chi}^-_1 \to W^{(\star)}W^{(\star)}\widetilde{\chi}^0_1\widetilde{\chi}^0_1 \to W^{(\star)}W^{(\star)}\gamma\gamma + \not{E}_T$, $\widetilde{\ell}_R\widetilde{\ell}_R \to \ell^+\ell^-\widetilde{\chi}^0_1\widetilde{\chi}^0_1 \to \ell^+\ell^-\gamma\gamma + \not{E}_T$, $\widetilde{\ell}_L\widetilde{\ell}_L \to \ell^+\ell^-\widetilde{\chi}^0_1\widetilde{\chi}^0_1 \to \ell^+\ell^-\gamma\gamma + \not{E}_T$, *etc.*.

– The $ee\gamma\gamma + \not{E}_T$ event of CDF has hard e's $\Rightarrow$ best interpreted as $\widetilde{\ell}_L\widetilde{\ell}_L$ production, but for reasonable probability for such an event we need prompt decays (small $\sqrt{F}$) and big $m_{\widetilde{\ell}_L} \Rightarrow$ need model with $F/\langle F_S\rangle \sim 1$. However, where are:

  * $\widetilde{\nu}_L\widetilde{\ell}_L \to \ell\gamma\gamma + \not{E}_T$ and $\widetilde{\nu}_L\widetilde{\nu}_L \to \gamma\gamma + \not{E}_T$ events, which have comparable rates in generic model.
  * Presumably $\widetilde{\chi}^0_2\widetilde{\chi}^\pm_1$ and $\widetilde{\chi}^+_1\widetilde{\chi}^-_1$ rates would be significant too and lead to $X\gamma\gamma + \not{E}_T$ with $X = \ell^\pm, \ell^+\ell'^-, \ell^+\ell^-\ell'^\pm$.

LEP,NLC:

– $e^+e^- \to \widetilde{\chi}^0_1\widetilde{\chi}^0_1 \to \gamma\gamma + \not{E}_T$ with $\frac{1}{4}\sqrt{s}(1-\beta) \le E_\gamma \le \frac{1}{4}\sqrt{s}(1+\beta)$ and flat.

– There might be a small excess of such events in the LEP2 data, but the level of background is still under debate.

2. NLSP $= \widetilde{H}_{1,2}$ (higgsino):

   $\widetilde{H}_{1,2} \to G + h^0, H^0, A^0$, depending on masses.

   Note: need $|\mu|$ small, but this is ok in GMSB since EWSB is almost automatic, independent of RGE.

   Signals if $c\tau$ small

   Tevatron/LHC and LEP/NLC: get $h^0h^0X + \not{E}_T$ final states, or higher Higgs, where $X =$ cascade decay products.

3. NLSP $= \widetilde{\ell}_R$ ($N_m \ge 2$):

   Decays are: $\widetilde{\ell}^\pm_R \to G + \ell^\pm$ and $\widetilde{\ell}^\pm_L \to \ell^\pm\widetilde{\chi}^{0(\star)}_1 \to \ell^\pm(\widetilde{\ell}^\pm_R\ell^\mp)' \to$

$\ell^{\pm}(\ell^{\pm}\ell^{\mp})'G$. For $N_m = 4$, $m_{\widetilde{\chi}_1^0} \sim 1.9 m_{\widetilde{\ell}_R}$.

Signals if $c\tau$ small

Tevatron/LHC and NLC: $\widetilde{\ell}_R\widetilde{\ell}_R \to \ell^+\ell^- + \not{E}_T$ (flat E_ℓ spectrum in $\widetilde{\ell}_R\widetilde{\ell}_R$ cm, *e.g.* e^+e^- cm at NLC) and $\widetilde{\ell}_L^{\pm}\widetilde{\ell}_L^{\mp} \to 6\ell + \not{E}_T$.

Because of larger Yukawa coupling $\tilde{\tau}_1$ might be lightest of the $\widetilde{\ell}_R$ — if sufficiently light that *e.g.* $\widetilde{\mu}_R \to \mu\tilde{\tau}_1\tau$ (via $\widetilde{B}$ component of $\widetilde{\chi}_1^{0\star}$) allowed, then all final states could cascade to τ's.

- If $\sqrt{F}$ is not sufficiently small for $c\tau$ to be small (as more natural in models with separate hidden and messenger sectors since they have large $F/\langle F_S \rangle$) then signals are very different.

What if $\sqrt{F} \sim 1000 - 2000$ TeV?

The number of decays where one or both $NLSP$'s decay within radial distance R is

$$\propto [1 - \exp(-2R/[c\tau])] \sim 2R/[c\tau].$$

For large $c\tau$, most decays would be non-prompt, with many occurring in the outer parts of the detector or completely outside the detector. To maximize sensitivity to GMSB models and fully cover the $(\sqrt{F}, \Lambda)$ parameter space, we must develop signals sensitive to decays that are delayed, but not necessarily so delayed as to be beyond current detector coverage and/or specialized extensions of current detectors.

The strategy will depend very much upon whether it is the $\widetilde{\chi}_1^0$ or the $\tilde{\ell}_R$ that is the NLSP.

$\tilde{\ell}_R$ =NLSP:

- For small $\sqrt{F}$, we look for the prompt multi-lepton plus $\not{E}_T$ signals described earlier.
- For moderate $\sqrt{F}$ such that the $\tilde{\ell}_R$ decays mainly before reaching the EM calorimeter, we look for a charged lepton that suddenly appears a finite distance from the interaction region, with non-zero impact parameter as measured by either the vertex detector or the EM calorimeter. Leading up to this decay would be a heavily ionizing track with $\beta < 1$ (as could be measured if magnetic field is present).
- For large $\sqrt{F}$, the $\tilde{\ell}_R$ will reach the EM and hadronic calorimeters, and behave much like a heavy muon, presumably exciting if it does not decay first. Limits on such objects should be pursued. Limits are currently quoted by D0 and CDF for pseudo-stable charged strongly

produced particles (stable quarks, squarks, . ..), but the GMSB cross section is not the same. The $\tilde{\ell}_R$'s will come from all kinds of sources (including gluino pair. squark pair, chargino pair, ... production as well as direct slepton pair production). A detailed calculation is in progress. Based purely on the slepton pair cross section estimate alone, we believe that charged pseudo-stable $\tilde{\ell}_R$'s can be ruled out up to about $80-100$ GeV. I have been told that similar limits will come from the LEP2 data.

$\widetilde{\chi}_1^0$ =NLSP:

This is a much more difficult case.

- For small $\sqrt{F}$, we look for the prompt γ plus $\not{E}_T$ signals described earlier.
- For moderate $\sqrt{F}$, we look for delayed γ appearance. This case will be considered in more detail shortly.
- For large $\sqrt{F}$, we return to standard SUSY signals since the $\widetilde{\chi}_1^0$ simply yields $\not{E}_T$. GMSB models yield specific boundary conditions for the normal sparticle masses to be used in assessing the reach of the standard SUSY signals.

Table 4: Michelin guide to gravity-mediated vs. gauge-mediated S$\not{U}$SY models.

	Gravity-Mediated	Gauge-Mediated
Flavor Problem	*	***
μ Problem	**	*?
Doublet-triplet splitting Problem	?	**
Dark matter Problem	***	*?
Experimental Observability	***	*****

A more detailed look at $\widetilde{\chi}_1^0 = NLSP$ at the Tevatron

If the hidden sector is separated from the messenger sector, leading to large $F/\langle F_S\rangle$, then we have seen that the parameter space is squeezed so that $\sqrt{F}$ should be large and $m_{\widetilde{\chi}_1^0}$ (and Λ) must be very modest in size. SUSY production rates at the Tevatron will then be substantial.

$\Rightarrow$ We should work hard to learn how to dig out the possible signals for small to moderate Λ.

We begin by considering three signals.

- The standard SUSY signal of jets plus missing energy, dominant when the $c\tau$ for the $\widetilde{\chi}_1^0$ is large. We employ D0 cuts: (a) $n(\text{jets}) \geq 3$ ($|\eta_{\text{jet}}| < 3.5$ and $E_T^{\text{jet}} > 25$ GeV for $\Delta R_{\text{coal.}} = 0.5$) — labelled $k = 1, 2, 3$ according to decreasing E_T; (b) no isolated ($E_T^{\text{had.}}(\Delta R \leq 0.3) < 5$ GeV) leptons with $E_T > 15$ GeV; (c) $\not{E}_T > 75$ GeV; (d) $0.1 < \Delta\phi(\not{E}_T, j_k) < \pi - 0.1$ and $\sqrt{(\Delta\phi(\not{E}_T, j_1) - \pi)^2 + (\Delta\phi(\not{E}_T, j_2))^2} > 0.5$. The background cross section level has been estimated by D0 to be $\sigma_B = 2.35$ pb. The signal will be deemed observable if: (i) there are at least 5 signal events; (ii) $\sigma_S/\sigma_B > 0.2$; and (iii) $N_S/\sqrt{N_B} > 5$, where N_S and N_B are the numbers of signal and background events.

- The prompt 2γ signal, dominant when $c\tau$ for the $\widetilde{\chi}_1^0$ is small. Following Baer etal, we require: (a) at least two photons with $|\eta_\gamma| < 1$, $E_T^\gamma > 12$ GeV and $E_T^{\rm had.}(\Delta R \leq 0.3) < 4$ GeV; (b) $\not\!\!E_T > 30$ GeV. Each photon is required to emerge from a $\widetilde\chi_1^0$ decay that occurs before the $\widetilde\chi_1^0$ has reached the electromagnetic calorimeter. Detection efficiency of 80% (100%) is assumed if $E_T^\gamma < 25$ GeV (> 25 GeV). It is presumed that this signal is completely free of background. It will be deemed observable if there are 5 or more events.

- A delayed γ appearance signal, useful for moderate to large $c\tau$ values. The best such signal is highly detector dependent. We have focused on the D0 detector, for which the central hadronic calorimeter is radially segmented into three sections (as well as segmented in ΔR). The cells of the outer section have radial size $2\mathrm{m} \lesssim r \lesssim 2.5\mathrm{m}$ and η–ϕ size of $\Delta R = 0.1$. Consider an event in which a $\widetilde\chi_1^0 \to \gamma G$ decay occurs inside one of the outer hadronic calorimeter (OHC) cells. The γ will deposit all its energy in the cell. If the γ energy is substantial and there is no jet pointing to the same cell with sizeable energy deposits in the inner cells of the hadronic calorimeter, the standard model background to such an event is very small.† In order to guarantee negligible backgrounds we require one of the following: (1) that there is at least one such isolated $\widetilde\chi_1^0$ decay in an OHC cell in association with three energetic jets and missing energy; (2) that there are two isolated $\widetilde\chi_1^0$ decays in different OHC cells in association with missing energy; or (3) that there is one isolated $\widetilde\chi_1^0$ decay in an OHC cell in association with one or more isolated photons from prompt $\widetilde\chi_1^0$ decay and missing energy. Isolation for the outer hadronic calorimeter cell

†Long-lived kaons interact strongly and will be absorbed before reaching the outer hadronic cells.

case is defined by requiring that there be no energetic jet emerging near the cell in which the $\widetilde{\chi}_1^0$ decay occurs. The specific cuts for these three classes of events are:

1. (a) $n(\text{jets}) \geq 3$ ($|\eta_{\text{jet}}| < 3.5$, $E_T^{\text{jet}} > 25$ GeV using $\Delta R_{\text{coal.}} = 0.5$); (b) one or more $\widetilde{\chi}_1^0 \to \gamma G$ decays in central OHC cells with $E_T^{\gamma} >$ 15 GeV and $\Delta R(j, \text{vertex}) > 0.5$; (c) $\not{E}_T > \not{E}_T^{\text{min}}$. Observability is assumed if there are 5 or more such events.
2. (a) any number of jets (as defined above); (b) two or more $\widetilde{\chi}_1^0$ decays in (central) OHC cells, each with $E_T^{\gamma} > 15$ GeV and $\Delta R(j, \text{vertex}) > 0.5$; (c) $\not{E}_T > \not{E}_T^{\text{min}}$. Observability is assumed if there are 5 or more such events.
3. (a) at least one photon with $|\eta_\gamma| < 1$, $E_T^{\gamma} > 12$ GeV and $E_T^{\text{had.}}(\Delta R \leq 0.3) < 4$ GeV emerging from a $\widetilde{\chi}_1^0$ decay that occurs before the $\widetilde{\chi}_1^0$ has reached the electromagnetic calorimeter. Detection efficiency of 80% (100%) is assumed if $E_T^{\gamma} < 25$ GeV (> 25 GeV). (b) one or more $\widetilde{\chi}_1^0 \to \gamma G$ decays in OHC cells with $E_T^{\gamma} > 15$ GeV and $\Delta R(j, \text{vertex}) > 0.5$; (c) $\not{E}_T > \not{E}_T^{\text{min}}$. Observability is assumed if there are 5 or more such events.

Experimental Monte Carlo work is needed to learn what an appropriate $\not{E}_T^{\text{min}}$ is for a given total L. We have made what we think are quite conservative choices: $\not{E}_T^{\text{min}} = 30, 50, 70$ GeV for $L = 100\ \text{pb}^{-1}, 2\ \text{fb}^{-1}, 30\ \text{fb}^{-1}$, respectively. If these cuts can be weakened, then signal event rates will increase.

A detector issue that is currently being explored is that of "hot cells". Occasionally, a calorimeter cell will fire simply because of accumulated charge. Some cells are worse than others and can simply be eliminated. Also, a hot cell firing in conjunction with the jet and $\not{E}_T$ requirements is likely to be improbable. Finally, a true signal γ will have some shower leakage to nearby cells, whereas this would not be present for a hot-cell firing. The detector people who have begun to look at this are rather optimistic that the OHC signal will not be impaired by this phenomenon.

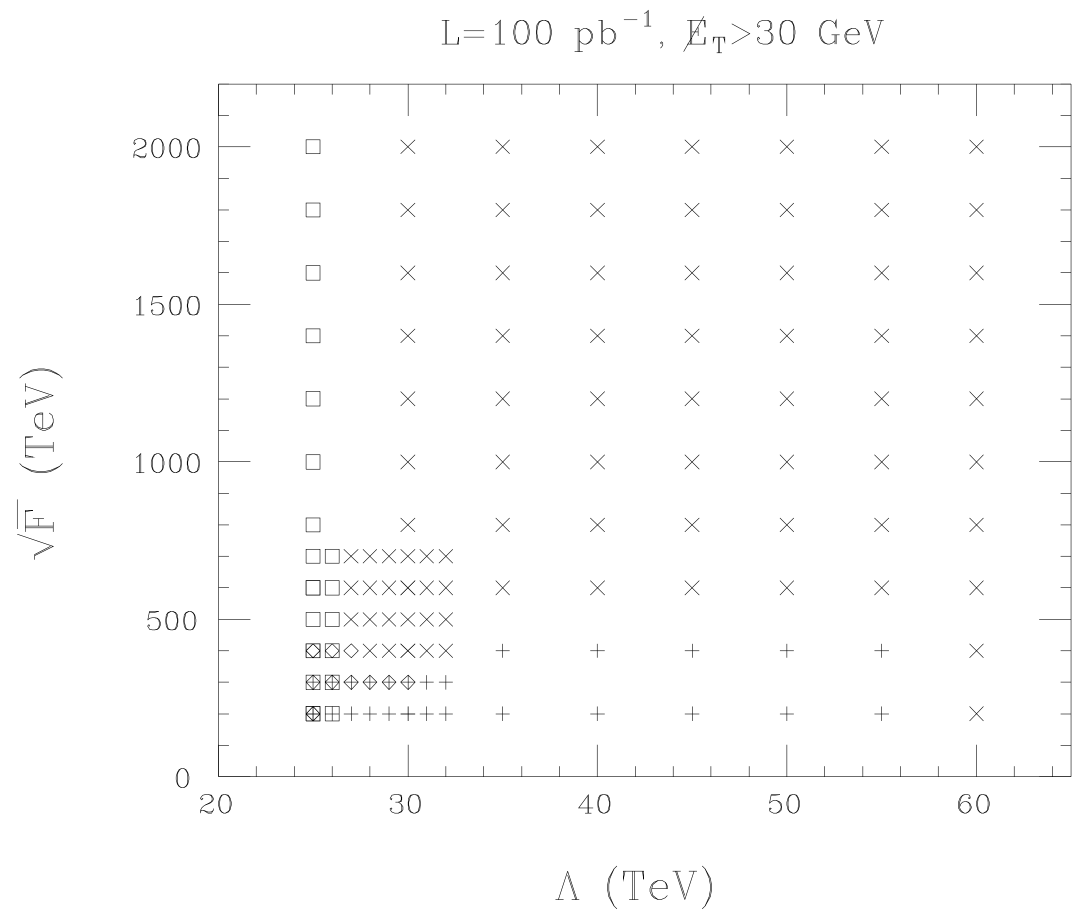

Figure 4: For $L = 100$ pb^{-1} and $\not{E}_T^{\min} = 30$ GeV, we display those points in $(\Lambda, \sqrt{F})$ parameter space for which we can observe the following GMSB SUSY signals: $\Box$, jets plus $\not{E}_T$; $+$, prompt 2γ; $\Diamond$, OHC delayed-decay. At points labelled by $\times$, no signal is observable.

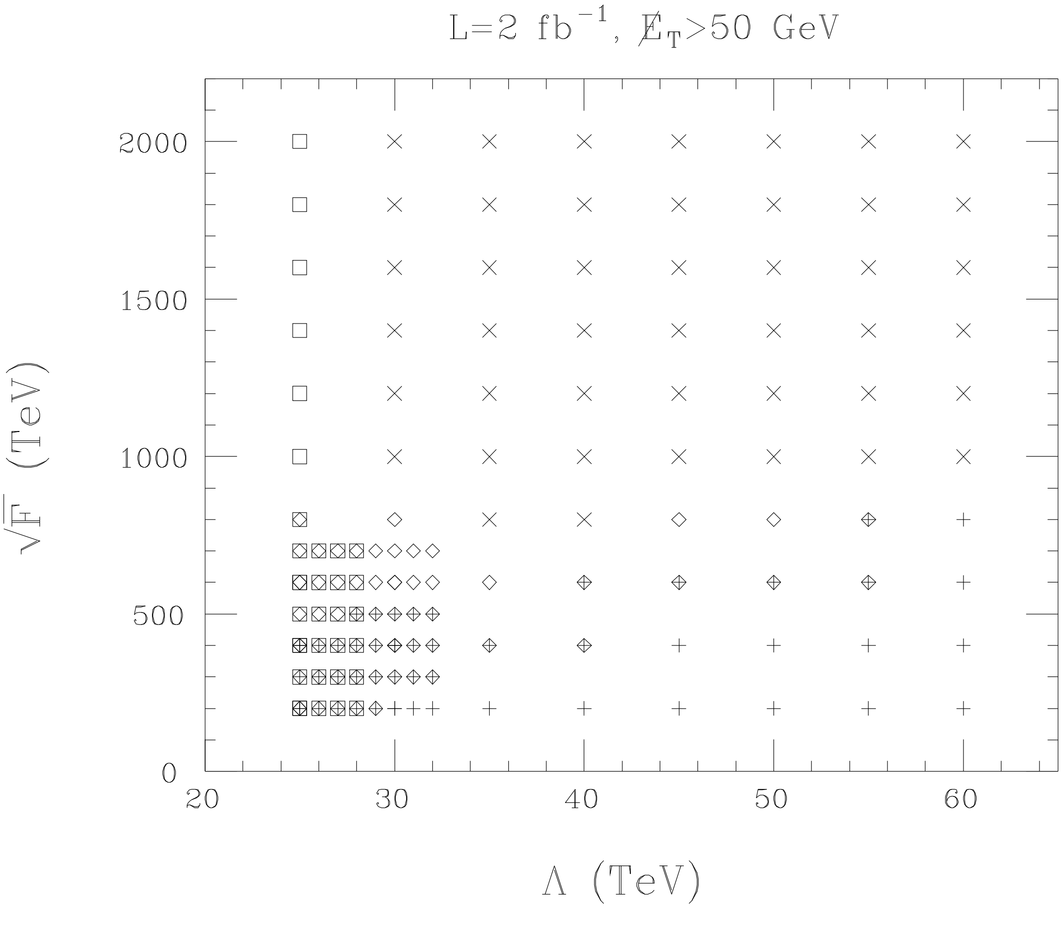

Figure 5: As in Fig. 4, but for $L = 2$ fb^{-1} and $\not{E}_T^{\min} = 50$ GeV.

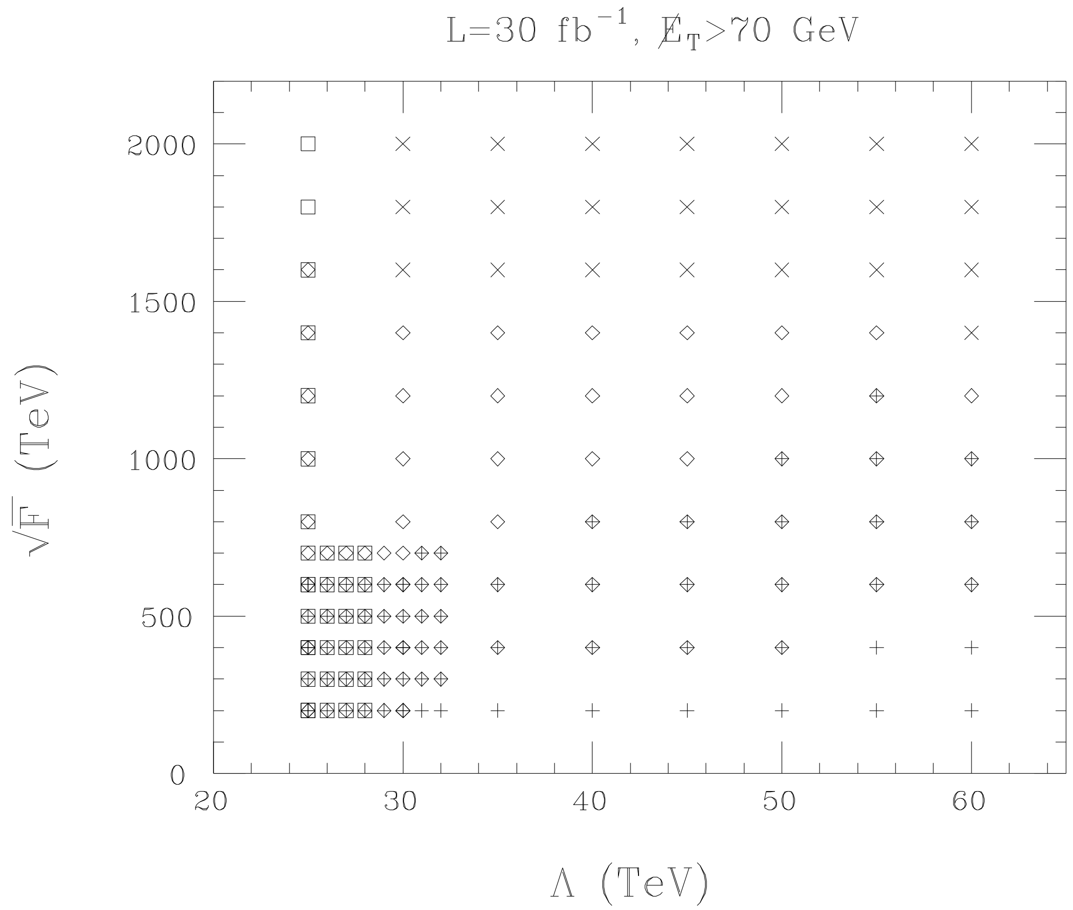

Figure 6: As in Fig. 4, but for $L = 30$ fb^{-1} and $\not{E}_T^{\rm min} = 70$ GeV.

Of course, there are many other possible signals for delayed decays. We have begun to examine several.

1. Non-zero impact parameter for a photon observed in the EM calorimeter.

   - in Run I, resolution in b is $\sim$ 10cm.
   - in Run II, a preshower next to EM calorimeter will improve resolution in b to $\sim$ 0.2cm!
   - An idea of the usefulness of this signal is obtained by examining some parameter space points which were on the edge of observability using the OHC signals in the case of $L = 2$ fb^{-1}. We require 3 jets (as defined in OHC case), $\not{E}_T > 50$ GeV, and $b > 50$cm, i.e. 5σ larger than the current resolution. For such requirements we presume the signal will be background free. The cross sections and event rates for the two parameter points considered so far are given in Table 5.

Table 5: Cross section for 3 jets, $\not{E}_T > 50$ GeV, and $b > 50$cm.

$(\Lambda, \sqrt{F})$ (TeV)	$\sigma(\text{ fb}^{-1})$	$N_{\text{events}}(L = 2 \text{ fb}^{-1})$
(30,800)	7	14
(35,800)	4	8

Both the event rates listed are better than obtained via the OHC signal, indicating that this signal will be very useful at moderate $\sqrt{F}$, especially with improved b resolution from the preshower which will allow larger background free rates.

2. Scintillator (with sheet of ? to cause γ showering) or other array placed outside the detector (i.e. beyond the muon chambers). Roughly, for D0 the outer radius of the muon chambers is at $\sim$ 7m.

   - The more volume covered, the better. We have looked at an array which covers $-12 < z < +12$m and various regions of r.
   - We require 3 jets (defined as in OHC study), $\not{E}_T > 30$ GeV, and decay outside the detector. The resulting cross sections are tabulated in Table 6 for a moderate value of $\Lambda = 35$ TeV and two $\sqrt{F}$ values, one near the upper cosmology limit.

Table 6: Cross section for 3 jets, $\not{E}_T > 30$ GeV, and photon emergence in $-12 < z < +12$m and indicated r region.

r region	$\sigma(\sqrt{F} = 800 \text{ TeV}, \Lambda = 35 \text{ TeV})$	$\sigma(\sqrt{F} = 1600 \text{ TeV}, \Lambda = 35 \text{ TeV})$
$7 < r < 10$m	35 fb	3 fb
$10 < r < 13$m	30 fb	2.8 fb
$13 < r < 16$m	17 fb	2.4 fb
$16 < r < 19$m	19 fb	1.8 fb

Of course, full 360 degree coverage is not possible because of the physical set up of the D0 detector. Scintillators cannot be placed below the detector or to the outer ring side of the detector. Cost will also be a factor. Let us suppose $\Delta\phi/360 \sim 0.3$ coverage. If we can sample out to $r = 19$m, then even at $\sqrt{F} = 1600$ TeV we get a total event rate of 6 ($L = 2$ fb^{-1}), enough to claim a signal. Thus, at modest Λ (as most consistent with a hidden sector that is separated from a messenger sector by some new gauge interactions), we can probe out near the highest $\sqrt{F}$ values allowed by non-special cosmology.

3. Direct timing information for the energy deposit of the γ's in the calorimeters. We have not yet explored this signal quantitatively, since we need more detector information than we currently have.

   In Run I, CDF had limited timing information, but D0 had none.

   In Run II, both CDF and D0 will have timing information.

   Even if timing information is not adequate on its own to allow a background-free signal, our hope is that the timing information would allow reduction in the other requirements needed for a background-free signal, thereby improving event rates and, hence, leading to greater sensitivity to the GMSB signals.

The main lesson from this Tevatron study is that CDF and D0 upgrades and LHC detector plans should be sure to incorporate features needed for sensitivity to the "delayed decay" signals that will be crucial for sensitivity to the full parameter space for GMSB models.

Even if prompt γ or ℓ signals are seen, it will be very important to determine $\sqrt{F}$. This can only be accomplished by observation of delayed-decay signals — comparing non-prompt to prompt signal rates will give a measure of $c\tau$ and, hence, of $\sqrt{F}$.

SUSY Conclusions

- Supersymmetry=dream-come-true if seen:
  - theorists $\Rightarrow$ overall theoretical idea correct = triumph;
  - experimentalists $\Rightarrow$ detailed spectrum requires decades of experimental work and theorists will be waiting in the wings for new results;
  - once spectrum, . . . , is known, use RGE, . . ., to extrapolate back up to the messenger scale(s);

    $\Rightarrow$ maybe we can figure out what the 0-mode sector of string theory is (and, thence, figure out more about the string theory), or find GMSB boundary conditions and work from there;
- Worry?:

  If there are too many possible theories of SU$\not{S}$Y , boundary conditions, . . ., maybe measuring 105 parameters at low-E will not suffice to pin down the model.

  $\Rightarrow$ Hopefully the boundary conditions will have an elegant and relatively easily recognized nature.

HIGGS SECTORS OF THE MSSM AND BEYOND

OUTLINE

- How precisely will we know m_{h^0} and how useful will it be?
- Prospects for and means for distinguishing the MSSM h^0 or other SM-like light Higgs bosons from the SM h_{SM} via branching ratios and couplings, and implications.
- Strategies for finding the MSSM H^0 and A^0 and the role of the MC.
- What can we learn from the branching ratios of the H^0, A^0 in the supersymmetric GUT context?
- Is there a no-lose theorem for the NMSSM (two-doublet plus one-singlet supersymmetric model) at the LHC + LEP2?
- A new sum rule and current limits from LEP2 on a CP-violating 2HDM or 2D1S Higgs sector.
- Precision measurement of the couplings for a general CPV 2HDM Higgs boson at a high energy e^+e^- collider.
- Exotic Higgs sectors: complementarity of LHC and s-channel processes at electron and muon colliders.

Since the muon collider (MC) will be an important ingredient in some of what follows, I give a brief outline of the MC energy resolution and luminosity possibilities.

A muon collider facility can be developed in stages, each successive stage building upon the previous one. Three stages are currently envisioned.

- Low-energy Higgs factory collider: $\sqrt{s} \sim 100$ GeV.
- Intermediate-energy collider: $\sqrt{s} \lesssim 500$ GeV.
- High-energy collider: $\sqrt{s} \sim 3 - 4$ TeV.

The instantaneous luminosity, $\mathcal{L}$, that can be achieved at each stage is still somewhat uncertain. For rather conservative designs of relatively low cost, current minimal expectations are:

- $\mathcal{L} \sim 1, 2, 10 \times 10^{31}\mathrm{cm}^{-2}\mathrm{s}^{-1}$ at $\sqrt{s} \sim 100$ GeV for beam energy resolutions of $R = 0.003\%, 0.01\%, 0.1\%$, respectively — the very excellent $R = 0.003\% \rightarrow$

  $$\sigma_{\sqrt{s}} \sim 2 \text{ MeV} \left(\frac{R}{0.003\%}\right) \left(\frac{\sqrt{s}}{100 \text{ GeV}}\right) , \tag{0.11}$$

  which is as small as the natural width of a light SM-like Higgs boson of same mass. A direct scan measurement of Γ_h^{tot} then becomes possible.

  It is also important to note that the beam energy can be very precisely tuned: $\Delta E_{\mathrm{beam}} \sim 10^{-5} E_{\mathrm{beam}}$ is 'easy'; 10^{-6} is achievable and very important for scanning a narrow Higgs boson.

- $\mathcal{L} \sim 1 \times 10^{33}\mathrm{cm}^{-2}\mathrm{s}^{-1}$, at $\sqrt{s} \sim 400$ GeV for $R \sim 0.14\%$.
- $\mathcal{L} \sim 1 \times 10^{35}\mathrm{cm}^{-2}\mathrm{s}^{-1}$, at $\sqrt{s} = 3 - 4$ TeV with $R \sim 0.16\%$.

(For yearly integrated luminosities, we use the standard convention of $\mathcal{L} = 1 \times 10^{32}\mathrm{cm}^{-2}\mathrm{s}^{-1} \Rightarrow L = 1\ \mathrm{fb}^{-1}/\mathrm{yr}$.)

Of course, the totally unique feature of a muon collider that is crucial to Higgs physics is the possibility of s-channel Higgs production, $\mu^+\mu^- \to h$.

Compute $\overline{\sigma}_h$ by convoluting a Gaussian $\sqrt{s}$ distribution of width $\sigma_{\sqrt{s}}$ with the standard s-channel Breit Wigner Higgs resonance cross section. For $\sqrt{s} = m_h$, one obtains

$$\overline{\sigma}_h \simeq \frac{\pi\sqrt{2\pi}\Gamma(h \to \mu\mu)\, BF(h \to X)}{m_h^2 \sigma_{\sqrt{s}}} \times \left(1 + \frac{\pi}{8}\left[\frac{\Gamma_h^{\rm tot}}{\sigma_{\sqrt{s}}}\right]^2\right)^{-1/2} . \qquad (0.12)$$

Eq. (0.12) $\Rightarrow$ small $\Gamma_h^{\rm tot}$ and $\sigma_{\sqrt{s}} \sim \Gamma_h^{\rm tot} \to$ big $\overline{\sigma}_h$.

Although smaller R implies smaller $\mathcal{L}$, the correlation is such that for small $\Gamma_h^{\rm tot}$ (*e.g.* a SM-like Higgs boson with $m_h \lesssim 2m_W$) it is best to use the smallest R that can be achieved.

Implications of a precise measurement of m_{h^0}:

- Discovery of h^0 guaranteed at NLC, MC and, if $m_{A^0} \gtrsim 150$ GeV, the LHC.
- m_{h^0} will be precisely determined: $\Delta m_{h^0} \lesssim 100$ MeV or better is achievable at NLC and LHC. The MC yields $\Delta m_{h^0} \lesssim 1$ MeV via s-channel scan.
- m_{h^0} will inaugurate a new precision game.

  At one-loop (no mixing, *etc.*.),

  $$\Delta m_{h^0}^2 = \frac{3g^2 m_t^4}{8\pi^2 m_W^2} \ln \frac{m_{\widetilde{t}}^2}{m_t^2}$$

  For $m_{h^0} = 100$ GeV, $\Delta m_{h^0} = \pm 100$ MeV $\Rightarrow$ constraints of order $\Delta m_t = \pm 170$ MeV, $\Delta m_{\widetilde{t}} = \pm 2$ GeV. More generally and at two-loops, A and μ parameters enter.

  This level of constraint on $m_{\widetilde{t}}, \ldots$ probably exceeds that achievable experimentally by direct measurements.

  Also, can we really get theory to $\Delta m_{h^0} = \pm 100$ MeV level? Two-loop RGE-improved result only reliable to a few GeV.

  $\Rightarrow$ accuracy of experimental m_{h^0} measurement entirely adequate for the precision 1-loop m_{h^0} game.

Discriminating among SM-like light Higgs bosons, *e.g.* $\boldsymbol{h^0}$ **vs.** $\boldsymbol{h_{SM}}$**.** (J.G., L. Poggioli, R. Van Kooten + . .)

With no NLC or MC:

- It is hard. Snowmass96 study $\Rightarrow$ precision inadequate in 'decoupling' sort of limit of particular interest. In particular, very hard to probe the fermionic (*e.g.* $b\overline{b}$) couplings that $\rightarrow$ largest deviations in the decoupling limit. $m_h \sim m_Z$ = best case: LEP2, TeV33 and LHC data all available.

  LEP2 + TeV33

  - The inclusive $e^+e^- \rightarrow Zh$ with $Z \rightarrow e^+e^-, \mu^+\mu^-$ determines $(ZZh)^2$ to $\sim \pm 26\%$.
  - The ratio $\sigma(Zh)BF(h \rightarrow b\overline{b})/\sigma(Zh)$ determines $BF(h \rightarrow b\overline{b})$; biggest error is that on $\sigma(Zh)$ from above $\Rightarrow$ error on $BF(h \rightarrow b\overline{b})$ also $\sim \pm 26\%$.
  - The ratio

    $$\frac{[\sigma(p\overline{p} \rightarrow W^\star \rightarrow Wh)BF(h \rightarrow b\overline{b})]_{\mathrm{TeV33}}}{[\sigma(e^+e^- \rightarrow Zh)BF(h \rightarrow b\overline{b})]_{\mathrm{LEP2}}} \tag{0.13}$$

    determines $(WWh)^2/(ZZh)^2$. Including theoretical systematics, $\Rightarrow \sim \pm 20\%$ error for the ratio.
  - The ratio

    $$\frac{[\sigma(p\overline{p} \rightarrow W^\star \rightarrow Wh)BF(h \rightarrow b\overline{b})]_{\mathrm{TeV33}}}{[\sigma(p\overline{p} \rightarrow Z^\star \rightarrow Zh)BF(h \rightarrow b\overline{b})]_{\mathrm{TeV33}}} \tag{0.14}$$

    $\Rightarrow$ 2nd determination of $(WWh)^2/(ZZh)^2$ with $\sim \pm 20\%$ error; combine with previous to get $\sim \pm 14\%$ error for $(WWh)^2/(ZZh)^2$.

- Combine above and multiply by $(ZZh)^2$ determination to get $(WWh)^2$ with $\sim \pm 30\%$ error.
- The ratios

$$\frac{[\sigma(Wh)BF(h\to b\bar{b})]_{\rm TeV33}}{[BF(h\to b\bar{b}]_{\rm LEP2}} \quad \frac{[\sigma(Zh)BF(h\to b\bar{b})]_{\rm TeV33}}{[BF(h\to b\bar{b}]_{\rm LEP2}} \tag{0.15}$$

  $\Rightarrow$ $(WWh)^2$ and $(ZZh)^2$, respectively, with $\sim\ \pm 30\%$ and $\sim$ $\pm 32\%$ error. Combine with previous determinations

  $\Rightarrow$ $(WWh)^2$ and $(ZZh)^2$ to $\sim \pm 20\%$ and $\sim \pm 22\%$, respectively.

Bring in the LHC:

-

$$\frac{[pp\to W^\star\to Wh\to W\gamma\gamma]}{[pp\to W^\star\to Wh\to Wb\bar{b}]} \tag{0.16}$$

  and similar for $t\bar{t}h$ final state $\Rightarrow$ $BF(h\to\gamma\gamma)/BF(h\to b\bar{b})$ with error of $\sim \pm 17\%$. Given $\sim \pm 26\%$ error on $BF(h\to b\bar{b})$ $\Rightarrow$ $\pm 31\%$ error for $BF(h\to\gamma\gamma)$.
- The ratio

$$\frac{\sigma(pp\to gg\to h\to\gamma\gamma)}{BF(h\to\gamma\gamma)} \tag{0.17}$$

  $\Rightarrow$ $(ggh)^2$; error dominated by $BF(h\to\gamma\gamma)$.
- The ratio

$$\frac{[pp\to t\bar{t}h\to t\bar{t}\gamma\gamma]}{[pp\to W^\star\to Wh\to W\gamma\gamma]} \tag{0.18}$$

  $\Rightarrow$ $(t\bar{t}h)^2/(WWh)^2$ and similar for $b\bar{b}$ decay channel. Multiply by $(WWh)^2$ (combined error from above $\sim \pm 20\%$) yields $\sim \pm 30\%$ error for $(t\bar{t}h)^2$.

No direct access to $(b\bar{b}h)^2$ or $(\tau^+\tau^-h)^2$ or $(\gamma\gamma h)^2$ couplings: need total width to convert branching ratios to couplings.

Summary table for LEP2, TeV33 plus LHC:

Table 7: Summary of approximate errors for branching ratios and couplings-squared at $m_{h_{SM}} \sim m_Z$ in the M1 mass region. Where appropriate, estimated systematic errors are included. Quantities not listed cannot be determined in a model-independent manner. As discussed in the text, directly measured products of couplings-squared times branching ratios can often be determined with better accuracy.

Quantity	Error
$BF(b\overline{b})$	$\pm 26\%$
$(WWh_{SM})^2/(ZZh_{SM})^2$	$\pm 14\%$
$(WWh_{SM})^2$	$\pm 20\%$
$(ZZh_{SM})^2$	$\pm 22\%$
$(\gamma\gamma h_{SM})^2/(b\overline{b}h_{SM})^2$	$\pm 17\%$
$BF(\gamma\gamma)$	$\pm 31\%$
$(ggh_{SM})^2$	$\pm 31\%$
$(t\overline{t}h_{SM})^2/(WWh_{SM})^2$	$\pm 21\%$
$(t\overline{t}h_{SM})^2$	$\pm 30\%$

At higher masses, LEP2 disappears, and TeV33 is stretched.

Overall, without NLC and/or MC data, we will know that the Higgs is SM-like, but we will not be able to discriminate between different SM-like possibilities without going to NLC and MC.

Table 8: Summary of approximate errors for coupling-squared ratios at $m_{h_{SM}} = 100, 110, 120, 130$ GeV in the M2 mass region. As discussed in the text, directly measured products of couplings-squared times branching ratios can often be determined with better accuracy. Includes TeV33 input.

Quantity	Errors			
Mass (GeV)	100	110	120	130
$(WWh_{SM})^2/(ZZh_{SM})^2$	$\pm 23\%$	$\pm 26\%$	$\pm 34\%$	$-$
$(\gamma\gamma h_{SM})^2/(b\bar{b}h_{SM})^2$	$\pm 17\%$	$\pm 19\%$	$\pm 22\%$	$\pm 25\%$
$(t\bar{t}h_{SM})^2/(WWh_{SM})^2$	$\pm 21\%$	$\pm 21\%$	$\pm 21\%$	$\pm 21\%$

Table 9: We tabulate the statistical errors at $m_{h_{SM}} = 120, 130, 150$ GeV in the determinations of $(\gamma\gamma h_{SM})^2/(ZZh_{SM})^2$ and $(WWh_{SM})^2/(ZZh_{SM})^2$, assuming $L = 600$ fb^{-1} at the LHC. Assumes no input from TeV33.

Quantity	Errors		
Mass (GeV)	120	130	150
$(\gamma\gamma h_{SM})^2/(ZZh_{SM})^2$	$\pm 25\%$	$\pm 11\%$	$\pm 10\%$
$(WWh_{SM})^2/(ZZh_{SM})^2$	$\pm 27\%$	$\pm 11\%$	$\pm 6\%$

NLC data alone:

- The best 'bet' for discriminating between SM-like Higgs bosons for $m_h \leq 130$ GeV is $\sigma BF(h \to c\overline{c})/\sigma BF(h \to b\overline{b})$; for $m_h \geq 130$ GeV (as in NMSSM), $\sigma BF(h \to WW^\star)/\sigma BF(h \to b\overline{b})$ valuable.
  - New results from Snowmass96 use 'topological tagging' (*e.g.* primary, secondary, tertiary for b jet but only primary and secondary for c jet). With state of the art vertex detector can separate with remarkable efficiency.
  - For $L = 200$ fb^{-1} at $\sqrt{s} = 500$ GeV and $m_h \leq 130$ GeV (and combining Zh, ZZ-fusion and WW-fusion production processes), $\Rightarrow$ statistical error in $BF(c\overline{c})/BF(b\overline{b})$ of $\sim \pm 7\%$.
  - Theoretical uncertainty in $m_c(m_c)$ and $m_b(m_b)$ (sum rules, lattice) and QCD running should reach $< 10\%$ level in a few years $\to$ net error of $\lesssim 10\%$.

    $\Rightarrow$ distinguish h^0 from h_{SM} at $\geq 2\sigma$ level for $m_{A^0} \leq 450$ GeV for typical $m_{h^0} = m_{h_{SM}} = 110$ GeV mass case.

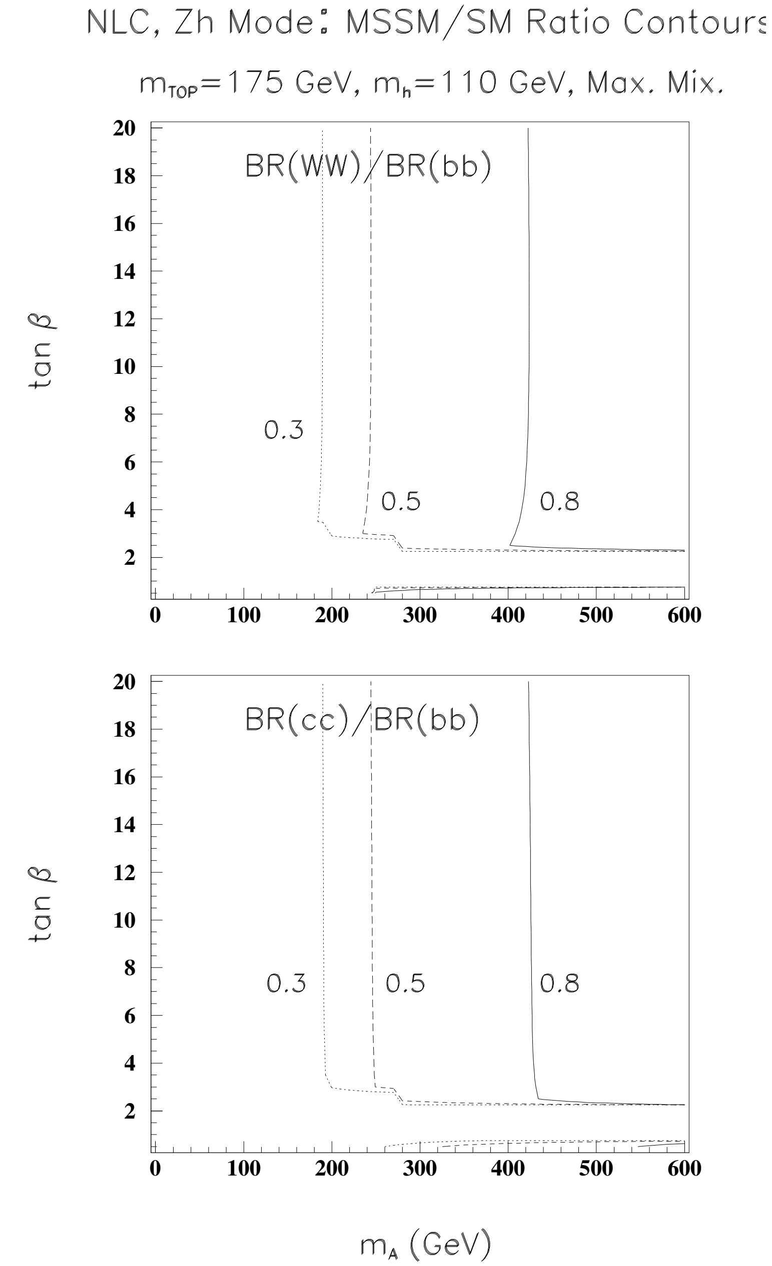

Figure 7: Constant value contours in $(m_{A^0}, \tan\beta)$ parameter space for the ratios $[WW^\star/b\overline{b}]_{h^0}/[WW^\star/b\overline{b}]_{h_{SM}}$ and $[c\overline{c}/b\overline{b}]_{h^0}/[c\overline{c}/b\overline{b}]_{h_{SM}}$. We assume "maximal mixing" in the squark sector and present results for the case of fixed $m_{h^0} = m_{h_{SM}} = 110$ GeV. The band extending out to large m_{A^0} at $\tan\beta \sim 2$ is where $m_{h^0} = 110$ GeV is theoretically disallowed in the case of maximal mixing. For no mixing, the vertical contours are essentially identical — only the size of the disallowed band changes.

- For NMSSM, the determination of $(ZZh)^2$ coupling squared could be very valuable for checking

$$\sum_i (ZZh_i)^2 = \sum_i (WWh_i)^2 = 1 \tag{0.19}$$

(where the $(VVh_i)^2$ – $V = W, Z$ – are defined relative to the SM-values). $(ZZh)^2$ is also crucial to getting many quantities in NLC only analysis.

How well can we do? $\Rightarrow$ recent analysis of ZZ-fusion mode, often ignored. (J.G., T. Han, R. Sobey)

Find: in $\sqrt{s} = 500$ GeV running and for low m_h, ZZ-fusion ($e^+e^- \rightarrow e^+e^-h$) analysis in missing-mass recoil peak technique $\Rightarrow$ better accuracy than $e^+e^- \rightarrow Zh$ channel (SLD-type detector). Combining errors in the $m_h < 150$ GeV range $\Rightarrow \pm 3\% - \pm 4\%$ error in $(ZZh)^2$.

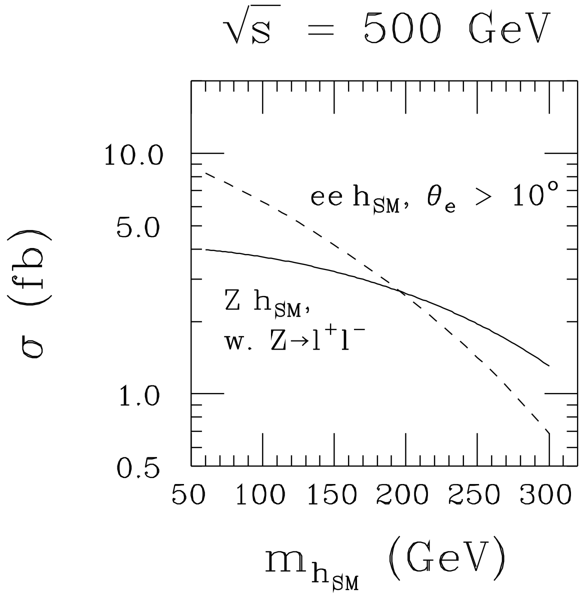

Figure 8: $\sigma(Zh_{SM})BF(Z \rightarrow \ell^-\ell^+)$ ($\ell = e, \mu$, no cuts) and $\sigma(e^+e^-h_{SM})$ (with a cut of $\theta > 10^\circ$ on the e^+ and e^- in the final state) as a function of $m_{h_{SM}}$ for $\sqrt{s} = 500$ GeV.

- $(WWh)^2$ measurement is more involved.

  1. For $m_h \le 140$ GeV, must measure $\sigma(\nu\overline{\nu}h)BF(h \to b\overline{b})$, and divide by $BF(h \to b\overline{b})$ as computed from $\sigma(Zh)BF(h \to b\overline{b})/\sigma(Zh)$ and $\sigma(e^+e^-h)BF(h \to b\overline{b})/\sigma(e^+e^-h)$.

     $\Rightarrow \sim \pm 5\% - \pm 6\%$ error for $(WWh)^2$ when $m_h \le 140$ GeV

  2. For $m_h \ge 150$ GeV, measure $\sigma(\nu\overline{\nu}h)BF(h \to WW^\star)$ and divide by $BF(h \to WW^\star)$ as computed from $\sigma(Zh)BF(h \to WW^\star)/\sigma(Zh)$ and $\sigma(e^+e^-h)BF(h \to WW^\star)/\sigma(e^+e^-h)$.

     $\Rightarrow \sim \pm 8\% - \pm 10\%$ error for $(WWh)^2$.

- Note: So far we have no determination of $\Gamma_h^{\rm tot}$. $\Gamma_h^{\rm tot}$ is needed to compute $(Xh)^2 = BF(h \to X)\Gamma_h^{\rm tot}$. Sketch indirect procedure for $m_h \le 130$ GeV.

  $\Rightarrow$ need to determine $BF(h \to \gamma\gamma)$ as well as possible and use $\gamma\gamma$ collisions to determine $\Gamma(h \to \gamma\gamma)$ and then compute

  $$\Gamma_h^{\rm tot} = \frac{\Gamma(h \to \gamma\gamma)}{BF(h \to \gamma\gamma)} \tag{0.20}$$

  Problem: $BF(h \to \gamma\gamma)$ cannot be well measured at NLC alone. Must use complicated game involving LHC and NLC data (complementarity!).

- $BF(h \to \gamma\gamma)$ at the NLC:

  – Measure $\sigma(e^+e^- \to Zh_{SM})BF(h_{SM} \to \gamma\gamma)$ and compute $BF(h_{SM} \to \gamma\gamma)$ as

  $$\frac{[\sigma(Zh_{SM})BF(h_{SM} \to \gamma\gamma)]}{\sigma(Zh_{SM})}; \tag{0.21}$$

– Measure $\sigma(e^+e^- \to \nu\overline{\nu}h_{SM})BF(h_{SM} \to \gamma\gamma)$ and $\sigma(e^+e^- \to \nu\overline{\nu}h_{SM})BF(h_{SM} \to b\overline{b})$ (both being WW-fusion processes) and compute $BF(h_{SM} \to \gamma\gamma)$ as

$$\frac{[\sigma(\nu\overline{\nu}h_{SM})BF(h_{SM} \to \gamma\gamma)]BF(h_{SM} \to b\overline{b})}{[\sigma(\nu\overline{\nu}h_{SM})BF(h_{SM} \to b\overline{b})]}. \tag{0.22}$$

For a calorimeter at the optimistic end of current plans for the NLC detector, the net error is predicted to range from $\sim \pm 22\%$ at $m_{h_{SM}} = 120$ GeV to $\sim \pm 35\%$ ($\sim \pm 53\%$) at $m_{h_{SM}} = 150$ GeV (70 GeV).

- Bring in LHC information:

Measure $\sigma(pp \to Wh_{SM})BF(h_{SM} \to \gamma\gamma)$ and $\sigma(pp \to t\overline{t}h_{SM})BF(h_{SM} \to \gamma\gamma)$ at the LHC. Errors: $\sim \pm 15\%$, each. Then,

1. Also measure $\sigma(pp \to t\overline{t}h_{SM})BF(h_{SM} \to b\overline{b})$ at the LHC and then compute $BF(h_{SM} \to \gamma\gamma) =$

$$\frac{BF(h_{SM} \to b\overline{b})_{\rm NLC}[\sigma(pp \to t\overline{t}h_{SM})BF(h_{SM} \to \gamma\gamma)]_{\rm LHC}}{[\sigma(pp \to t\overline{t}h_{SM})BF(h_{SM} \to b\overline{b})]_{\rm LHC}}. \tag{0.23}$$

   Using $[BF(h_{SM} \to b\overline{b})]_{\rm NLC}$ (error $\pm 4\% - \pm 5\%$, for $L = 200~{\rm fb}^{-1}$), error for $BF(h_{SM} \to \gamma\gamma)$ is dominated by $\gamma\gamma/b\overline{b}$ ratio (see Tables 7 and 8), $\to \pm 18\%$ to $\pm 26\%$ for $80 \leq m_h \leq 130$ GeV.

2. Use only $\sigma(pp \to Wh_{SM})BF(h_{SM} \to \gamma\gamma)$ (error $\sim \pm 15\%$) from the LHC, and then divide by the $\sigma(pp \to Wh_{SM})$ as computed using $[(WWh_{SM})^2]_{\rm NLC}$ (which has error $\sim \pm 6\%$). Including systematics, error in $\sigma(pp \to Wh_{SM}) \sim \pm 10\%$. Combining, $\Rightarrow \sim \pm 18\%$ error for $BF(h_{SM} \to \gamma\gamma)$.

Combine 1. and 2. $\Rightarrow BF(h \to \gamma\gamma)$ error of $\lesssim \pm 16\%$ for $m_h \lesssim 130$ GeV.

- $\Gamma(h_{SM} \to \gamma\gamma)$, the 2nd ingredient. Need $\gamma\gamma$ collider (complementarity!). Latest estimates (Bauer), including systematics, $\Rightarrow \Gamma(h_{SM} \to \gamma\gamma) BF(h_{SM} \to b\overline{b})$ error (for $L = 50~\mathrm{fb}^{-1}$) of 8%-10%. Given $\pm 5\% - \pm 6\%$ error for $BF(h_{SM} \to b\overline{b}) \Rightarrow \Gamma(h_{SM} \to \gamma\gamma)$ error of order $\pm 12\%$.

- Putting all this together $\Rightarrow \Gamma^{\rm tot}_{h_{SM}}$ error $\sim \pm 18\%$; not very wonderful.

Table 10: Summary of approximate errors for branching ratios, coupling-squared ratios, couplings-squared and $\Gamma^{\rm tot}_{h_{SM}}$ as determined using only data accumulated in $\sqrt{s}=500$ GeV running at the NLC, assuming $L=200$ fb^{-1} is accumulated. For $BF(h_{SM}\to\gamma\gamma)$ we have combined the NLC $\sqrt{s}=500$ GeV results with results obtained using LHC data; the net accuracy so obtained for $BF(h_{SM}\to\gamma\gamma)$ is also reflected in the determination of $\Gamma^{\rm tot}_{h_{SM}}$ following the indirect procedure. The errors for $\Gamma(h_{SM}\to\gamma\gamma)$ quoted are for $L=50$ fb^{-1} accumulated in $\gamma\gamma$ collider running at $\sqrt{s}\sim m_{h_{SM}}/0.8$, and are those employed in the indirect $\Gamma^{\rm tot}_{h_{SM}}$ determination.

Quantity	Errors			
$\mathbf{m_{h_{SM}}}$ **(GeV)**	**80**	**100**	**110**	**120**
$(c\overline{c}h_{SM})^2/(b\overline{b}h_{SM})^2$	$\sim\pm7\%$			
$(WWh_{SM})^2/(b\overline{b}h_{SM})^2$	–	–	–	$\pm23\%$
$(\gamma\gamma h_{SM})^2/(b\overline{b}h_{SM})^2$	$\pm52\%$	$\pm33\%$	$\pm29\%$	$\pm26\%$
$(ZZh_{SM})^2$	$\pm3\%-\pm4\%$			
$BF(h_{SM}\to b\overline{b})$	$\pm5\%$			
$BF(h_{SM}\to c\overline{c})$	$\sim\pm9\%$			
$BF(h_{SM}\to WW^\star)$	–			
$(WWh_{SM})^2$	$\pm5\%$			
$(ZZh_{SM})^2/(WWh_{SM})^2$	$\pm6\%-\pm7\%$			
$BF(h_{SM}\to\gamma\gamma)$	$\pm15\%$	$\pm14\%$	$\pm14\%$	$\pm14\%$
$(\gamma\gamma h_{SM})^2$	$\sim\pm12\%$			
$\Gamma^{\rm tot}_{h_{SM}}$ (indirect)	$\pm19\%$	$\pm19\%$	$\pm19\%$	$\pm18\%$
$(b\overline{b}h_{SM})^2$	$\pm20\%$	$\pm19\%$	$\pm19\%$	$\pm19\%$
$\mathbf{m_{h_{SM}}}$ **(GeV)**	**130**	**140**	**150**	**170**
$(c\overline{c}h_{SM})^2/(b\overline{b}h_{SM})^2$	$\pm7\%$	?		
$(WWh_{SM})^2/(b\overline{b}h_{SM})^2$	$\pm16\%$	$\pm8\%$	$\pm7\%$	$\pm16\%$
$(\gamma\gamma h_{SM})^2/(b\overline{b}h_{SM})^2$	$\pm27\%$	$\pm30\%$	$\pm41\%$	–
$(ZZh_{SM})^2$	$\pm4\%$			
$BF(h_{SM}\to b\overline{b})$	$\pm6\%$		$\pm9\%$	$\sim20\%$?
$BF(h_{SM}\to c\overline{c})$	$\sim\pm9\%$	?		
$BF(h_{SM}\to WW^\star)$	$\pm16\%$	$\pm8\%$	$\pm6\%$	$\pm5\%$
$(WWh_{SM})^2$	$\pm5\%$	$\pm5\%$	$\pm8\%$	$\pm10\%$
$(ZZh_{SM})^2/(WWh_{SM})^2$	$\pm7\%$	$\pm7\%$	$\pm9\%$	$\pm11\%$
$BF(h_{SM}\to\gamma\gamma)$	$\pm14\%$	$\pm20\%$?	$\pm41\%$	–
$(\gamma\gamma h_{SM})^2$	$\pm15\%$	$\pm17\%$	$\pm31\%$	–
$\Gamma^{\rm tot}_{h_{SM}}$ (indirect)	$\pm13\%$	$\pm9\%$	$\pm10\%$	$\pm11\%$
$(b\overline{b}h_{SM})^2$	$\pm14\%$	$\pm11\%$	$\pm13\%$	$\pm23\%$
$\mathbf{m_{h_{SM}}}$ **(GeV)**	**180**	**190**	**200**	**300**
$(ZZh_{SM})^2$	$\pm4\%-\pm5\%$		$\pm6\%$	$\pm9\%$
$(WWh_{SM})^2$	$\pm11\%$	$\pm12\%$	$\pm13\%$	$\pm24\%$
$(ZZh_{SM})^2/(WWh_{SM})^2$	$\pm12\%$	$\pm13\%$	$\pm14\%$	$\pm25\%$
$BF(h_{SM}\to WW)$	$\pm6\%$	$\pm7\%$	$\pm8\%$	$\pm14\%$?
$(\gamma\gamma h_{SM})^2$	$\pm13\%$	$\pm12\%$	$\pm12\%$	$\pm22\%$
$\Gamma^{\rm tot}_{h_{SM}}$ (indirect)	$\pm13\%$	$\pm14\%$	$\pm15\%$	$\pm28\%$

Bring in the muon collider:

- MC $\Rightarrow$ big further gain (if $m_h \neq m_Z$) by focusing on $\mu^+\mu^- \to h$ production at $\sqrt{s} \simeq m_h$. (J.G., Barger, Berger, Han)

  The crucial measurements are:

  - The very tiny Higgs width: $\Gamma_h^{\rm tot} = 1-10$ MeV for a SM-like Higgs with $m_h \lesssim 140$ GeV (i.e. mass as predicted for h^0 of SUSY).
  - $\sigma(\mu^+\mu^- \to h \to X)$ for $X = b\bar b, WW^\star, ZZ^\star$.[‡]

  Accuracy achievable? Employ optimized 3-point scan.

Table 11: Percentage errors (1σ) for $\sigma BF(h_{SM} \to b\bar b, WW^\star, ZZ^\star)$ (extracted from channel rates) and $\Gamma_{h_{SM}}^{\rm tot}$ for s-channel Higgs production at the MC assuming beam energy resolution of $R = 0.003\%$. Results are presented for two integrated four-year luminosities: $L = 4~{\rm fb}^{-1}$ ($L = 0.4~{\rm fb}^{-1}$). An optimized three-point scan is employed [which, for the cross section measurements, is equivalent to $L \sim 2~{\rm fb}^{-1}$ ($L = 0.2~{\rm fb}^{-1}$) at the $\sqrt{s} = m_{h_{SM}}$ peak].

Quantity	Errors			
Mass (GeV)	**80**	m_Z	**100**	**110**
$\sigma BF(b\bar b)$	0.8%(2.4%)	7%(21%)	1.3%(4%)	1%(3%)
$\sigma BF(WW^\star)$	–	–	10%(32%)	5%(15%)
$\sigma BF(ZZ^\star)$	–	–	–	62%(190%)
$\Gamma_{h_{SM}}^{\rm tot}$	3%(10%)	25%(78%)	10%(30%)	5%(16%)
Mass (GeV)	**120**	**130**	**140**	**150**
$\sigma BF(b\bar b)$	1%(3%)	1.5%(5%)	3%(9%)	9%(28%)
$\sigma BF(WW^\star)$	3%(10%)	2.5%(8%)	2.3%(7%)	3%(9%)
$\sigma BF(ZZ^\star)$	16%(50%)	10%(30%)	8%(26%)	11%(34%)
$\Gamma_{h_{SM}}^{\rm tot}$	5%(16%)	6%(18%)	9%(29%)	34%(105%)

At $L = 0.4~{\rm fb}^{-1}$ the errors for $\sigma BF(h_{SM} \to b\bar b)$ are still generally small but those for $\Gamma_{h_{SM}}^{\rm tot}$ are uncomfortably large. In fact, errors for $\Gamma_{h_{SM}}^{\rm tot}$ obtained indirectly using a combination of $L = 600~{\rm fb}^{-1}$ LHC

[‡]Note that $\sigma(\mu^+\mu^- \to h \to X)$ provides a determination of $\Gamma(h \to \mu^+\mu^-)BF(h \to X)$ unless $\sigma_{\sqrt{s}} \ll \Gamma_h^{\rm tot}$.

data, $L = 200$ fb^{-1} NLC data, and $L = 50$ fb^{-1} $\gamma\gamma$-collider data are often better: $\sim 19\%$ for $m_{h_{SM}} \lesssim 120$ GeV and $\sim 10\% - 13\%$ for 130 GeV $\lesssim m_{h_{SM}} \lesssim 180$ GeV.

- Can now combine with measurements from e^+e^- collisions at NLC and $\gamma\gamma$-collider facility at NLC $\Rightarrow$ determination of fundamental Higgs couplings.

  Best Example: 4 ways to determine $\Gamma(h \to \mu^+\mu^-)$:

  1) $\Gamma(h_{SM} \to \mu^+\mu^-) = \frac{[\Gamma(h_{SM}\to\mu^+\mu^-)BF(h_{SM}\to b\overline{b})]_{\rm MC}}{BF(h_{SM}\to b\overline{b})_{\rm NLC}}$;
  2) $\Gamma(h_{SM} \to \mu^+\mu^-) = \frac{[\Gamma(h_{SM}\to\mu^+\mu^-)BF(h_{SM}\to WW^\star)]_{\rm MC}}{BF(h_{SM}\to WW^\star)_{\rm NLC}}$;
  3) $\Gamma(h_{SM} \to \mu^+\mu^-) = \frac{[\Gamma(h_{SM}\to\mu^+\mu^-)BF(h_{SM}\to ZZ^\star)]_{\rm MC}\Gamma^{\rm tot}_{h_{SM}}}{\Gamma(h_{SM}\to ZZ^\star)_{\rm NLC}}$;
  4) $\Gamma(h_{SM} \to \mu^+\mu^-) = \frac{[\Gamma(h_{SM}\to\mu^+\mu^-)BF(h_{SM}\to WW^\star)\Gamma^{\rm tot}_{h_{SM}}]_{\rm MC}}{\Gamma(h_{SM}\to WW^\star)_{\rm NLC}}$.

  Resulting errors are labelled $(\mu^+\mu^- h_{SM})^2|_{\rm NLC+MC}$ in Table 12.

- Use these measurements to distinguish between h_{SM} and h^0 of the MSSM $\Rightarrow$ constraints on H^0 and A^0.

  – If only s-channel Higgs factory MC data are available (*i.e.* no Zh NLC or MC data) use

  $$(WW^\star h_{SM})^2/(b\overline{b}h_{SM})^2 \propto \sigma BF(WW^\star)/\sigma BF(b\overline{b}).$$

  If $110 \lesssim m_{h_{SM}} \lesssim 140$ GeV (a very likely region in the MSSM) then this ratio will be measured with a statistical accuracy of $\lesssim \pm 5\%$ for $L_{\rm tot} = 4$ fb^{-1} (see Table 11). Systematic errors of order $\pm 5\% - \pm 10\%$ from uncertainty in the b quark mass will also enter. A $> 2-3\sigma$ deviation will be observed if $m_{A^0} < 450$ GeV.

Table 12: Percentage errors (1σ) for combining $L = 600$ fb^{-1} LHC, $L = 200$ fb^{-1}–$\sqrt{s} = 500$ GeV NLC, $L = 50$ fb^{-1} $\gamma\gamma$-collider and MC $R = 0.003\%$ s-channel data, with errors for the latter as quoted in Table 11. Results are presented for two total four-year integrated MC luminosities: $L = 4$ fb^{-1} ($L = 0.4$ fb^{-1}).

Quantity	Errors			
Mass (GeV)	**80**	**100**	**110**	**120**
$(b\bar{b}h_{SM})^2\|_{\mathrm{NLC+MC}}$	6%(10%)	10%(16%)	7%(13%)	7%(13%)
$(c\bar{c}h_{SM})^2\|_{\mathrm{NLC+MC}}$	9%(13%)	12%(18%)	10%(15%)	10%(15%)
$(\mu^+\mu^- h_{SM})^2\|_{\mathrm{NLC+MC}}$	5%(5%)	5%(5%)	4%(5%)	4%(4%)
$(\gamma\gamma h_{SM})^2\|_{\mathrm{MC}}$	15%(18%)	17%(33%)	14%(21%)	14%(20%)
$(\gamma\gamma h_{SM})^2\|_{\mathrm{NLC+MC}}$	9%(10%)	10%(11%)	9%(10%)	9%(10%)
$\Gamma^{\mathrm{tot}}_{h_{SM}}\|_{\mathrm{NLC+MC}}$	3%(9%)	8%(16%)	5%(12%)	5%(12%)
Mass (GeV)	**130**	**140**	**150**	**170**
$(b\bar{b}h_{SM})^2\|_{\mathrm{NLC+MC}}$	8%(12%)	9%(10%)	13%(13%)	23%(23%)
$(c\bar{c}h_{SM})^2\|_{\mathrm{NLC+MC}}$	10%(14%)	?		
$(\mu^+\mu^- h_{SM})^2\|_{\mathrm{NLC+MC}}$	4%(5%)	4%	4%(5%)	13%(14%)
$(WW^\star h_{SM})^2\|_{\mathrm{MC}}$	17%(24%)	12%(30%)	33%(104%)	–
$(WW^\star h_{SM})^2\|_{\mathrm{NLC+MC}}$	5%	5%	6%(8%)	10%
$(\gamma\gamma h_{SM})^2\|_{\mathrm{MC}}$	14%(22%)	20%(34%)	48%(110%)	–
$(\gamma\gamma h_{SM})^2\|_{\mathrm{NLC+MC}}$	10%(12%)	13%(15%)	25%(29%)	–
$\Gamma^{\mathrm{tot}}_{h_{SM}}\|_{\mathrm{NLC+MC}}$	5%(10%)	6%(8%)	9%(10%)	11%(11%)

For $L_{\mathrm{tot}} = 0.4$ fb^{-1}, one would observe a $> 1.5 - 2\sigma$ deviation for $m_{A^0} < 450$ GeV.

– If $\sqrt{s} = 500$ GeV ($L_{\mathrm{tot}} = 200$ fb^{-1}) data available (presumably from NLC operation, but MC could also provide) $\Rightarrow$ use $\Gamma(h \to \mu^+\mu^-)$ (error $\lesssim 5\%$ for either MC $L_{\mathrm{tot}} = 0.4$ fb^{-1} or 4 fb^{-1}).

$\Rightarrow$ probes out to $m_{A^0} \gtrsim 600$ GeV for all $m_h \lesssim 2m_W$. No systematics.

– Note that Γ_h^{tot} alone cannot be used to distinguish between MSSM and SM in model-independent way. Γ_h^{tot} depends on many things, including (in MSSM) the squark-mixing model. However, deviations from SM are generally quite substantial if $m_{A^0} \lesssim 500$ GeV.

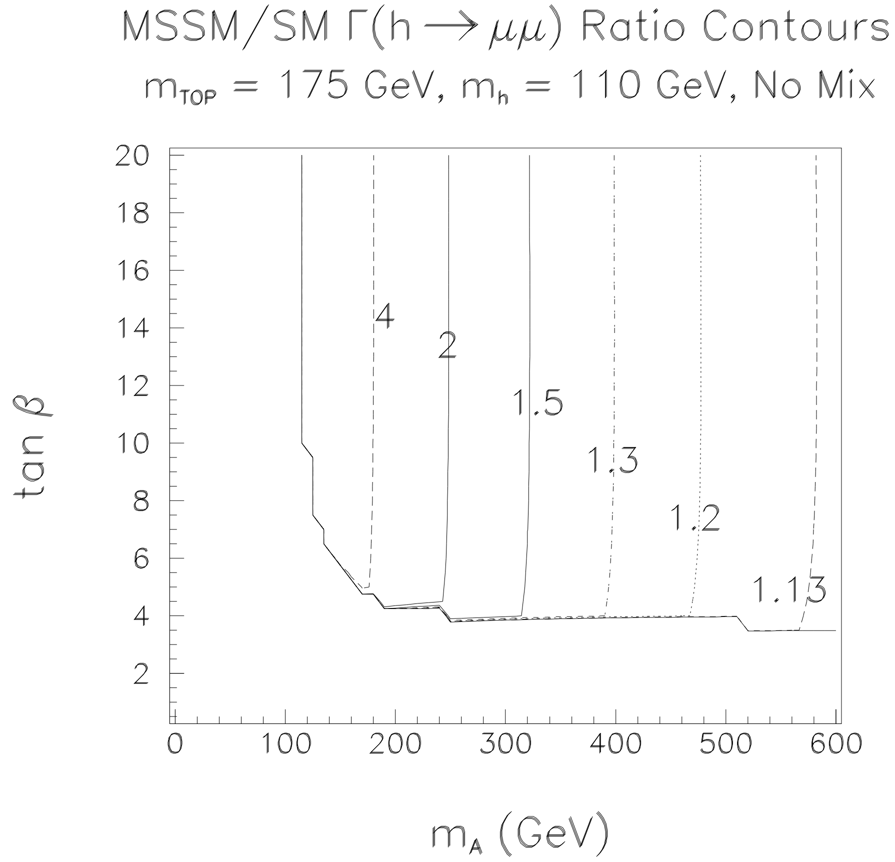

Figure 9: Constant value contours in $(m_{A^0}, \tan\beta)$ parameter space for the ratio $\Gamma(h^0 \to \mu^+\mu^-)/\Gamma(h_{SM} \to \mu^+\mu^-)$. We assume "no mixing" in the squark sector and present results for the case of fixed $m_{h^0} = m_{h_{SM}} = 110$ GeV. For "maximal mixing", the vertical contours are essentially identical — only the size of the allowed parameter range is altered. Contours for $\Gamma(h^0 \to b\bar{b})/\Gamma(h_{SM} \to b\bar{b})$ are identical.

Heavy Higgs of the MSSM and the MC

- Possibilities for H^0, A^0 are limited at other machines.
  - The LHC has "h^0-only" regions at moderate $\tan\beta \gtrsim 3$, $m_{A^0} \geq 200$ GeV (see figure).
  - At the NLC $e^+e^- \to Z^\star \to H^0 A^0$ is limited to $m_{H^0} \sim m_{A^0} \lesssim \sqrt{s}/2$ — *i.e.* 230 – 240 GeV at $\sqrt{s} = 500$ GeV.
  - A $\gamma\gamma$ collider could probe up to $m_{H^0} \sim m_{A^0} \sim 0.8\sqrt{s}_{e^+e^-}$, but this would require $L \sim 150 - 200\ \mathrm{fb}^{-1}$, especially if m_{A^0} near 400 GeV and $\tan\beta$ is large.

- In contrast, $\mu^+\mu^- \to H^0, A^0$ potentially allows production and study of H^0, A^0 up to $m_{A^0} \sim m_{H^0} \lesssim \sqrt{s}$. For $L = 50\ \mathrm{fb}^{-1}$ (5 yrs running at $< \mathcal{L} >= 1 \times 10^{33}$, as possibly achievable for $R \gtrsim 0.14\%$ for $\sqrt{s} = 300 - 500$ GeV):
  - with preknowledge/restrictions on m_{A^0} (from h^0 data, LHC or NLC discovery, *etc.*) $\mu^+\mu^- \to H^0$ and $\mu^+\mu^- \to A^0$ can be studied with precision for all $\tan\beta \gtrsim 1$. In particular, a scan to determine their widths would be no problem. Fine resolution ($R \sim 0.01\%$) might be required to separate A^0 from H^0 if $\tan\beta$ is large. (Lower expected L for such a small R would be ok once the overall peak location had been determined.)
  - without preknowledge, $\mu^+\mu^- \to H^0, A^0$ discovery by scanning from 250 – 500 GeV at the MC will be possible for most of $(m_{A^0}, \tan\beta)$ parameter space such that they cannot be discovered at the LHC (in particular, if $m_{A^0} \gtrsim 250$ GeV and $\tan\beta \gtrsim 4$).We

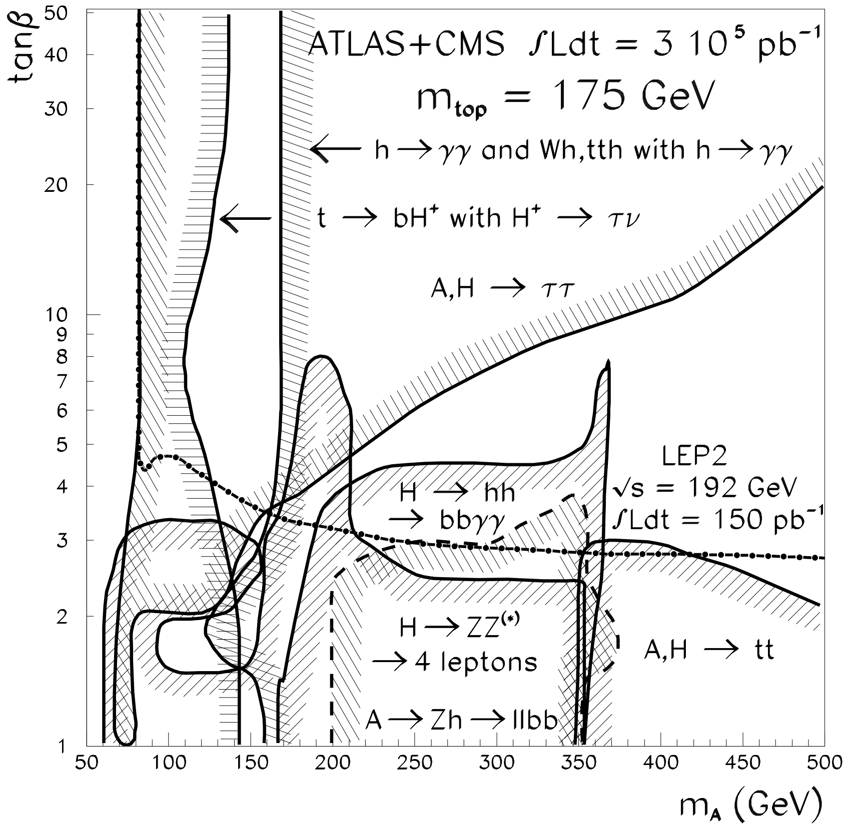

Figure 10: Discovery contours (5σ) in the parameter space of the minimal supersymmetric model for ATLAS+CMS at the LHC: $L = 300$ fb^{-1}. Two-loop/RGE-improved radiative corrections to the MSSM Higgs sector are included assuming $m_{\widetilde{t}} = 1$ TeV and no squark mixing.

might be left with a small gap in the $3 \lesssim \tan\beta \lesssim 4$ part of parameter space.

– If no NLC, first run FMC at $\sqrt{s} = 500$ GeV (or whatever). Use bremsstrahlung tail to detect H^0, A^0 if $m_{A^0} \geq \sqrt{s}/2$. Observation of A^0, H^0 peaks in $m_{b\bar{b}}$ distribution may be possible. For $m_{b\bar{b}}$ mass resolution of order ± 5 GeV (either via direct reconstruction or hard photon recoil) and $L = 50$ fb^{-1} (200 fb^{-1}) at $\sqrt{s} = 500$ GeV, the A^0, H^0 peak(s) are observable for $\tan\beta \geq 5 - 6$ $(3.5 - 4.5)$

if 250 GeV $\leq m_{A^0} \leq$ 500 GeV — *i.e.* the LHC/FMC gap for $\tan\beta \gtrsim 3$ is essentially closed at the higher luminosity.

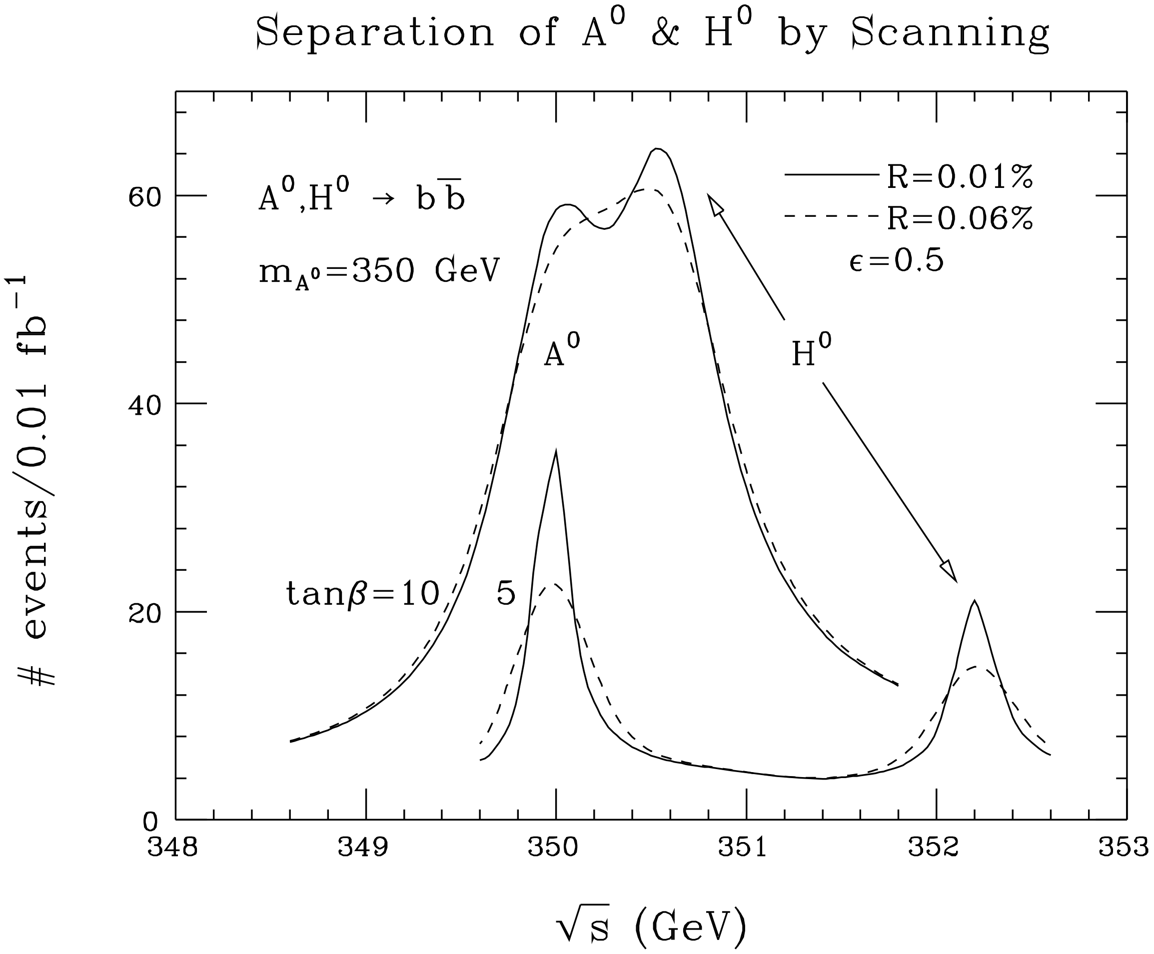

Figure 11: Plot of $b\bar{b}$ final state event rate as a function of $\sqrt{s}$ for $m_{A^0} = 350$ GeV, in the cases $\tan\beta = 5$ and 10, resulting from the H^0, A^0 resonances and the $b\bar{b}$ continuum background. We have taken $L = 0.01\ \mathrm{fb}^{-1}$ (at any given $\sqrt{s}$), $\epsilon = 0.5$, $m_t = 175$ GeV, and included two-loop/RGE-improved radiative corrections to Higgs masses, mixing angles and self-couplings using $m_{\tilde{t}} = 1$ TeV and neglecting squark mixing. SUSY decays are assumed to be absent. Curves are given for two resolution choices: $R = 0.01\%$ and $R = 0.06\%$

$\Rightarrow$ Together, the LHC and MC come close to guaranteeing discovery of the A^0, H^0 if they lie in the $\lesssim 500$ GeV range, assuming MC energy can be adjusted up to $\sqrt{s} \gtrsim 500$ GeV maintaining full luminosity. For higher m_{H^0}, m_{A^0}, higher MC energies are required. Without some restrictions or . . . from other data on m_{A^0}, the scan interval becomes large and discovery might be missed if $\tan\beta$ is not large.

- If no NLC, first run MC at $\sqrt{s} = 500$ GeV (or whatever). Use bremsstrahlung tail to detect H^0, A^0 if $m_{A^0} \geq \sqrt{s}/2$. Observation of A^0, H^0 peaks in $m_{b\bar{b}}$ distribution may be possible. For $m_{b\bar{b}}$ mass resolution of order ± 5 GeV and $L = 50~\mathrm{fb}^{-1}$ ($200~\mathrm{fb}^{-1}$) at $\sqrt{s} = 500$ GeV, the A^0, H^0 peak(s) are observable for $\tan\beta \geq 5-6$ ($3.5-4.5$) if 250 GeV $\leq m_{A^0} \leq$ 500 GeV — *i.e.* the LHC/MC gap for $\tan\beta \gtrsim 3$ is essentially closed at the higher luminosity.

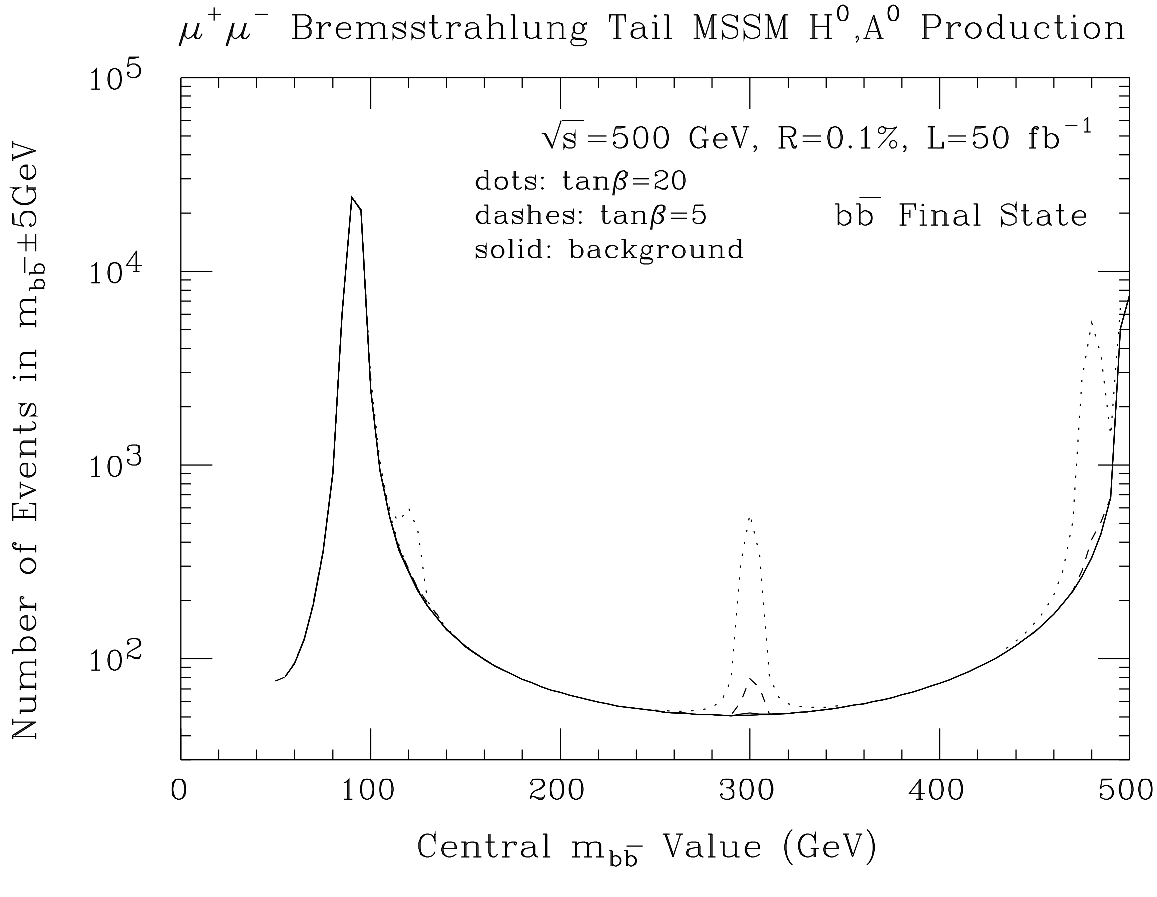

Figure 12: Taking $\sqrt{s} = 500$ GeV, integrated luminosity $L = 50~\mathrm{fb}^{-1}$, and $R = 0.1\%$, we consider the $b\bar{b}$ final state and plot the number of events in the interval $[m_{b\bar{b}} - 5~\mathrm{GeV}, m_{b\bar{b}} + 5~\mathrm{GeV}]$, as a function of the location of the central $m_{b\bar{b}}$ value, resulting from the low $\sqrt{\hat{s}}$ bremsstrahlung tail of the luminosity distribution. MSSM Higgs boson H^0 and A^0 resonances are present for the parameter choices of $m_{A^0} = 120$, 300 and 480 GeV, with $\tan\beta = 5$ and 20 in each case. Enhancements for $m_{A^0} = 120$, 300 and 480 GeV are visible for $\tan\beta = 20$; $\tan\beta = 5$ yields visible enhancements only for $m_{A^0} = 300$ and 480 GeV. Two-loop/RGE-improved radiative corrections are included, taking $m_t = 175$ GeV, $m_{\tilde{t}} = 1$ TeV and neglecting squark mixing. SUSY decay channels are assumed to be absent.

$H^0 A^0$ and H^+H^- Pair Production

Value of H^0A^0 and H^+H^- pair production is great. (JFG, Kelly)

$\Rightarrow$ must build muon collider if NLC can't be built with needed energy.

- Discovery of H^0A^0 in their $b\bar{b}$ or $t\bar{t}$ decay modes and H^+H^- in their $t\bar{b}$ and $b\bar{t}$ decays will be easy for expected luminosities, even if SUSY decays are present.
- Measurement of mass with reasonable accuracy will be possible.
- Measurement of branching ratios in combination with measurement of $m_{A^0} \sim m_{H^0} \sim m_{H^\pm}$ and, say, $m_{\widetilde{\chi}_1^\pm}$ (chargino) discriminates with incredible statistical significance between different closely similar GUT scenarios.

  Example: suppose $m_{A^0} = 349.7$ GeV and $m_{\widetilde{\chi}_1^\pm} = 149.5$ GeV.

  1. Consider 6 supergravity/superstring models: Dilaton, No-Scale, High-Scale, with sign(μ)= $\pm$.
  2. m_{A^0} and $m_{\widetilde{\chi}_1^\pm}$ fix the two independent parameters $\tan\beta$ and $m_{1/2}$ within any one of these models.

Table 13: The values of $m_{1/2}$ (in GeV) and $\tan\beta$ required in each of the six scenarios in order that $m_{A^0} = 349.7$ GeV and $m_{\widetilde{\chi}_1^\pm} = 149.5$ GeV.

	D^-	D^+	NS^-	NS^+	HS^-	HS^+
$m_{1/2}$	201.7	174.4	210.6	168.2	203.9	180.0
$\tan\beta$	7.50	2.94	3.24	2.04	12.06	3.83
m_{H^0}	350.3	355.8	353.9	359.0	350.1	353.2

3. Branching ratios are very different: SUSY modes are measurable and especially powerful discriminators. Assume D$^-$ model correct:

Table 14: $\Delta\chi^2_i$ assuming m_{A^0} and $m_{\widetilde{\chi}^\pm_1}$ are 349.7 GeV and 149.5 GeV, respectively. SUSY channels are resolved into final states involving a fixed number of leptons. Results for $L_{\rm eff} = 80$ fb^{-1} at $\sqrt{s} = 1$ TeV *assuming that the D$^-$ scenario is the correct one.*

Ratio	D$^+$	NS$^-$	NS$^+$	HS$^-$	HS$^+$
$\langle H^0, A^0\rangle$					
$[0\ell][\geq 0j]/b\overline{b}, t\overline{t}$	12878	1277	25243	0.77	10331
$[1\ell][\geq 0j]/b\overline{b}, t\overline{t}$	13081	2.41	5130	3.6	4783
$[2\ell][\geq 0j]/b\overline{b}, t\overline{t}$	4543	5.12	92395	26.6	116
$h^0h^0/b\overline{b}$	109	1130	1516	10.2	6.2
H^+					
$[0\ell][\geq 0j]/t\overline{b}$	12.2	36.5	43.2	0.04	0.2
$[1\ell][\geq 0j]/t\overline{b}$	1.5	0.3	0.1	5.6	0.06
$h^0W/t\overline{b}$	0.8	0.5	3.6	7.3	0.3
$\tau\nu/t\overline{b}$	43.7	41.5	47.7	13.7	35.5
$\Sigma_i \Delta\chi^2_i$	30669	2493	124379	68	15272

Bottom line: Higgs pair production **and measurement of their decays** will be a powerful tool in determining the correct GUT-scale boundary conditions.

Is there a LHC no-lose theorem for the NMSSM? (J.G., Haber, Moroi)

- At least one of the MSSM Higgs bosons can be discovered either at LEP2 or at the LHC throughout all of the standard $(m_{A^0}, \tan\beta)$ parameter space.

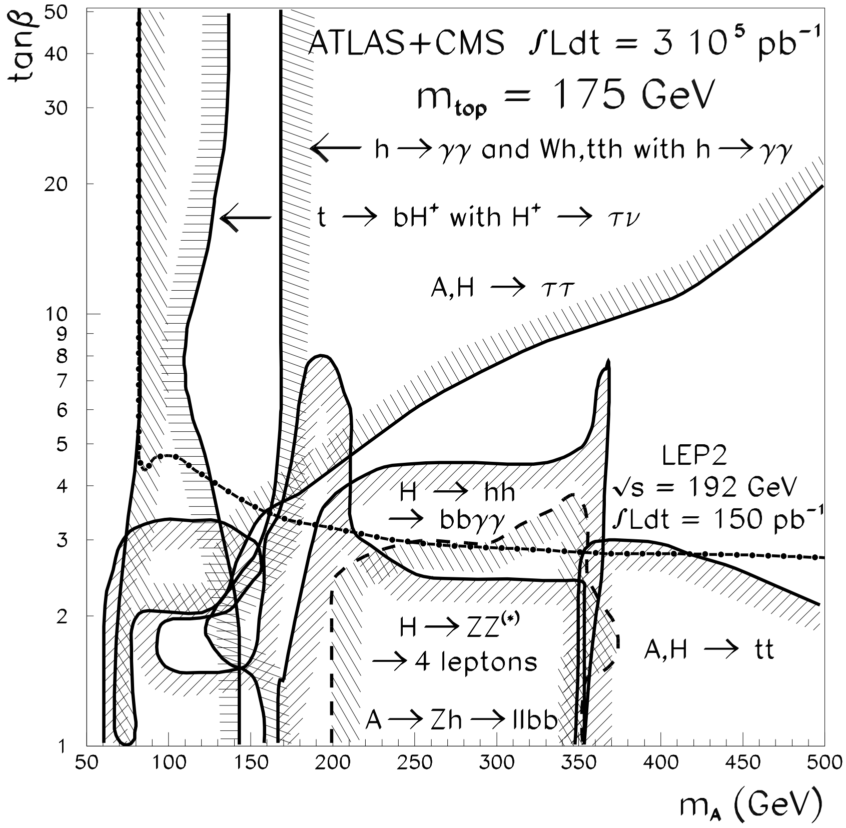

Figure 13: Discovery contours (5σ) in the parameter space of the minimal supersymmetric model for ATLAS+CMS at the LHC: $L = 300$ fb^{-1}. Two-loop/RGE-improved radiative corrections to the MSSM Higgs sector are included assuming $m_{\widetilde{t}} = 1$ TeV and no squark mixing.

- Employ same detection modes for the NMSSM. 1) $Z^\star \to Zh$ at LEP2; 2) $Z^\star \to ha$ at LEP2; 3) $gg \to h \to \gamma\gamma$ at LHC; 4) $gg \to h \to ZZ^\star$ or $ZZ \to 4\ell$ at LHC; 5) $t \to H^+ b$ at LHC; 6) $gg \to b\overline{b}h, b\overline{b}a \to$

$b\bar{b}\tau^+\tau^-$ at LHC; 7) $gg \to h, a \to \tau^+\tau^-$ at LHC. Additional Higgs decay modes that could be considered, but not reliably, at the LHC include: a) $a \to Zh$; b) $h \to aa$; c) $h_j \to h_i h_i$; d) $a, h \to t\bar{t}$. Avoid any choice of NMSSM parameters for which a)-d) might be relevant.

- $\Rightarrow$ Even over this restricted region of parameter space, NMSSM parameter choices can be found such that there are no observable Higgs signatures at either LEP2 or the LHC.

- Free parameters: $\tan\beta$, m_{h_1}, λ, $\alpha_{1,2,3}$, and m_a. h_1 = lightest CP-even Higgs mass eigenstate, a = lightest CP-odd scalar (2nd CP-odd scalar taken to be much heavier), λ from $W \ni \lambda \hat{H}_1 \hat{H}_2 \hat{N}$, with $\lambda \lesssim 0.7$ for perturbativity during evolution from m_Z to M_U. λ limit $\to$ a $\tan\beta$-dependent upper limit on m_{h_1} below $\lesssim 140$ GeV. $\alpha_{1,2,3}$ parameterize orthogonal matrix which diagonalizes the CP-even Higgs mass-squared matrix.

- Moderate $\tan\beta$ yields worse case: for low $\tan\beta \leq 1.5$, $\gamma\gamma, 4\ell, \ldots$ standard modes work; for high $\tan\beta \geq 10-11$, $b\bar{b}h$ and $b\bar{b}a$ modes are strong.

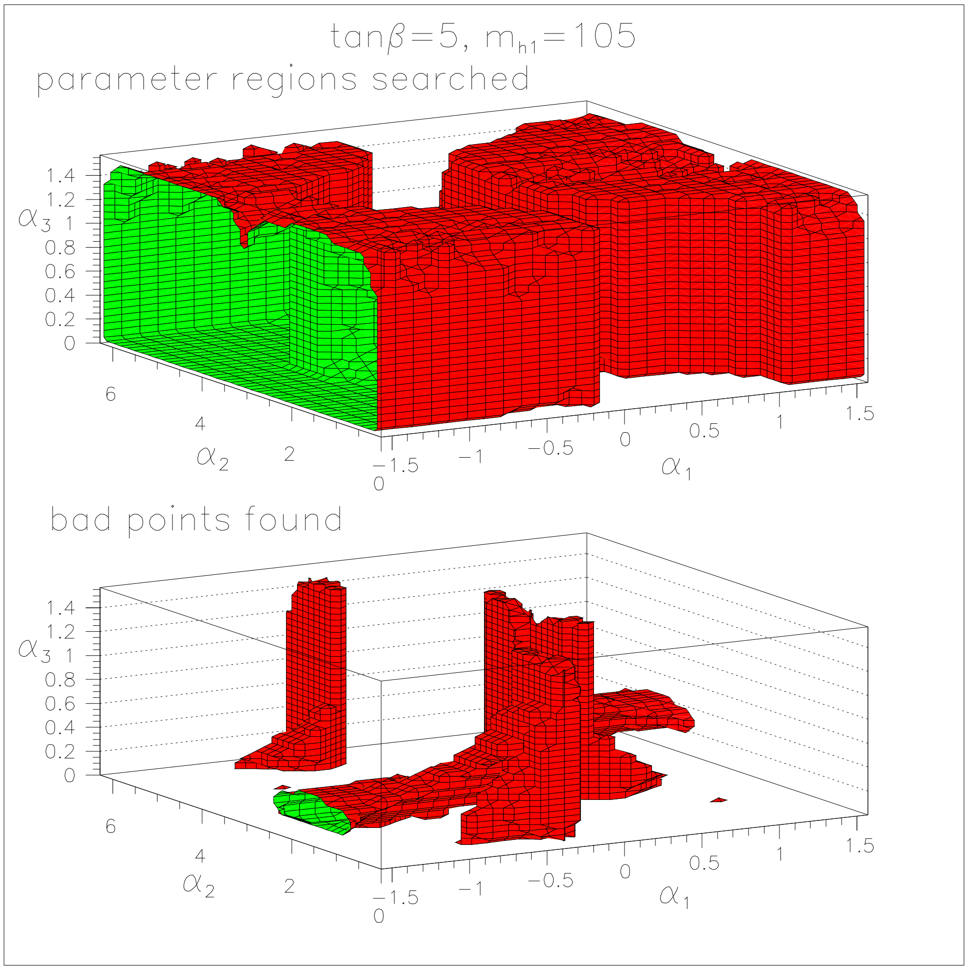

Figure 14: For $\tan\beta = 5$ and $m_{h_1} = 105$ GeV, we display in three dimensional $(\alpha_1, \alpha_2, \alpha_3)$ parameter space the parameter regions searched (which lie within the surfaces shown), and the regions therein for which the remaining model parameters can be chosen so that no Higgs boson is observable (interior to the surfaces shown).

A New Sum Rule (J.G., Grzadkowski, Haber, Kalinowski)

2HDM example:

- Define:

$$g_{ZZh_i} \equiv \frac{gm_Z}{c_W} C_i \,, \quad g_{Zh_ih_j} \equiv \frac{g}{2c_W} C_{ij} \,, \quad g_{ZZh_ih_j} = \frac{g^2}{2c_W^2} \delta_{ij} \,, \quad (0.24)$$

- Previously it was well known that

$$C_{h^0}^2 + C_{H^0}^2 = \sin^2(\beta - \alpha) + \cos^2(\beta - \alpha) = 1 \,. \quad (0.25)$$

$$C_{h^0}^2 + C_{h^0 A^0}^2 = \sin^2(\beta - \alpha) + \cos^2(\beta - \alpha) = 1 \,. \quad (0.26)$$

yields limits in CP-conserving case, but in CP-violating case naive sum rules involve three, not just two, of the $h_{1,2,3}$ mixed Higgs. However, can show [using $WW \to WW$, $WW \to ZZ$ *and* $ZZ \to h_ih_j$ unitarity sum rules (J.G., Haber, Wudka)]

$$C_i^2 + C_j^2 + C_{ij}^2 = 1 \,, \quad \text{any } i \neq j. \quad (0.27)$$

Combining Higgs pair and Zh limits from LEP (ALEPH) prove that 2 or more of the Higgs cannot be light.

- Generalization to 2D1S (and beyond is possible). In CP-violating case

$$C_1^2 + C_2^2 + C_3^2 + C_{12}^2 + C_{13}^2 + C_{23}^2 = 1 + C_{45}^2 \,. \quad (0.28)$$

and three (or more) of the 5 mixed $h_{1,2,3,4,5}$ cannot all be light.

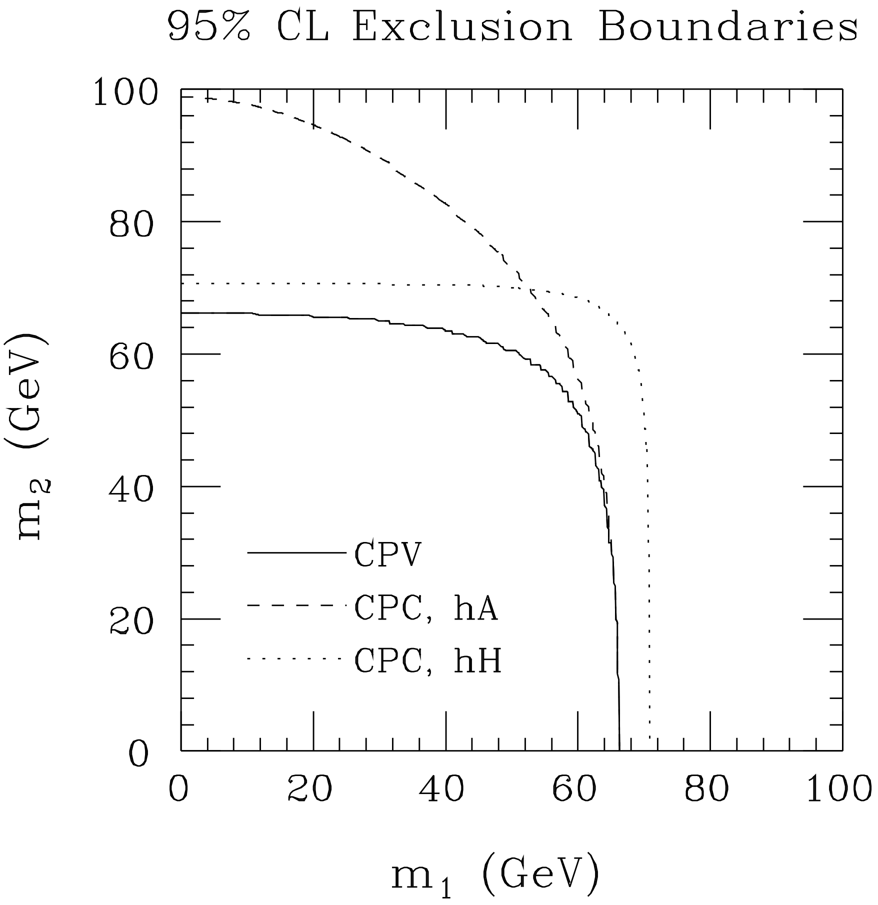

Figure 15: The LEP 95% confidence level boundaries (based on our use of the latest ALEPH results and earlier LEP1 results) in the (m_1, m_2) plane for three two-Higgs-doublet model cases: (i) the CP-conserving (CPC) model where $h_1 = h^0$, $h_2 = H^0$ (dotted curve); (ii) the CPC model where $h_1 = h^0$, $h_2 = A^0$ (dashed curve); (iii) the CP-violating (CPV) model where h_1 and h_2 are the two lightest neutral Higgs bosons (solid curve). This figure is based on including just two constraints: a particular choice of masses is excluded (a) if some ZZh_i coupling must lie above the 95% CL upper limit for the assumed m_{h_i} or (b) if one or more events are expected in $e^+e^- \to h_i h_j$ production at the 95% CL for some choice of $i \neq j$. For details, see the Appendix.

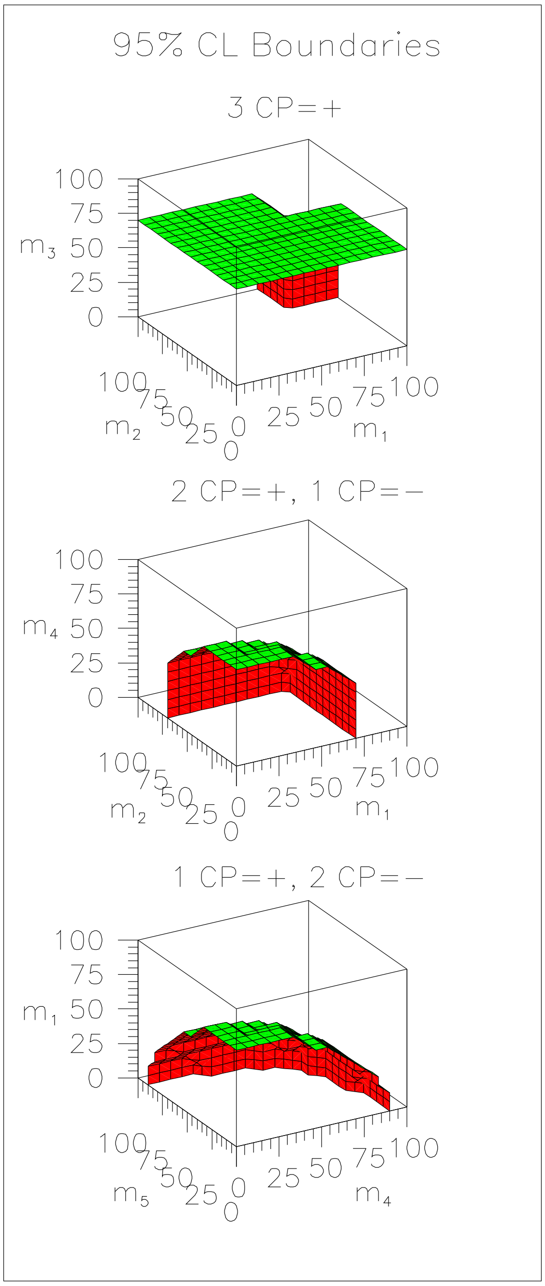

Figure 16: The LEP 95% confidence level boundaries for the two-doublet plus one-singlet CP-conserving Higgs sector in the (m_1, m_2, m_3), (m_1, m_2, m_4) and (m_4, m_5, m_1) spaces for three CP-even, two CP-even plus one CP-odd, and two CP-odd plus one CP-even Higgs bosons, respectively. Mass axes are in GeV units. Constraints are as in Fig. 15.

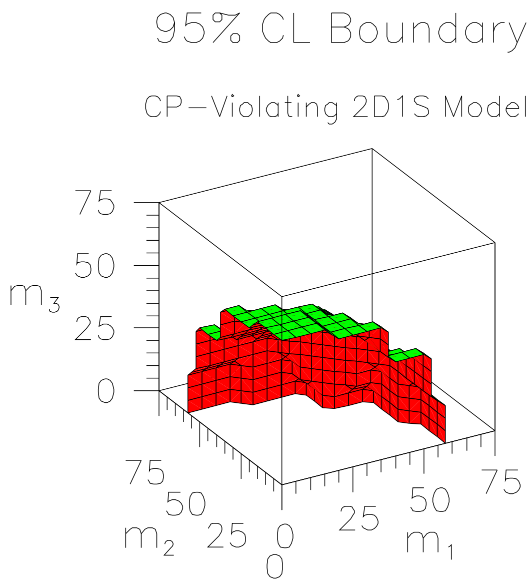

Figure 17: The LEP 95% confidence level boundary for the two-doublet plus one-singlet CP-violating Higgs sector in the (m_1, m_2, m_3) parameter space. Mass axes are in GeV units. Constraints are as in Fig. 15.

Precision measurements of 2HDM Higgs boson couplings. (J.G., X.-G. He)

- The $t\bar{t}$ and ZZ couplings of a neutral Higgs boson take the form:
$$t\bar{t}h : -\bar{t}(a+ib\gamma_5)t\frac{gm_t}{2m_W}\ , \quad ZZh : c\frac{gm_Z}{cos(\theta_W)}g_{\mu\nu}\ , \qquad (0.29)$$
where for the SM $a=1, b=0, c=1$. In the 2HDM,
$$a=\frac{R_{2j}}{\sin\beta}\ , \quad b=R_{3j}\cot\beta\ , \quad c=R_{1j}\cos\beta+R_{2j}\sin\beta\ , \qquad (0.30)$$
where $j=1,2,3$ indicates one of the three Higgs mass eigenstates, R_{ij} is a 3×3 orthogonal matrix for 2HDM Higgs fields $\rightarrow$ mass eigenstates. Result:
$$a=-\frac{s_1c_2}{\sin\beta}\ , \quad b=s_1s_2\cot\beta\ , \quad c=c_1\cos\beta-s_1c_2\sin\beta\ , \quad (0.31)$$
where $s_i=\sin\alpha_i$ and $c_i=\cos\alpha_i$ and $\alpha_{1,2}$ are free parameters in the range $0\le\alpha_{1,2}<2\pi$. The h has CP-violating couplings if either $ab\ne 0$ or $bc\ne 0$.

- Assume $L=500$ fb^{-1} (2 1/2 years) at $\sqrt{s}=1$ TeV. The total χ^2 is computed by combining the $t\bar{t}h$ and Zh processes:
$$\chi^2=\chi^2(t\bar{t}h)+\chi^2(Zh)\,; \qquad (0.32)$$
$\chi^2(t\bar{t}h)$ is computed using the full correlated error matrix for the optimal technique.
  - $e^+e^-\rightarrow Zh$ kinematically trivial; only useful observable is $\sigma_T(Zh)$, $\propto c^2$.
  - The differential $e^+e^-\rightarrow t\bar{t}h$ cross section contains five distinct terms: $\frac{d\sigma}{d\phi}=\Sigma_{i=1}^5 c_if_i(\phi)$, where
$$c_1=a^2\,;\quad c_2=b^2\,;\quad c_3=bc\,;\quad c_4=c^2\,;\quad c_5=ac\,, \qquad (0.33)$$

and the $f_i(\phi)$ are kinematically known functions. The $c_3 = bc$ term is explicitly CP-violating. It is vital to use information embodied in full detailed dependence of $d\sigma/d\phi$ on the ϕ phase space variables.

– Employ $w_i(\phi)$ such that $\int w_i(\phi)[d\sigma/d\phi] = c_i$, where the $w_i(\phi)$ are chosen for optimal statistics. Result:

$$c_i = \sum_k X_{ik} I_k = \sum_k M_{ik}^{-1} I_k\,, \quad \text{where} \quad I_k \equiv \int f_k(\phi) d\phi\,, \tag{0.34}$$

with

$$M_{ik} \equiv \int \frac{f_i(\phi) f_k(\phi)}{[d\sigma/d\phi]} d\phi\,. \tag{0.35}$$

– The covariance matrix from M_{ik} of Eq. (0.35) is

$$V_{ij} \equiv \langle \Delta c_i \Delta c_j \rangle = \frac{M_{ij}^{-1} \sigma_T(t\bar{t}h)}{N(t\bar{t}h)}\,, \tag{0.36}$$

where $N(t\bar{t}h) = L_{\rm eff}(t\bar{t}h)\sigma_T(t\bar{t}h)$ is the total number of events, with $L_{\rm eff}(t\bar{t}h)$ being the effective luminosity:

- We discuss in detail. the 2HDM model with $\tan\beta = 0.5$, $\alpha_1 = \pi/4$ and $\alpha_2 = \pi/2$ as our input model. (If $\tan\beta$ large $\to b\bar{b}h$.) For the alternative models, we considered $\tan\beta = 0.5$, $\tan\beta = 1.0$ and $\tan\beta = 1.5$, and computed χ^2 as a function of α_1 and α_2 assuming the 2HDM forms of a, b, c of Eq. (0.31).

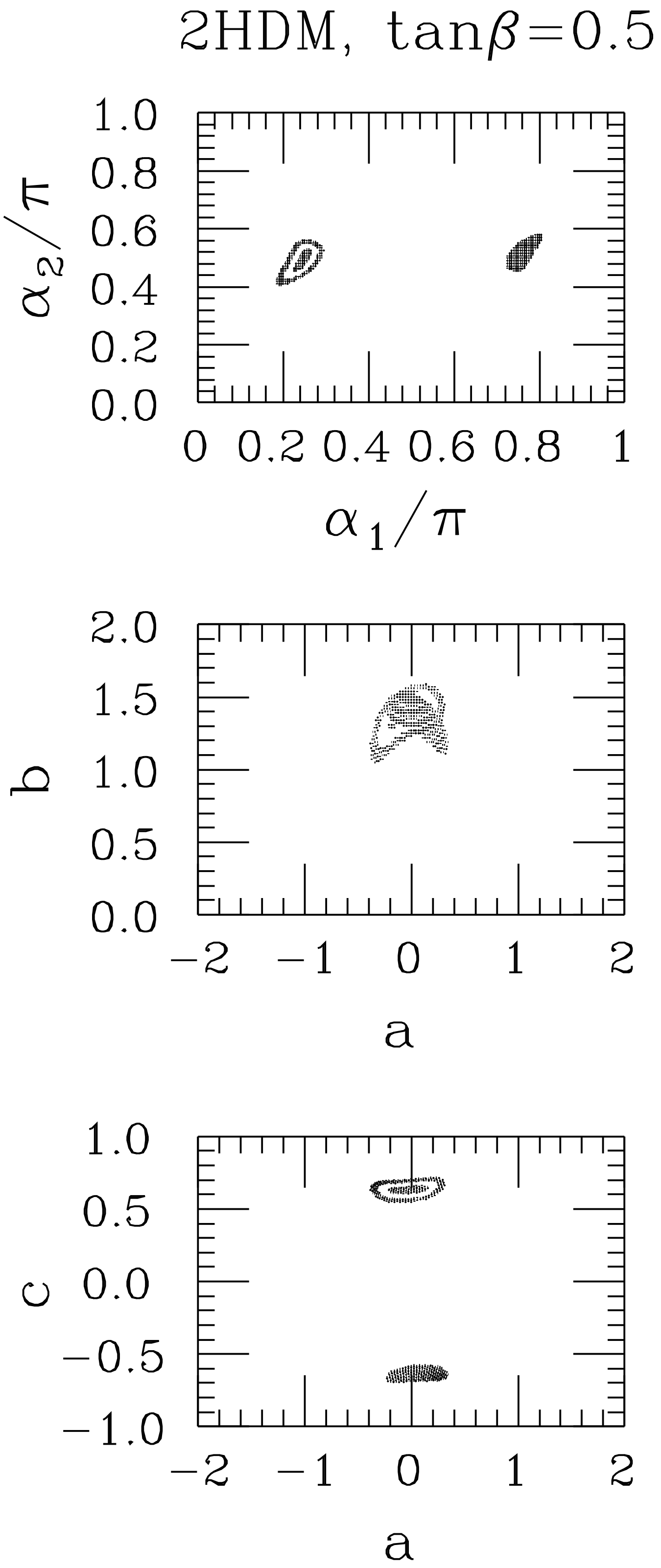

Figure 18: $\chi^2 \leq 1$, $1 < \chi^2 \leq 4$ and $4 < \chi^2 \leq 9$ regions in the $(\alpha_1/\pi, \alpha_2/\pi)$, (a, b) and (a, c) planes, assuming as input a 2HDM model with $\tan\beta = 0.5$, $\alpha_1 = \pi/4$ and $\alpha_2 = \pi/2$.

Exotic Higgs Sectors: Complementarity of LHC, NLC and FMC

- Doubly-Charged Higgs Bosons (Δ^{--}):

  Theoretical issues:

  – Consider models where $\rho = 1$ is natural (not infinitely renormalized).

    $\Rightarrow$ vev of any neutral member of the same multiplet $= 0$. $\Rightarrow$ no $W^-W^- \to \Delta^{--}$ coupling. $\Rightarrow$ narrow width in general, especially if $\Delta^{--} \to W^-\Delta^-$ is kinematically forbidden (as is likely).

  – Coupling constant unification good in non-SUSY Standard Model with a single $|Y| = 2$ triplet representation in addition to standard $|Y| = 1$ doublet.

  – In MSSM, triplet Higgs field(s) destroy unification if intermediate scale matter not included.

  – Especially interesting = lepton-number-violating $e^-e^- \to \Delta^{--}$ coupling. For $Q = T_3 + \frac{Y}{2} = -2$ the allowed cases are:

$$
\begin{aligned}
e^-_R e^-_R &\to \Delta^{--}(T = 0, T_3 = 0, Y = -4)\,, \\
e^-_L e^-_R &\to \Delta^{--}(T = \tfrac{1}{2}, T_3 = -\tfrac{1}{2}, Y = -3)\,, \\
e^-_L e^-_L &\to \Delta^{--}(T = 1, T_3 = -1, Y = -2)\,.
\end{aligned}
\tag{0.37}
$$

    Note the above cases do not include the $T = 3, Y = -4$ representation that yields $\rho = 1$ even with vev$\neq 0$, nor the $T = 1, Y = -4$ triplet with no neutral member, but do include the $T = 1/2, Y = -3$ doublet representation with no neutral member, and the popular $T = 1, Y = -2$ triplet representation.

– In the case of a $|Y|=2$ triplet representation (to which we now specialize) the lepton-number-violating coupling to (left-handed) leptons is specified by the Lagrangian form:

$$\mathcal{L}_Y = i h_{ij} \psi_{iL}^T C \tau_2 \Delta \psi_{jL} + \text{h.c.}\,, \tag{0.38}$$

where $i,j = e,\mu,\tau$ are generation indices, the ψ's are the two-component left-handed lepton fields ($\psi_{\ell L} = (\,\nu_\ell, \ell^-\,)_L$), and Δ is the 2×2 matrix of Higgs fields:

$$\Delta = \begin{pmatrix} \Delta^+/\sqrt{2} & \Delta^{++} \\ \Delta^0 & -\Delta^+/\sqrt{2} \end{pmatrix} . \tag{0.39}$$

– Limits on the h_{ij} by virtue of the $\Delta^{--} \to \ell^-\ell^-$ couplings include: Bhabbha scattering, $(g-2)_\mu$, muonium-antimuonium conversion, and $\mu^- \to e^-e^-e^+$.

$$\begin{aligned} &|h_{ee}^{\Delta^{--}}|^2 \lesssim 10^{-5} m_{\Delta^{--}}^2(\text{ GeV}) \\ &|h_{\mu\mu}^{\Delta^{--}}|^2 \lesssim 4\times 10^{-5} m_{\Delta^{--}}^2(\text{ GeV}) \\ &|h_{ee}^{\Delta^{--}} h_{\mu\mu}^{\Delta^{--}}| \lesssim 6\times 10^{-5} m_{\Delta^{--}}^2(\text{ GeV}) \\ &|h_{e\mu}^{\Delta^{--}} h_{ee}^{\Delta^{--}}| \lesssim 5\times 10^{-11} m_{\Delta^{--}}^2(\text{ GeV}) \end{aligned} \tag{0.40}$$

from the above respective sources. Last suggests small off-diagonal couplings as we shall assume. Adopt convention

$$|h_{\ell\ell}^{\Delta^{--}}|^2 \equiv c_{\ell\ell} m_{\Delta^{--}}^2(\text{ GeV})\,, \tag{0.41}$$

where $c_{ee} \lesssim 10^{-5}$ is the strongest of the limits.

– For a $T=1, Y=-2$ triplet,

$$\begin{aligned} \Gamma(\Delta^{--} \to \Delta^- W^-) &= (1.3\text{ GeV}) \left(\tfrac{m_{\Delta^{--}}}{100\text{ GeV}}\right)^3 \beta^3_{\Delta^- W^-}\,, \\ \Gamma(\Delta^{--} \to \ell\ell) &= (0.4\text{ GeV}) \left(\tfrac{c_{\ell\ell}}{10^{-5}}\right) \left(\tfrac{m_{\Delta^{--}}}{100\text{ GeV}}\right)^3 . \end{aligned} \tag{0.42}$$

Consider $m_{\Delta^{--}} = 360$ GeV, $m_{\Delta^{-}} = 250$ GeV. From Eq. (0.42) we find $\Gamma(\Delta^{--} \to \Delta^{-}W^{-}) \sim 2$ GeV and $\Gamma(\Delta^{--} \to \ell^{-}\ell^{-}) = 19$ GeV $\left(\frac{c_{\ell\ell}}{10^{-5}}\right)$. For very small c's, the $\Delta^{-}W^{-}$ mode is likely to be dominant if it is kinematically allowed. For extremely tiny c's, virtual versions of $\Delta^{-}W^{-}$ can enter.

Strategy:

– Discover Δ^{--} in $p\overline{p} \to \Delta^{--}\Delta^{++}$ with $\Delta^{--} \to \ell^-\ell^-, \Delta^{++} \to \ell^+\ell^+$ ($\ell = e, \mu, \tau$) at TeV33 or LHC (J.G., Loomis, Pitts).

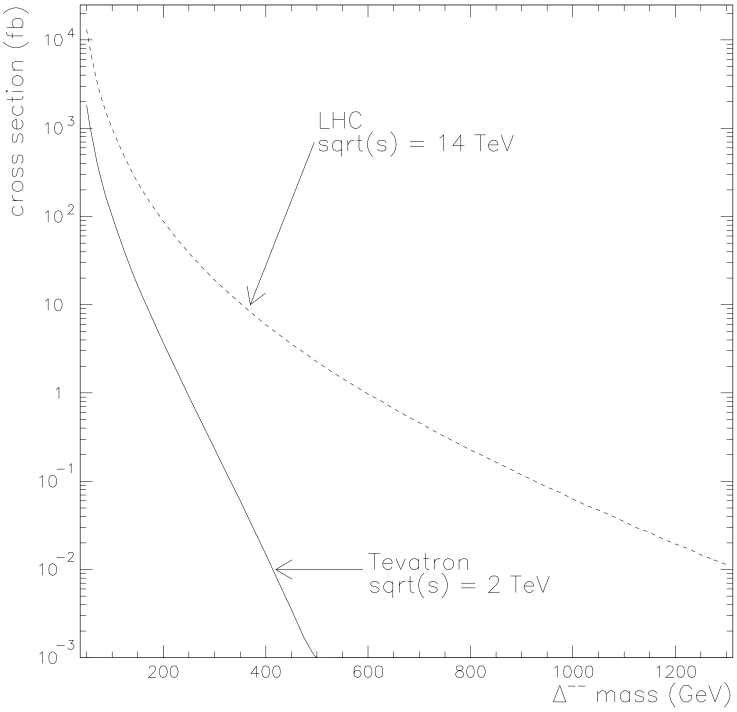

Figure 19: $\Delta^{++}\Delta^{--}$ pair production cross section as a function of Δ^{--} mass for both the Tevatron and the LHC.

$\Rightarrow$ Δ^{--} detection at the Tevatron ($\sqrt{s} = 2$ TeV, $L = 30$ fb^{-1}) ok for $m_{\Delta^{--}}$ up to 300 GeV for $\ell = e$ or μ and 180 GeV for $\ell = \tau$. (Criteria: $\sim$ 10 evts. for $\ell = e, \mu$ and $\sim$ 300 evts. for $\ell = \tau$). At LHC $m_{\Delta^{--}}$ discovery ok up to roughly 925 GeV (1.1 TeV) for $\ell = e, \mu$ and 475 GeV (600 GeV) for $\ell = \tau$, for $L = 100$ fb^{-1} ($L = 300$ fb^{-1}).

$\Rightarrow$ TeV33 + LHC will tell us if such a Δ^{--} exists in the mass range accessible to NLC and FMC.

– Study in e^-e^- and $\mu^-\mu^-$ s-channel collisions via the allowed Majorana-like bi-lepton coupling.

* At e^+e^- machine, spectrum approximated by a Gaussian in the vicinity of the peak energy, with a 1σ rms resolution of $\sigma \sim 0.2\%\sqrt{s}$, accompanied by a tail (coming from the beam-strahlung and bremsstrahlung). Roughly 38% of the total luminosity will reside in the narrow Gaussian centered at the nominal machine energy. Assume a few years $\Rightarrow L = 50$ fb^{-1} in the central 0.2% Gaussian peak.

* A useful mnemonic for the Gaussian rms resolution, taking $\sqrt{s} = m_{\Delta^{--}}$, is

$$\sigma \sim 0.2 \text{ GeV} \left(\frac{m_{\Delta^{--}}}{100 \text{ GeV}}\right)\left(\frac{R}{0.2\%}\right) , \qquad (0.43)$$

where R is the resolution in percent. The crucial issue is how σ compares to $\Gamma_{\Delta^{--}}$. For $c_{\ell\ell} = 10^{-5}$ and $R = 0.2\%$, Eq. (0.42) predicts that $\Gamma(\Delta^{--} \to \ell^-\ell^-) = \sigma$ for $m_{\Delta^{--}} \sim 70$ GeV. If all c's $\ll 10^{-5}$, the Δ^{--} is light, and the $\Delta^{--} \to H^-W^-$ decay is either strongly suppressed or disallowed, $\Rightarrow \Gamma_{\Delta^{--}} \ll \sigma$.

* The resulting cross section is denoted by $\overline{\sigma}_{\Delta^{--}}$. For $\sqrt{s} = m_{\Delta^{--}}$,

$$\overline{\sigma}_{\Delta^{--}} = \begin{cases} \frac{4\pi BR(\Delta^{--}\to e^-e^-)}{m^2_{\Delta^{--}}}, & \Gamma_{\Delta^{--}} \gg \sigma; \\ \frac{\sqrt{\pi}}{2\sqrt{2}} \frac{4\pi \frac{\Gamma(\Delta^{--}\to e^-e^-)}{\sigma}}{m^2_{\Delta^{--}}}, & \Gamma_{\Delta^{--}} \ll \sigma \ . \end{cases} \qquad (0.44)$$

* Taking $L = 50$ fb^{-1}, and using Eq. (0.43) for σ and the result in Eq. (0.42) for $\Gamma(\Delta^{--} \to e^-e^-)$, we find from Eq. (0.44) an

event rate of

$$N(\Delta^{--}) \sim 3 \times 10^{10} \left(\frac{c_{ee}}{10^{-5}}\right)\left(\frac{0.2\%}{R}\right) ; \tag{0.45}$$

$\Rightarrow$ an enormous event rate if c_{ee} near its upper bound. Note that if the Δ^{--} is observed at the LHC or NLC, we will know ahead of time what final state to look in.

Note: if $\Gamma_{\Delta^{--}} \ll \sigma$, Eq. (0.45) $\Rightarrow$ event rate alone is sufficient to determine c_{ee}, unlike in the $\Gamma_{\Delta^{--}} \gg \sigma$ case. Direct measurement of $\Gamma_{\Delta^{--}}$ and/or observation of $\Delta^{--} \to e^-e^-$ decays not required.

* Ultimate sensitivity to c_{ee} when $\Gamma_{\Delta^{--}} \ll \sigma$: suppose 100 events are required. From Eq. (0.45), we predict 100 Δ^{--} events for

$$c_{ee}|_{100\text{ events}} \sim 3.3 \times 10^{-14}(R/0.2\%)\,, \quad \Gamma_{\Delta^{--}} \ll \sigma\,, \tag{0.46}$$

independent of $m_{\Delta^{--}}$. $\Rightarrow$ dramatic sensitivity. Even in the worst case scenario of requiring 1000 events when the semi-virtual modes dominate the final state, we are able to achieve a nearly 8 orders of magnitude improvement over the current limits on c_{ee}. If the $\mu^-\mu^-$ final state were dominant, as few as 10 events would probably constitute a viable signal.

* A $\mu^+\mu^-$ collider with

$$\sigma \sim 0.007 \text{ GeV} \left(\frac{m_{\Delta^{--}}}{100 \text{ GeV}}\right)\left(\frac{R}{0.007\%}\right) , \tag{0.47}$$

would do a factor of 30 better, and directly determine $c^2_{\mu\mu}$ in the narrow width regime, even if $BF(\Delta^{--} \to \tau^+\tau^-) \sim 1$.

Conclusion

Higgs boson physics remains as exciting as ever. Measurements of their production rates, decays, couplings and widths provide a very powerful probe of a wide range of new physics. Once we have accelerators capable of detecting Higgs bosons, we will be very busy.